ANCR-1228
NRC-2

THERMAL-HYDRAULIC RESPONSE OF THE SEMISCALE MOD-1 SYSTEM— ISOTHERMAL TEST SERIES

Aerojet Nuclear Company

IDAHO NATIONAL ENGINEERING LABORATORY

Idaho Falls, Idaho — 83401

DATE PUBLISHED—OCTOBER 1975

PREPARED FOR THE
ENERGY RESEARCH AND DEVELOPMENT ADMINISTRATION
IDAHO OPERATIONS OFFICE UNDER CONTRACT E (10-1)-1375

DISTRIBUTION OF THIS DOCUMENT IS UNLIMITED

DISCLAIMER

Printed in the United States of America
Available from
National Technical Information Service
U. S. Department of Commerce
5285 Port Royal Road
Springfield, Virginia 22161
Price: Printed Copy $5.45; Microfiche $2.25

ANCR-1228

Distribution Under Category:
NRC-2
Water Reactor Safety Research
Systems Engineering
TID-4500, R63

THERMAL-HYDRAULIC RESPONSE OF THE SEMISCALE MOD-1 SYSTEM – ISOTHERMAL TEST SERIES

by

C. E. Cartmill

AEROJET NUCLEAR COMPANY

Date published – October 1975

PREPARED FOR THE
U.S. ENERGY RESEARCH AND DEVELOPMENT ADMINISTRATION
IDAHO OPERATIONS OFFICE
UNDER CONTRACT NO. E(10-1)-1375

ACKNOWLEDGMENTS

The author wishes to express his thanks to the personnel of the Fluids Laboratory Division for their efforts in conducting the tests and gathering the test data, to the personnel of the Test Integration and Coordination Section for verification and documentation of the data, to D. J. Hanson for technical support, to K. A. Dietz for her efforts in editing and improving the quality of the overall report, to L. K. Keller and L. A. Nelson for their patience in typing the report, to G. W. Johnsen and D. C. Mecham for their work in setting up the RELAP4 computer model of the isothermal system and for supplying the computer calculations, and to D. L. Caraher and J. K. Meier for supplying model verification information on break flows and pressurizer response, respectively.

ABSTRACT

Selected experimental thermal-hydraulic data from the recent isothermal blowdown test series performed in the Semiscale Mod-1 geometry are analyzed from an experimental viewpoint with emphasis on explaining differences between the data and expected results. Comparisons are made between the trends measured by the system instrumentation and the trends predicted by analytical tools, including the RELAP4 computer code, to aid in understanding the interactions between phenomena occurring in different parts of the system. The analyses presented in this report are valuable for evaluating the adequacy and improving the predictive capability of analytical models developed to predict the system of a pressurized water reactor during a postulated loss-of-coolant accident (LOCA).

SUMMARY

The Semiscale Mod-1 Program is intended to provide transient thermal- hydraulic data from a simulated loss-of-coolant accident (LOCA) using a small-scale experimental system. The Semiscale Mod-1 Program is a major contributor of experimental data that will aid in understanding the reponse of the system, the response of the individual components, and the interactions that occur between the major components and subsystems. These data provide a means of evaluating the adequacy of the overall system analytical models as well as the models of the individual system components. The objectives of the Semiscale Mod-1 experimental program are to: (a) produce integral and separate effects experimental thermal-hydraulic data that are needed to provide an experimental basis for analytical model assessment, (b) provide data for assessing the requirements and reliability of selected loss-of-Fluid Test (LOFT) Program instrumentation, and (c) produce experimental data to aid in optimizing the selection of test parameters and the evaluation of test results from the LOFT Program.

The isothermal test series was the first series conducted in the Semiscale Mod-1 program and contributed to fulfilling successfully the three Semiscale Mod-1 program objectives. The isothermal test series consisted of eight blowdown tests, each of which simulated an offset shear of either the hot or cold leg. Each of the cold leg break configuration tests was conducted by establishing system fluid conditions at about 540°F and 2,250 psig, allowing the piping and various metal components to approach the fluid temperature, and simulating a rupture in the broken loop cold leg piping to cause the system fluid to flow out through the two rupture nozzles and into a pressure suppression tank. Each of the hot leg break configuration tests was conducted at 1,600 psig and 540°F with the rupture in the broken loop hot leg piping. The decompression, or blowdown process, lasted between 40 and 50 seconds depending on the type of break. Seven of the tests included emergency core coolant (ECC) injection during blowdown, with ECC being injected into one of the three principal locations: the intact Loop cold leg, the downcomer distributor annulus, or the lower plenum.

In addition to the Semiscale Mod-1 program objectives, general tests series objectives were developed for the isothermal tests. These objectives relate to phenomena which strongly influence system behavior. The studies conducted included: (a) an investigation of the break phenomena, (b) an investigation of the performance and effect of the intact loop pump, (c) an investigation of the emergency core coolant influence, (d) a determination of the energy transfer from the steam generator, and (e) a determination of the performance and effect of the pump and steam generator simulators, and (f) an investigation of the effect of the pressurizer on system response. In addition, specific objectives were selected to evaluate the repeatability of the phenomena occurring during tests with similar initial conditions and the effect on system response of changing the configuration of a part of the system. The specific test objectives were met through differential comparisons of data from separate tests to investigate the effect on system response of: (a) changing intact loop flow resistance, (b) changing break location and size, (c) changing from water to nitrogen in the steam generator secondary (a reduction in heat transfer from the steam generator to the blowdown fluid), and (d) having the 40-rod core installed rather than the core simulator.

This report provides an evaluation of the thermal-hydraulic response of the system relative to the general and specific objectives outlined. System parameters having the most influence on fluid blowdown response are discussed from an experimental viewpoint with emphasis on explaining the trends of the data rather than the test-by-test results. Selected experimental data from the isothermal blowdown test series include data that describe blowdown and ECC related phenomena throughout the entire system, with emphasis on the core region, break areas, and pump region. Data from these parts of the system are presented together with calculated results, including results from the RELAP4 computer code. A detailed discussion of the results is included only when the experimental data deviate significantly from the expected system behavior. The discussion of the analysis begins with the phenomena which most strongly influence system behavior and proceeds with a subsequent discussion of differential test[a] analyses that are related to objectives which are specific to individual tests.

Phenomena Strongly Influencing System Behavior

The flow rates at the rupture nozzles strongly influence the system decompression rate and, therefore, affect much of the phenomena occurring throughout the system. The effect of blowdown on system fluid response is principally a function of the break and pump conditions during blowdown. The break and pump conditions compete with each other in determining the magnitudes and direction of fluid flow through the Semiscale Mod-1 system during blowdown. The principal influence of the break fluid conditions on system response occurs within the core region.

Knowledge of core fluid properties during blowdown is important to blowdown analysis in that high core flow rates and low fluid qualities result in more energy removal from the core. The core fluid properties are influenced by other components within the system, principally the pump and the breaks. Therefore, accurate prediction of core phenomena can only result from properly accounting for the various influences imposed on the core from the other components in the system. Analysis has shown that use of a critical break flow model in the RELAP4 code which correctly represents the physical phenomena occurring at the breaks is important in analytically determining the core fluid behavior. Of the present options in RELAP4, a critical break flow model in which the Henry break flow model is used for subcooled blowdown, followed by a sonic choking model for saturated blowdown, gives the best, but not optimum results. Various other critical flow models where subsequently studied to determine whether improvements could be obtained in approximating flow conditions during both portions of the blowdown. The homogeneous equilibrium model (HEM) appears to predict break flows better than the other models.

[a] Differential tests within the Semiscale Mod-1 system are defined as two or more tests the results of which are compared to evaluate the effect on system response of changing the configuration or initial blowdown conditions of a part of the system.

The principal influence of the pump on system response for the isothermal tests occurs within the first several seconds of blowdown. The pump model for the Semiscale Mod-1 system contained in the RELAP4 computer program appeared to calculate the trends of the data resonably well. However, without more accurately defined two-phase head and torque degradation multipliers, better prediction in terms of magnitudes of the Semiscale Mod-1 pump variables is difficult. In addition, the two-phase homologous head curves used in the RELAP4 pump model appear to be slightly low in the steady state operating region.

An analysis of the emergency core coolant influence in the system indicates that periodic oscillatory flow existed about the injection point within the intact loop cold leg during ECC injection. Significant condensation occurred near the injection location causing the establishment of the oscillatory flow pattern. The complex phenomena that occurred in the downcomer region during ECC injection influenced the time of delivery and the rate of deliver of ECC to the lower plenum. Downcomer countercurrent flow, bypass flow, and heat transfer phenomena were the controlling variables as to when ECC water reached the lower plenum. Lower plenum ECC injection was found to provide about 26 seconds of additional cooling for the core as compared to cold leg injection.

The results of the piping heat transfer and steam generator analysis indicate that the intact and broken loop piping heat transfer is sensitive to azimuthal location in a given pipe, location of the pipe in both the intact and broken loops, and the broken loop break characteristics. Maximum heat transfer has been shown to occur in the bottom of horizontal pipe sections and this phenomenon is attributable to the phase separation of the blowdown fluid.

The sensitivity of piping heat transfer to location in the intact loop is relatable to the location of the intact loop primary fluid stagnation point. The sensitivity to location in the broken loop is caused by unequal division of break flows and the presence of bypassed ECC in the broken loop vessel inlet side of the break.

In general, the isothermal test series provided data which were quite repeatable up to the time of accumulator ECC injection. The general performance (that is, the trends of the data) was also repeatable after initiation of ECC injection even though the magnitudes were different.

Comparison of Results from Differential Tests

In order to establish the importance of operating loop resistance during blowdown, Tests S-01-2 and S-01-4A were conducted with different intact loop flow resistances: A high resistance based on volumetric scaling in Test S-01-2 and a lower resistance based on core area scaling in Test S-01-4A. The effect of the use of these two resistance values on system performance was studied during the first 20 seconds of blowdown (prior to ECC injection) at measurement locations throughout the system. The effect on system response of having different intact loop flow resistances during blowdown was to change the fluid behavior near the intact loop pump and, more significantly, within the core region. The fluid density at the inlet to the core was significantly changed, although the change was not consistent with RELAP4 calculations. The turbine flowmeter measurement at the core inlet also

showed a difference of results for the two tests of interest. However, the effect on core performance on high versus low intact loop resistance cannot be conclusively stated because the turbine flowmeter measurement for Test S-01-2 is in question.

The effect on system response of the energy transfer from the secondary side of the steam generator is demonstrated through an analysis and comparison of data from Tests S-01-4 and S-01-5. Both tests were 200% offset shear cold leg break tests and utilized ECC injection into the cold leg of the intact loop. Intact loop secondary to primary steam generator heat transfer was found to have little, if any, effect on overall system performance during the blowdown transient. Variations in system blowdown performance between Tests S-01-4 and S-01-5 were noted primarily between the steam generator outlet and the intact loop vessel inlet. The local variations in blowdown response noted in comparing the results of the two tests had very little effect on overall system performance.

The effect of break size and location of break on system response was demonstrated to be large when results from a 100% hot leg break test were compared with those from a 200% cold leg break test. The most significant difference in results for the hot leg break in comparison to the cold leg break occurred within the core region. The positive flow through the core throughout blowdown for the hot leg break resulted in a much higher density within the core than existed for the cold leg break and led to the conclusion that better cooling characteristics existed within the core for the 100% hot leg break configuration than for the 200% cold leg break configuration.

CONTENTS

FIGURES

TABLES

THERMAL-HYDRAULIC RESPONSE OF THE SEMISCALE MOD-1 SYSTEM – ISOTHERMAL TEST SERIES

I. INTRODUCTION

The Semiscale Mod-1 experimental program conducted by Aerojet Nuclear Company is part of an overall Nuclear Regulatory Commission sponsored research and development program to investigate the behavior of a pressurized water reactor (PWR) system during a hypothesized loss-of-coolant accident (LOCA). The Semiscale Mod-1 Program is intended to provide transient thermal-hydraulic data from a simulated LOCA using a small-scale experimental system and is a major contributor of experimental data that will aid in understanding the response of PWR system, the response of the individual components, and the interactions that occur between the major components and subsystems. These data provide a means of evaluating the adequacy and facilitating the improvement of system analytical models as well as models of individual components. The objectives of the Semiscale Mod-1 experimental program are to: (a)produce integral and separate effects experimental thermal-hydraulic data that are needed to provide an experimental basis for analytical model assessment, (b) provide data for assessing the requirements and reliability of selected Loss-of-Fluid Test (LOFT) Program instrumentation, and (c) produce experimental data to aid in optimizing the selection of test parameters and the evaluation of test results from the LOFT Program.

The isothermal test series consisted of a group of isothermal blowdown tests which contributed to fulfilling the Semiscale Mod-1 Program objectives. In addition the general program objectives, additional specific objectives were developed for the isothermal tests. These objectives were grouped into those objectives which were common to all tests within this series, and into those objectives which were unique to individual tests. The common test objectives were selected to provide an investigation of the component-related phenomena which most strongly influence the overall system behavior. The studies to fulfill these objectives include: (a) an investigation of the break phenomena, (b) an investigation of the performance of the intact loop pump, (c) a determination of the energy transfer from the steam generator, (d) a determination of the performance of the broken loop pump and steam generator simulators, (e) an investigation of the repeatability of the phenomena occurring during tests with similar initial conditions, and (f) an investigation of the effect of the pressurizer on system response. The specific objectives were selected to evaluate the effect on system response of changing the configuration of a part of the system. These objectives were met through differential comparisons of data from separate tests to investigate the effect on system response of: ,(a) Changing intact loop flow resistance, (b) changing break location and size, (c) changing from water to nitrogen in the steam generator secondary (a reduction in heat transfer from the steam generator to the blowdown fluid), and (d) having the 40-rod core installed rather than the core simulator.

This report provides an evaluation of the thermal-hydraulic response of the system relative to the common and specific objectives. A detailed discussion of the results is included only when the experimental data deviate significantly from the expected system behavior. Comparisons between experimental results and results calculated using the RELAP4[1] computer code are presented to aid in understanding the complex phenomena occurring during the LOCA. The RELAP4 model used in calculating the response during the Semiscale Mod-1 isothermal tests is discussed in Appendix A.

The isothermal test series consisted of eight blowdown tests, each of which simulated on offset shear of either the hot or cold leg. Each of the cold leg break configuration tests was conducted by establishing system fluid conditions at about 540°F and 2,250 psig, allowing the piping and various metal components to approach the fluid temperature, and simulating a rupture in the broken loop cold leg piping to cause the system fluid to flow out through the two rupture nozzles and into a pressure suppression tank. Each of the hot leg break configuration tests was conducted at 1,600 psig and 540°F with the rupture in the broken loop hot leg piping. The decompression, or blowdown process, lasted between 40 and 50 seconds depending on the type of break. All of the tests included emergency core coolant (ECC) injection during blowdown except Test S-01-2 which included ECC injection following blowdown (at 112 seconds after rupture). ECC was injected into one of the three principal locations: the intact loop cold leg, the downcomer distributor annulus, or the lower plenum. The prerupture conditions, test procedures, and uninterpreted results for the isothermal tests discussed in this report are provided in a series of system description and experiment data reports[2-8]. Companion reports are being prepared on the evaluation and interpretation of test results relating to specific topics[9-11].

II. EXPERIMENT DESCRIPTION

The Semiscale Mod-1 test apparatus, shown in Figures 1 and 2, was a high-pressure system having a water volume of approximately 8.5 ft^3. The system consisted of a pressure vessel with simulated reactor internals (downcomer, lower plenum, core region, and upper plenum); an intact loop with a steam generator, pump, and pressurizer; a broken loop with rupture diaphragm assemblies, simulated steam generator, and simulated pump; a pressure suppression system with suppression tank and header; and a simulated ECC injection system with accumulators and injection pumps. Detailed descriptions of the system components, including volumes and flow resistances, and of the measurement and data acquisition systems are contained in Reference 2.

The intact loop is a 1-30—volume scale model of three loops of a commercial PWR and consists of primary coolant piping, a steam generator, a pressurizer, and a circulating pump. The piping is primarily 3-inch Schedule 160 pipe. The steam generator is a tube-in-shell heat exchanger.

The blowdown loop is a volume-scaled representation of one loop of a four-loop PWR and consists of an inactive pump and steam generator simulators, two discharge nozzles, and two rupture assemblies which provide a simulated double-ended offset shear. The associated piping was primarily 2-inch Schedule 160 stainless steel. The simulated steam generator and simulated pump consist of piping with orifices to achieve the desired hydraulic resistances. The rupture assemblies contain a converging-diverging blowdown nozzle (to provide the desired break area) and two diaphragm rupture discs. The reflood bypass lines are incorporated to simulate, in terms of volume and location, the reflood bypass safety system used in LOFT.

The pressure suppression system consists of a 91.7-ft^3 pressure tank which is used to simulate the backpressure created by a containment building in a PWR system. The tank was maintained partially full of subcooled water, and a downcomer pipe projected below the water surface to accommodate the blowdown effluent. A 16-inch header connects the pressure suppression tank to the primary coolant system.

The ECC injection system includes three demineralized water injection subsystems: one compressed nitrogen-water accumulator subsystem and two pump subsystems. The ECC injection system interfaced with the vessel lower plenum, intact loop, and inlet distributor annulus.

The Semiscale Mod-1 isothermal tests discussed in this report consisted of two double-ended hot leg break configuration tests and six cold leg break configuration tests. Table I summarizes the test configurations.

Test S-01-1 was conducted with a 100% hot leg break with ECC injection into the inlet annulus. The initial pressure was 1,600 psig for this test. Test S-01-1B was identical to Test S-01-1 except ECC was injected into the cold leg of the intact loop. Test S-01-2 was

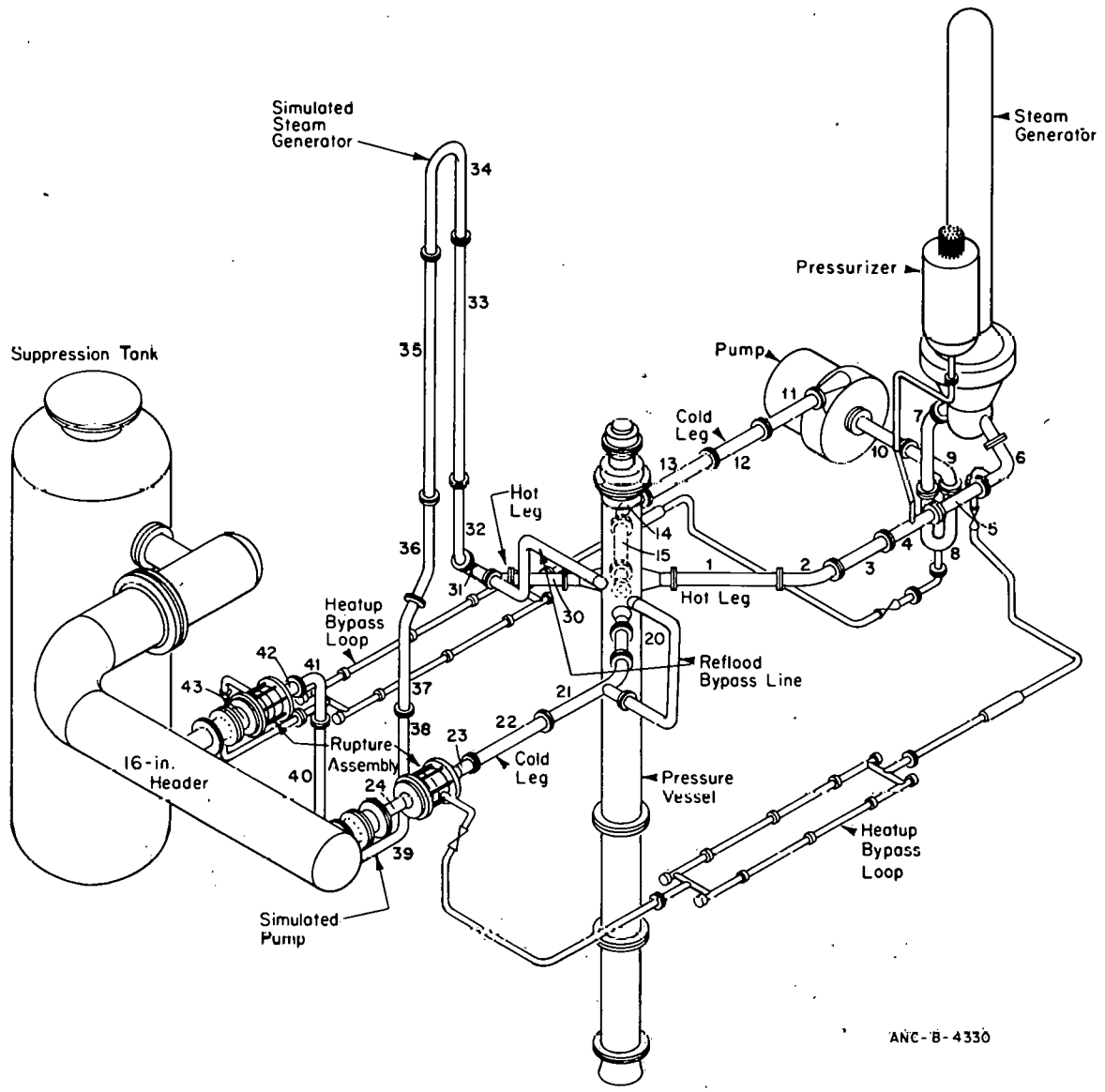

Fig. 1 Semiscale Mod-1 cold leg break configuration – isometric.

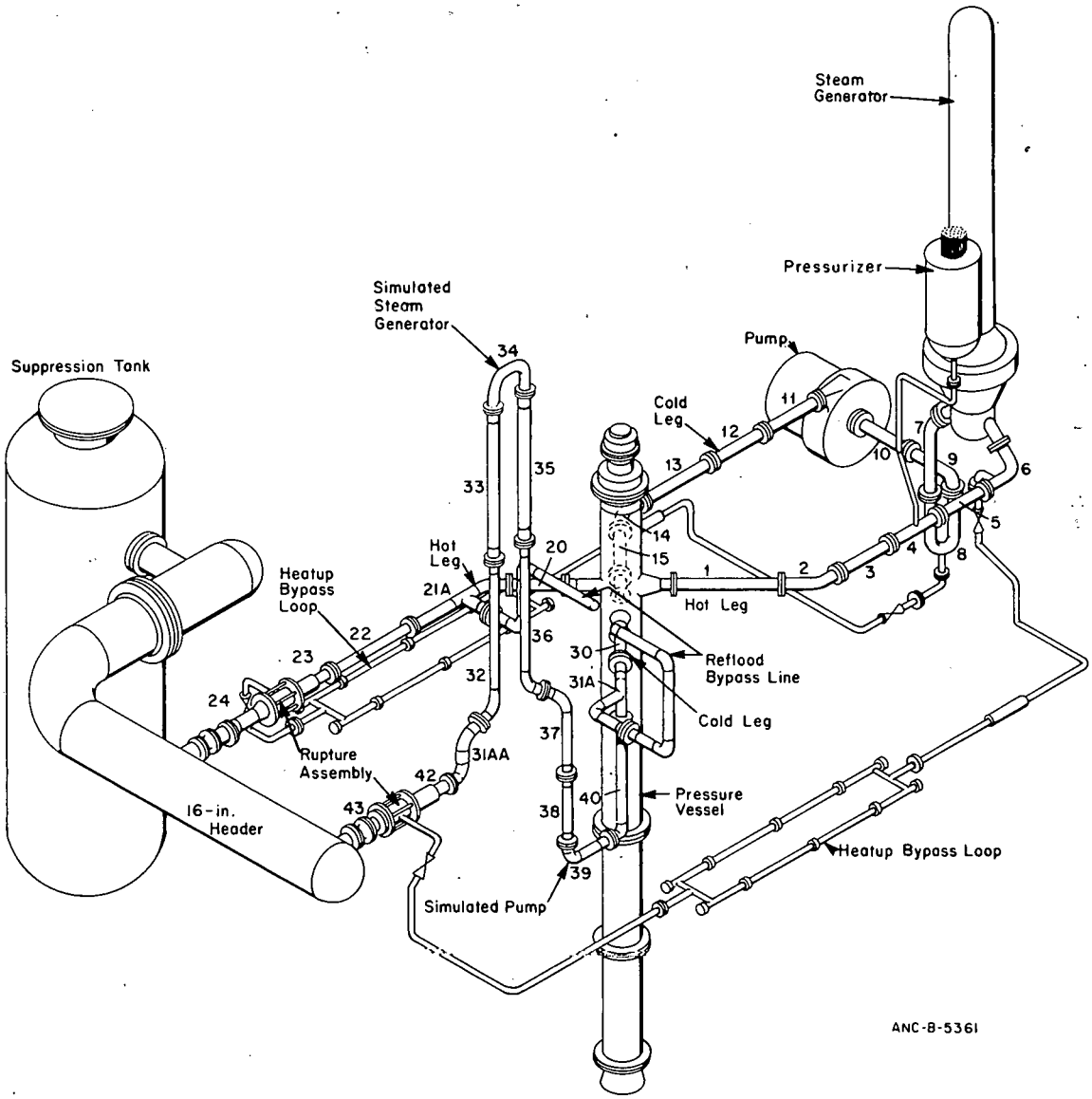

Fig. 2 Semiscale Mod-1 hot leg break configuration – isometric.

TABLE I

TEST DESCRIPTION OF ISOTHERMAL TEST SERIES

	Test							
	S-01-1	S-01-1B	S-01-2	S-01-3	S-01-4	S-01-4A[a]	S-01-5	S-01-6[b]
Break Size	100%[c]	100%	200%	200%	200%	200%	200%	200%
Break Type	Hot Leg	Hot Leg	Cold Leg	Cold Leg	Cold Leg	Cold Leg	Cold Leg	Cold Leg
Intact Loop Resistance	Low[d]	Low	High	Low	Low	Low	Low	Low
ECC Injection								
Location	Inlet[e] Annulus	Intact Loop Cold Leg	Intact Loop Cold Leg	Lower Plenum	Intact Loop Cold Leg	Intact Loop Cold Leg	Intact Loop Cold Leg	Intact Loop Cold Leg
Actuation Pressure or Time								
Accumulator	600 psig	600 psig	1112 sec after rupture)	600 psig	600 psig	600 psig	600 psig	600 psig
HPIS (High-Pressure Injection System)	at rupture	at rupture	---	35.5 sec after rupture	35.5 sec after rupture	35.5 sec after rupture	35.5 sec after rupture	35.5 sec after rupture
LPIS (Low-Pressure Injection System)	250 psig	250 psig	---	35.5 sec after rupture	35.5 sec after rupture	35.5 sec after rupture	35.5 sec after rupture	35.5 sec after rupture
Steam Generator Fluid (hot standby condition)	Steam-Water	Steam-Water	Steam-Water	Steam-Water	Steam-Water	Steam-Water	Nitrogen	Steam-Water

[a] Repeat of Test S-01-4 due to heatup line valve isolation failure during Test S-01-4.

[b] Repeat of Test S-01-4A except 40-heater-rod core installed instead of the core simulator.

[c] 100% break refers to a simulated failure in the broken loop with each break nozzle having an area of 0.00145 ft^2. 200% break refers to a simulated double-ended offset shear break in the broken loop with each break nozzle having an area of 0.00262 ft^2. The 200% break has a break area-to-system volume ratio equivalent to that ratio for a double-ended offset shear break in the cold leg of one loop of a four-loop pressurized water reactor.

[d] Low and high system resistance refers to the size of orifices located at the inlet and outlet of the intact loop steam generator. The high system resistance orifices have an approximate 1.35-inch-diameter hole and the low system resistance orifices have an approximate 1.6-inch-diameter hole.

[e] ECC injection configuration specified in Reference 2.

conducted with a 200% cold leg break with ECC injection only following blowdown. The intact loop flow resistance was high (volumetrically scaled) for this test and low (core area scaled) for the other tests of this test series. Test S-01-3 was conducted with a 200% cold leg break with ECC injection into the lower plenum. Test S-01-4 was conducted with a 200% cold leg break with ECC injection into the cold leg of the intact loop. Test S-01-4A was a repeat of Test S-01-4 due to the heater bypass lines blowing down into the primary system during Test S-01-4. Test S-01-5 duplicated Test S-01-4 with the exception that nitrogen was placed in the secondary side of the steam generator instead of steam and water, to determine the effect of the steam generator heat transfer on system response. Test S-01-6 was a repeat of Test S-01-4A except a 40-heater-rod core was installed instead of the core simulator. Tests S-01-2, S-01-3, S-01-4, S-01-4A, S-01-5, and S-01-6 were performed with the same initial conditions. The initial isothermal temperature was 540°F with the steam generator maintained in a hot standby condition. Initial system pressure was 2,250 psig.

The test sequence for the isothermal blowdown experiments was essentially the same for each blowdown: (a) the temperature and pressure of the fluid in the system were increased to their specified prerupture conditions, (b) fluid was circulated through the intact loop and vessel at approximately 17.3 lbm/sec, (c) a small bypass flow was circulated through the broken loop components to establish uniform conditions throughout the system, and (d) the water level on the secondary side of the steam generator was established. Once the initial conditions were established, the tests were initiated by breaking rupture discs in both the vessel inlet and vessel oulet sides of the broken loop. The flow rate was controlled by the phenomena occurring in the converging-diverging nozzles immediately upstream of the rupture discs in the broken loop.

III. RESULTS OF THE DATA ANALYSIS

The results of the data analysis are presented in two parts. Analyses related to phenomena which most strongly influence system behavior are discussed first. Included within this discussion are results from an investigation of: phenomena occurring at the breaks, intact loop pump performance, steam generator and piping heat transfer, broken loop pump and steam generator performance, repeatability of results, and pressurizer performance and hot leg fluid response. The behavior of the break flow is discussed in detail because of the strong influence of this phenomenon on the overall system performance and because the measured break flow was somewhat different than that predicted. The other subjects within this discussion are covered in somewhat less detail than the break flow phenomenon either because the observed test results agree well with calculated (expected) results or because the discussion represents a summary of a more detailed analysis presented in other topical reports on this test series.

The results of similar tests are compared in the second part of this section to evaluate the effect of changes in the system configuration. Included is an investigation of the effect on overall system response of: changing intact loop resistance (Tests S-01-2 and S-01-4A), changing break location and size (Tests S-01-1B and S-01-4A), reducing the amount of heat transferred from the steam generator secondary (Tests S-01-4 and S-01-5), and having the 40-heater-rod core installed instead of the core simulator (Tests S-01-6 and S-01-4A).

1. PHENOMENA WHICH STRONGLY INFLUENCE SYSTEM RESPONSE

Analyses of phenomena which strongly influence system response are presented in this section. Particular emphasis is placed on phenomena which affect core fluid response during blowdown.

Although all the isothermal tests were evaluated, the discussion has been limited to Tests S-01-4A and S-01-1B because these two tests produced typical results and provided the best quality data. The results of the other tests, which were conducted primarily to investigate specific parameters, are discussed when they deviate significantly from those observed during either Test S-01-4A or Test S-01-1B.

1.1 Break Flows

The phenomena occurring at the simulated breaks control the system depressurization rate and directly influence much of the phenomena occurring throughout the system. Initially, the fluid at the breaks is subcooled and the flow rates are high. When the pressure at the break falls to the saturation pressure of the fluid, choking at the break commences. Choking may occur at one break earlier (at the pump side of the break for a 200% cold leg break) than at the other and in so doing affect the system flow rates and directions. During saturated blowdown, the flow rates throughout the system are also affected by the conditions at the breaks competing with the conditions at the pump.

An accurate measurement of the flow properties at the break is thus necessary to properly interpret results at other places within the system. The measurements recorded at the breaks include fluid temperature, fluid pressure, fluid density, momentum flux, and differential pressure across the break assembly.

The break itself is simulated by a converging-diverging nozzle with the previously mentioned measurements located just upstream of the converging portion of the nozzle. Evaluation of these measurements and comparison of the Semiscale data with predictions obtained using various correlations provide a better understanding of the subcooled and saturated blowdown phenomena occurring at the breaks.

1.1.1. Subcooled Blowdown. The flow rate and duration of subcooled flow at the break nozzles is influenced by the pressure and the initial degree of subcooling at the break. After rupture, the break pressure dropped from the initial pressure (2,250 psig for the cold leg break) to the saturation pressure of 926 psia between 20 and 100 milliseconds depending on the side of the break considered. Since the pump and steam generator simulators have large hydraulic resistances, the pressure at the break downstream of the simulators (pump side) drops quickly to the saturation condition, whereas the pressure at the vessel side of the break drops more slowly. The subcooled blowdown pressure for Test S-01-4A is illustrated in Figure 3 which shows the pressure at the vessel side of the break dropping to the saturation pressure in 100 milliseconds, whereas the pressure at the pump side of the break dropped to the saturation pressure in 20 milliseconds. The flow rates at the break were large during the subcooled portion of blowdown due to the acceleration of the fluid. Figures 4 and 5 show the subcooled flow rates at the vessel and pump sides of the break for the 200% cold leg break configuration. The flow rate drops fairly rapidly when the fluid begins to decelerate measurably.

RELAP4 calculations have been used, in addition to the data, to investigate the subcooled portion of blowdown and its influences on system behavior. The subcooled critical break flow models used in RELAP4 to calculate the subcooled break flow rates were the Henry Model[12] and the momentum model[1]. The Henry critical flow model is based on a momentum balance, and the critical mass flux is obtained in tabular form as a function of stagnation pressure and enthalpy which are taken from the volume just upstream of the choking plane. Since the Henry model was originally developed for saturated blowdown, the tabular information is provided by an "extended" Henry table of values applicable to subcooled conditions. Once the mass flux is obtained, a contraction coefficient (multiplier) is used to account for the flow losses encountered in the fluid going through the converging-diverging nozzles at the break. The multiplier value of 0.6 was determined to be appropriate for the nozzle configuration used in the Semiscale system. The momentum model is based on the solution to the one-dimensional momentum equation in conjunction with the continuity equation. Figure 6 shows the subcooled blowdown pressure at the vessel side of the break for Test S-01-4A and includes RELAP4 calculations in which the two different subcooled break flow models were used.

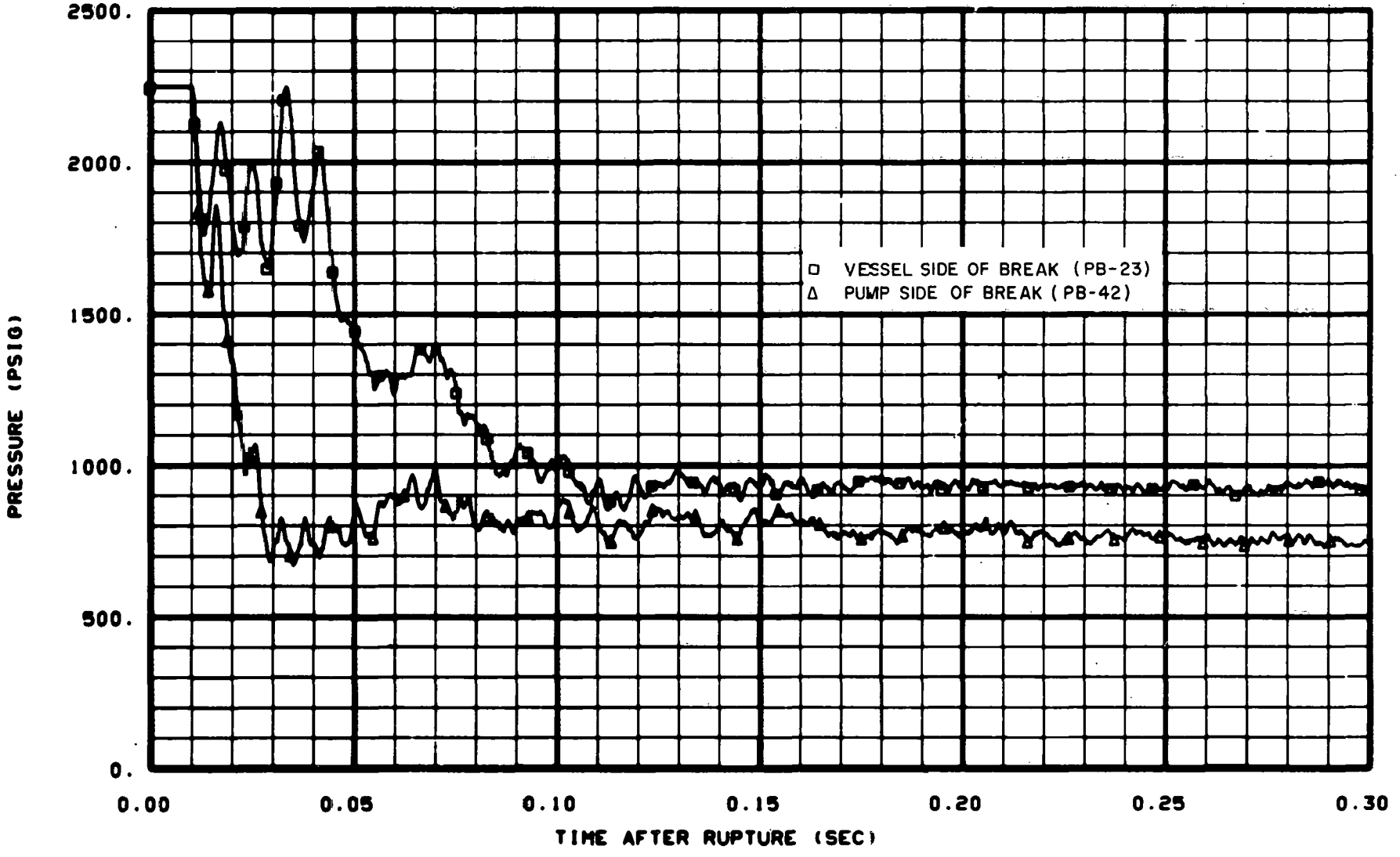

Fig. 3 Subcooled blowdown pressure at vessel and pump sides of break – Test S-01-4A.

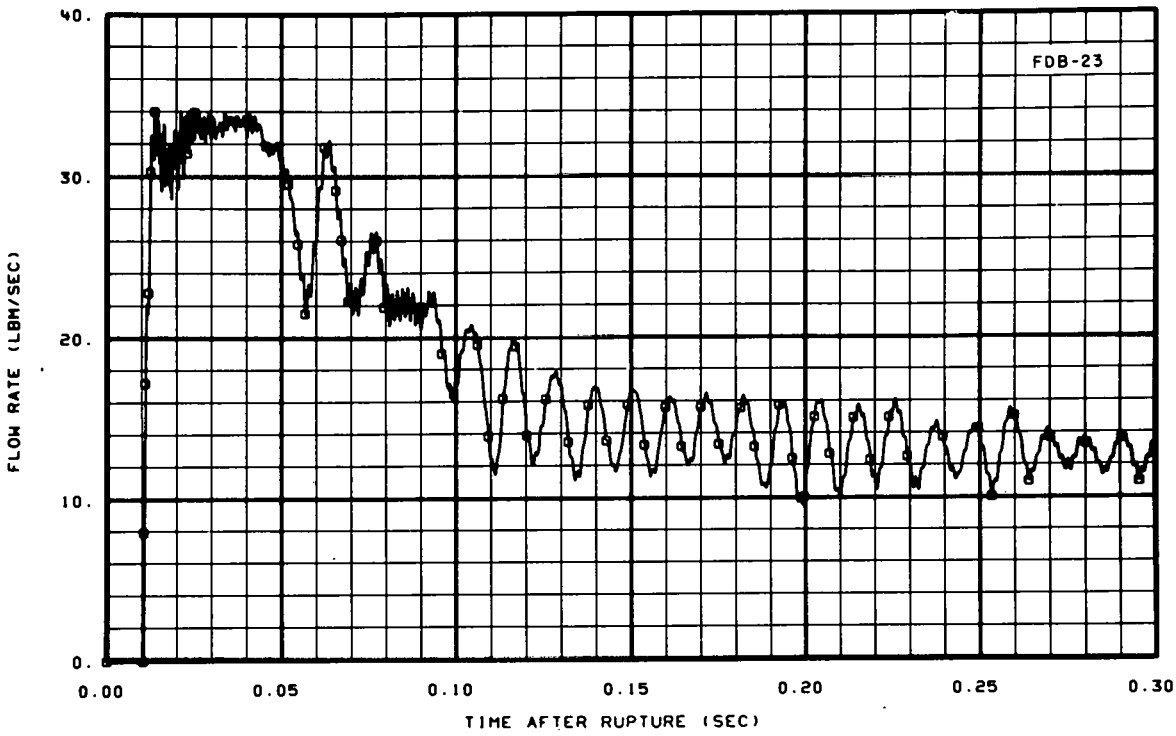

Fig. 4 Subcooled blowdown flow rate at vessel side of break – Test S-01-4A.

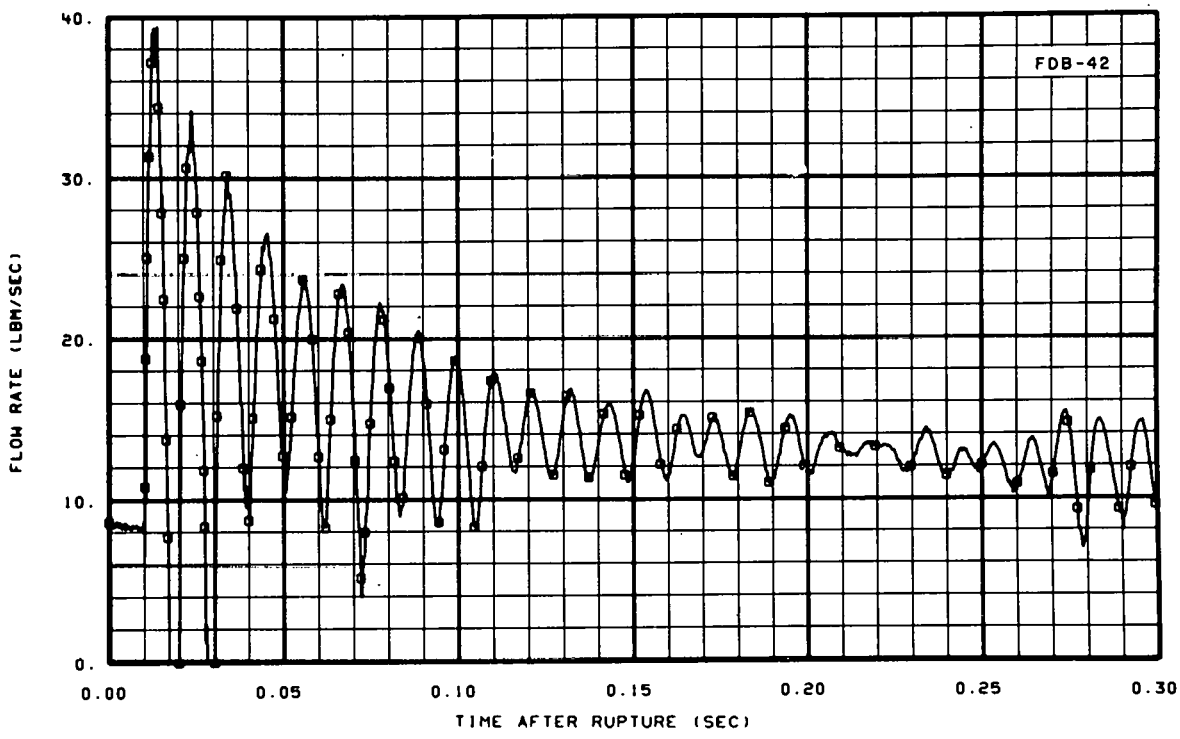

Fig. 5 Subcooled blowdown flow rate at pump side of break – Test S-01-4A.

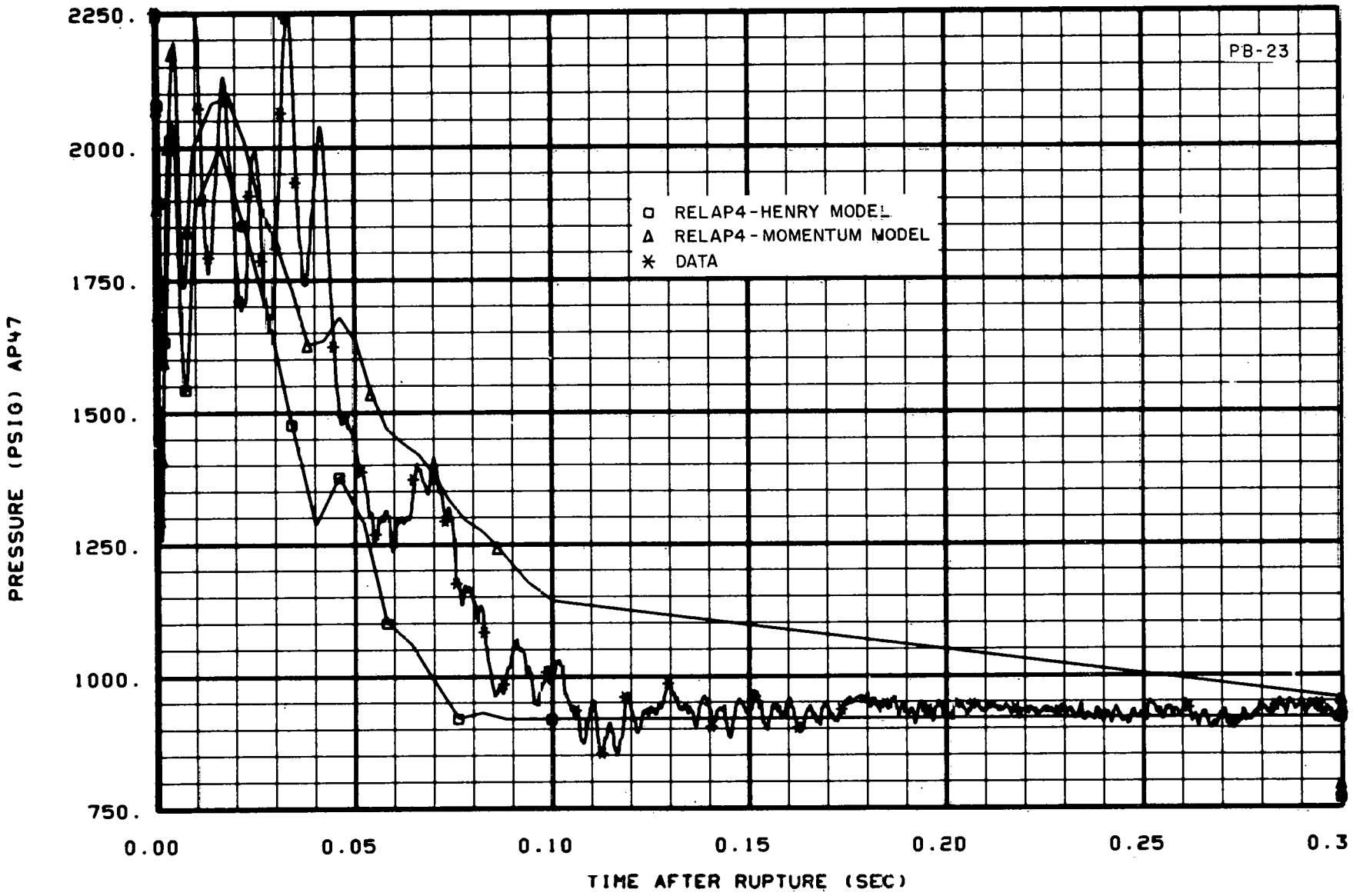

Fig. 6 Subcooled blowdown pressure – RELAP4 calculations for vessel side of break – Test S-01-4A.

The subcooled critical break flow model used in RELAP4 which most closely matched the data was the Henry model. Using the Henry model, RELAP4 calculates the pressure for the first 60 milliseconds of subcooled blowdown reasonably well. The momentum model, however, overpredicted the pressure, causing a slightly lower depressurization rate and a higher calculated flow rate than existed with the data. Figure 7 shows that the results of the flow rate obtained utilizing the Henry model more closely match the physical phenomena occurring at the break, than those obtained through use of the momentum model. A more nearly accurate determination of the density, resulting from a closer evaluation of the depressurization rate, accounts for the fact that the Henry model calculates values closer to the data than does the momentum model.

Calculations from the two RELAP4 models also aid in determining the influence of subcooled break flow on system response. The influence that the subcooled critical break flow had on system response is observed within the core region. Figure 8 compares the RELAP4 calculated core flow rates obtained through use of the previously mentioned break flow models with the data for Test S-01-4A. The momentum model predicts an extended period of subcooled flow and results in negative flow through the core during the subcooled blowdown, whereas the Henry model predicts a shorter period of subcooled flow and results in positive flow during the same time interval. The measured flow was positive. The core fluid behavior is therefore very sensitive to the critical break flow model used during subcooled blowdown, indicating the fluid conditions at the break strongly influence the core fluid behavior during subcooled blowdown.

1.1.2 Saturated Blowdown. The saturated blowdown flow rate is influenced by the pressure and fluid density at the break nozzles. The large initial change in the depressurization rate shown in Figure 9 and the corresponding large reduction in flow rate shown in Figure 10 indicate the change from subcooled to saturated flow. The slower depressurization rate for saturated blowdown (Figure 9) is due to smaller flow rates out the break and the degree of fluid flashing within the system. As was the case during the subcooled blowdown, the resistance in the simulators cause flow differences between the two break locations. The saturated blowdown history at the break indicates that 65% of the fluid leaving the system left the vessel side of the break for the 200% cold leg break configuration (35% flowed from the pump side of the break). The lower flow restrictive path out the vessel side of the break, as compared with that out the pump side, accounts for the difference in the percentage of the fluid out each break. In the hot leg break (100%) configuration, about 50% of the fluid leaving the system went out each side of the break. The difference in the relative distribution of flow out the breaks for the hot and cold leg break configurations is attributed to differences in the hydraulic resistance of the paths the flow takes to get to the break.

RELAP4 calculations have also been used to investigate the saturated portion of blowdown to aid in understanding the influence of the break on system fluid behavior. The saturated critical break flow models used in RELAP4 to calculate the saturated break flow rates were the Moody critical flow model[13] and the sonic model[1]. The Moody critical flow model is based on an energy balance using the first law of thermodynamics and takes

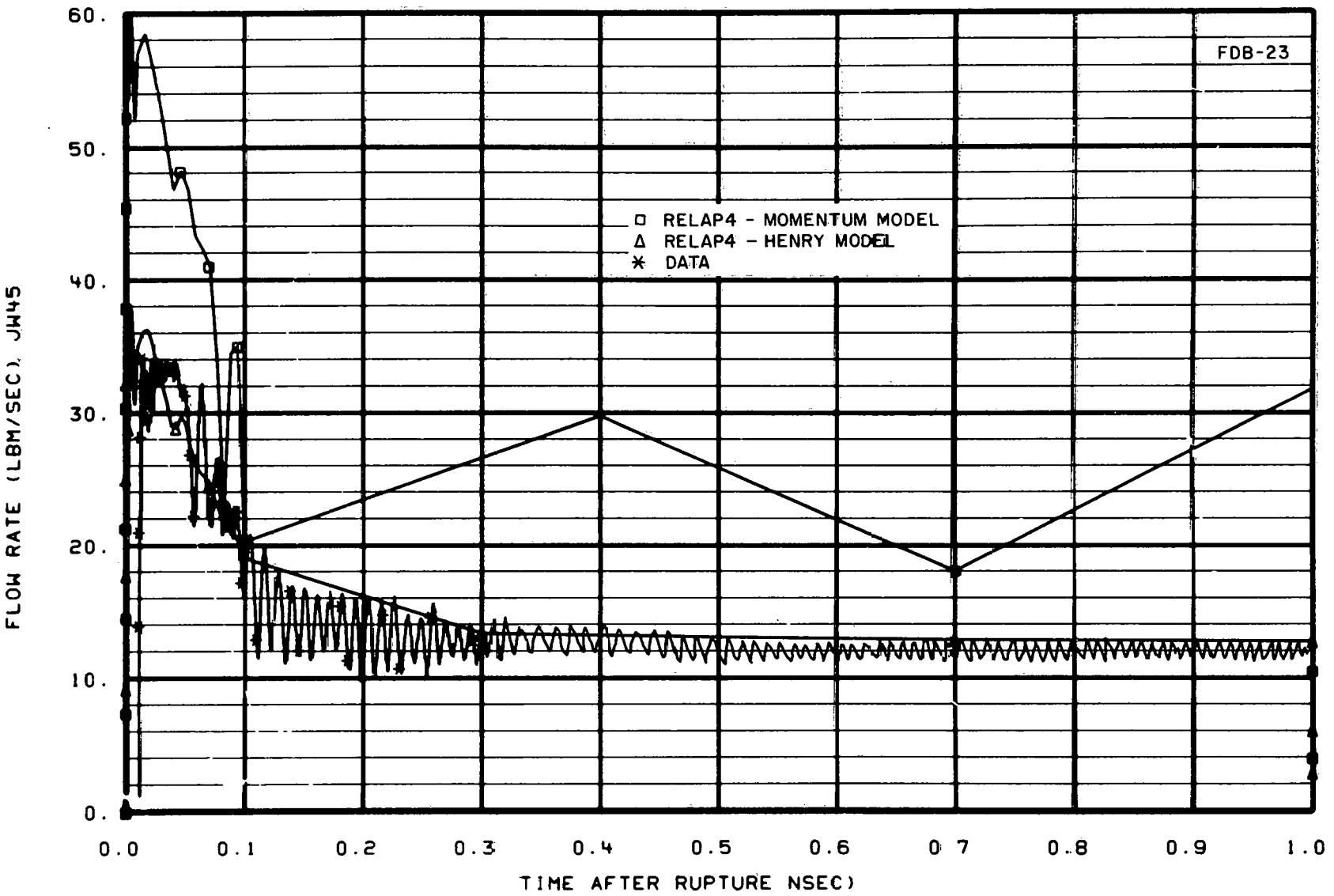

Fig. 7 Subcooled blowdown flow rate -- RELAP4 calculations for vessel side of break -- Test S-01-4A.

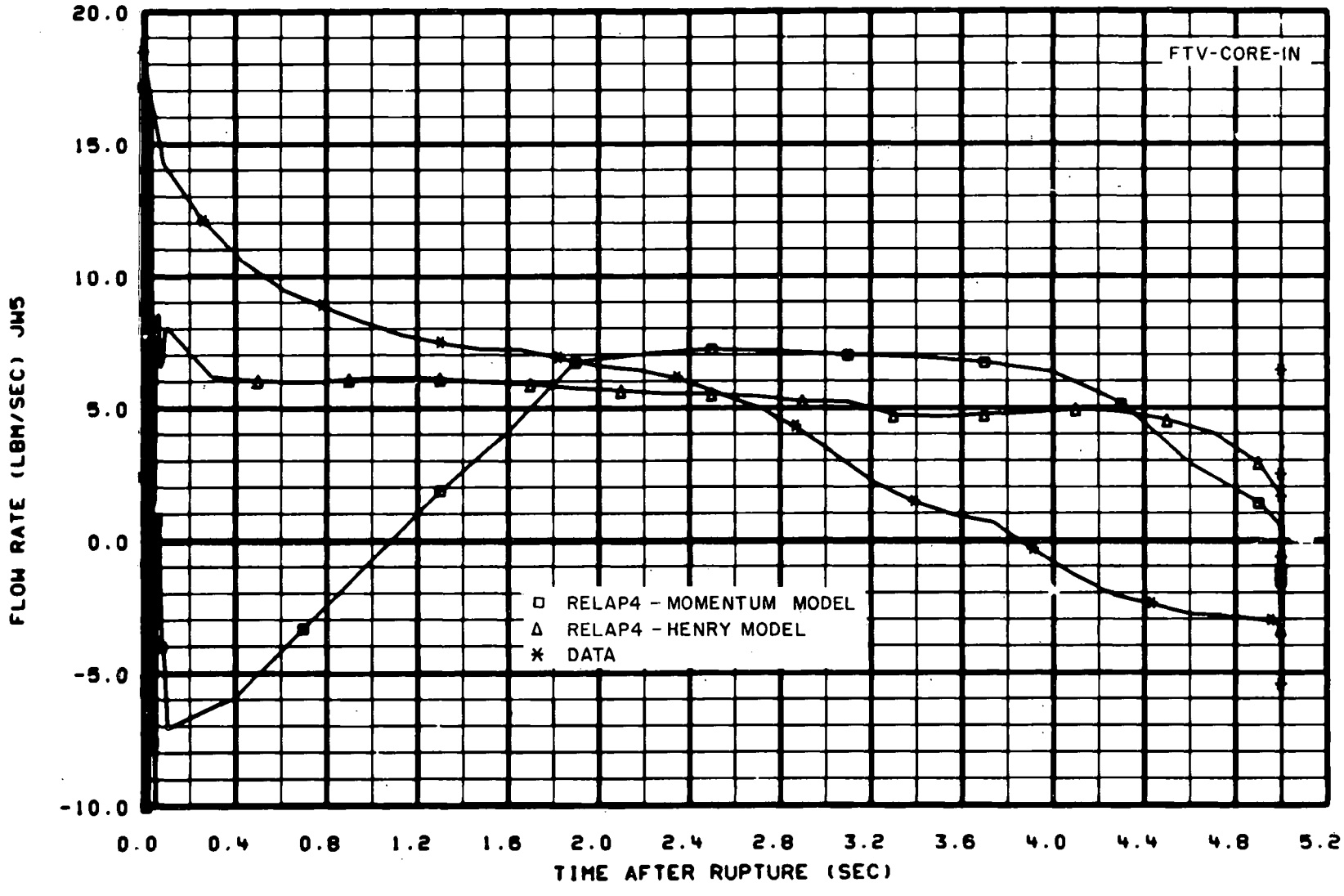

Fig. 8 Subcooled blowdown core flow rate – RELAP4 calculations for Test S-01-4A.

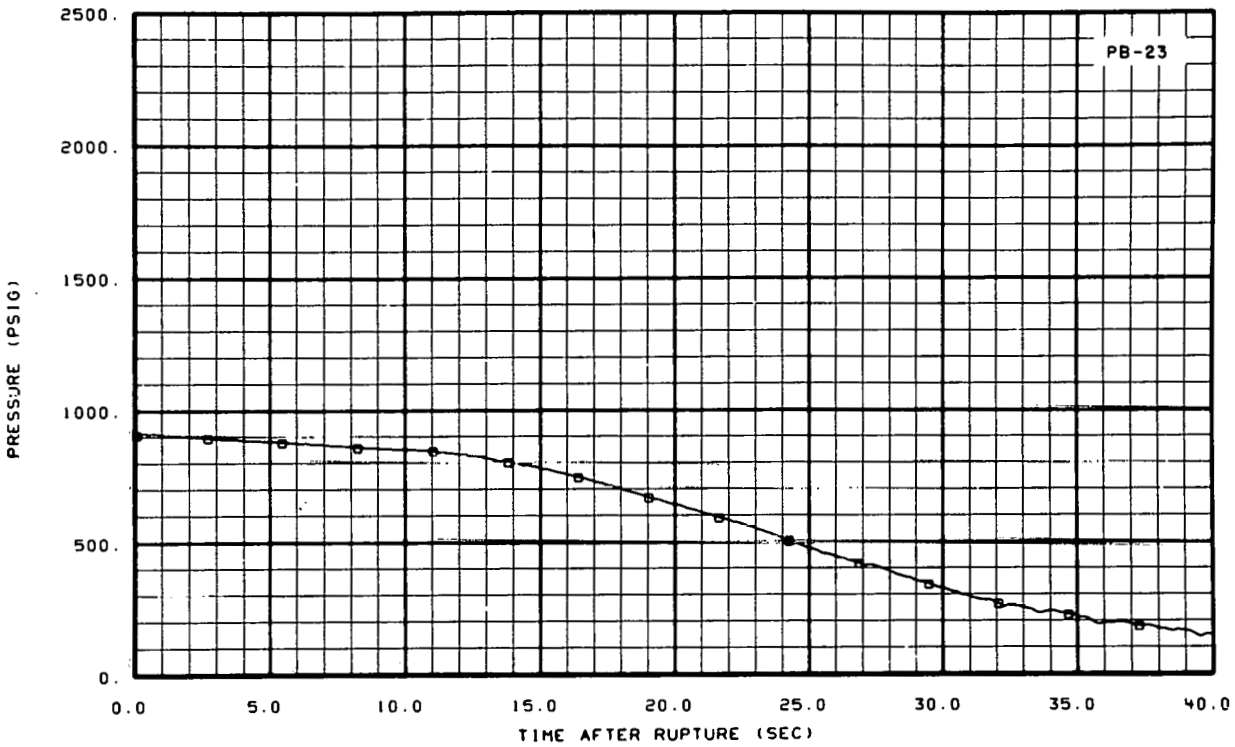

Fig. 9 Saturated blowdown pressure at vessel side of break – Test S-01-4A.

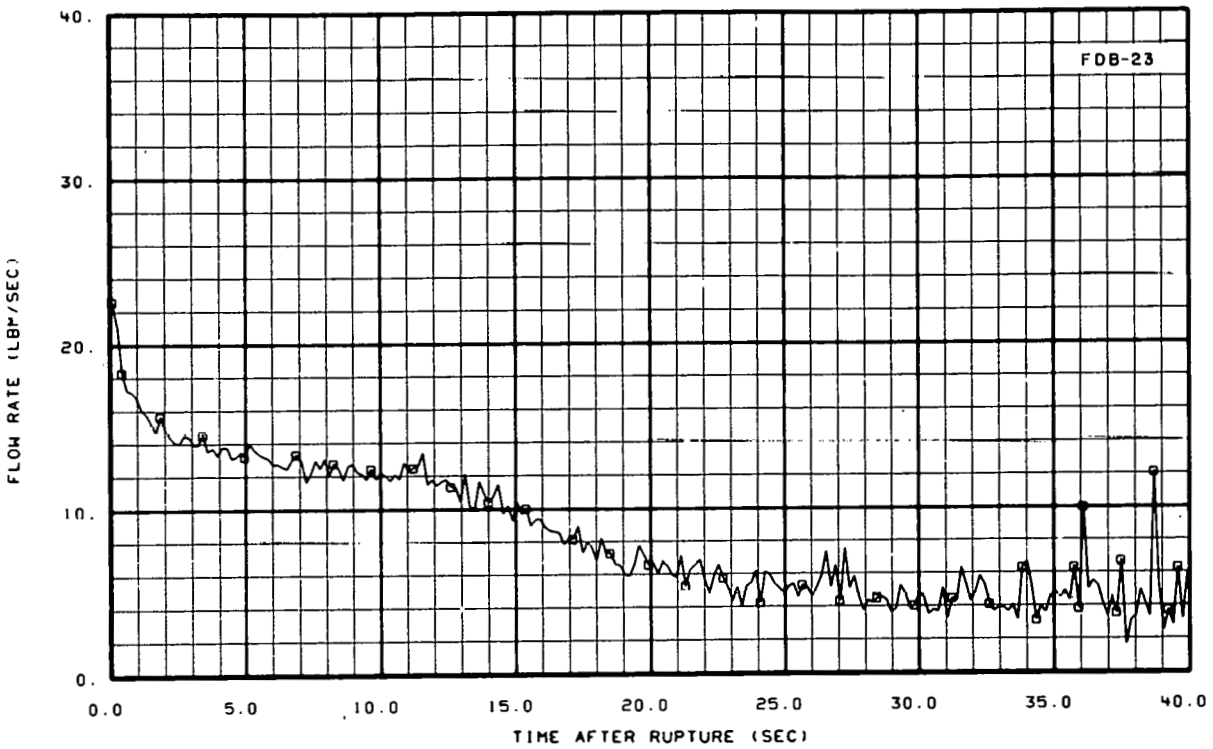

Fig. 10 Saturated blowdown flow rate at vessel side of break – Test S-01-4A.

into account slip within the two-phase mixture in calculating the break flow rate. The critical mass flux is obtained in tabular form as a function of stagnation pressure and enthalpy which are taken from the volume just upstream of the choking plane. The sonic critical flow model in RELAP4 calculates the sonic velocity at the break by means of the steam tables assuming homogeneous flow, using the specific volume and internal energy of the volume just upstream of the choking plane. Once the sonic velocity is determined, the mass flux is calculated through knowledge of the geometry at the choking plane. The principal difference between Moody's approach and the sonic velocity approach is that Moody's work takes into account slip at the break, whereas the sonic approach does not take slip into account.

RELAP4 calculations obtained using the Moody and sonic models, shown in Figure 11, are in general agreement with the data. Both RELAP4 calculations of the system pressure were higher than the data for the first 15 seconds of blowdown. The higher RELAP4 pressure resulted in higher calculated flow rates out the vessel side of the break as shown in Figure 12. In Figure 12 the use of the Moody critical flow model in RELAP4 (using an 0.6 contraction coefficient) resulted in considerable overprediction of the flow rate at the vessel side of the break during saturated blowdown, whereas the sonic model appears to predict the saturated blowdown fairly well. The fact that the sonic value more closely matches the Semiscale Mod-1 isothermal tests series experimental data implies that the fluid is homogeneous as it passes through the break nozzles. In fact, this implication is supported by the experimental configuration. The drag disc used to measure the momentum flux at the break has a target which is 0.406 inch in diameter and which is centered in a pipe 1.338 inches in diameter. The target is positioned just 1 inch upstream of the converging section of the break nozzles, and is thus just upstream of the choking plane. The target is thought to have disturbed the flow immediately upstream of the choking plane and to have caused homogenization of the flow at the throat of the break nozzle.

The break flow rates for the 100% hot leg break tests were also studied to determine the effect of the break size and configuration on break flow response during saturated blowdown. Because of the smaller break size (and hence lower depressurization rate) used for the hot leg break configuration, the fluid flow was not homogenized as for the larger 200% break tests and resulted in more flow "bubble separation". A slip model was therefore incorporated into the RELAP4 code for the parts of the system vertically oriented to account for the additional bubble rise phenomena. Figure 13 shows the flow from the vessel side of the break for Test S-01-1B and compares the experimental flow with that calculated by RELAP4 with and without the slip model included. The Henry and Moody critical break flow models with a 0.6 break flow multiplier were used for the subcooled and saturated portions of blowdown, respectively. The break flows in the hot leg break configuration for Tests S-01-1 and S-01-1B were underpredicted from 6 to 30 seconds. The RELAP4 calculation with slip appears to follow the data better. Although the slip model was not applied to horizontal piping and therefore did not calculate slip in the piping directly upstream of the simulated break nozzle, the calculation of density in vertical regions

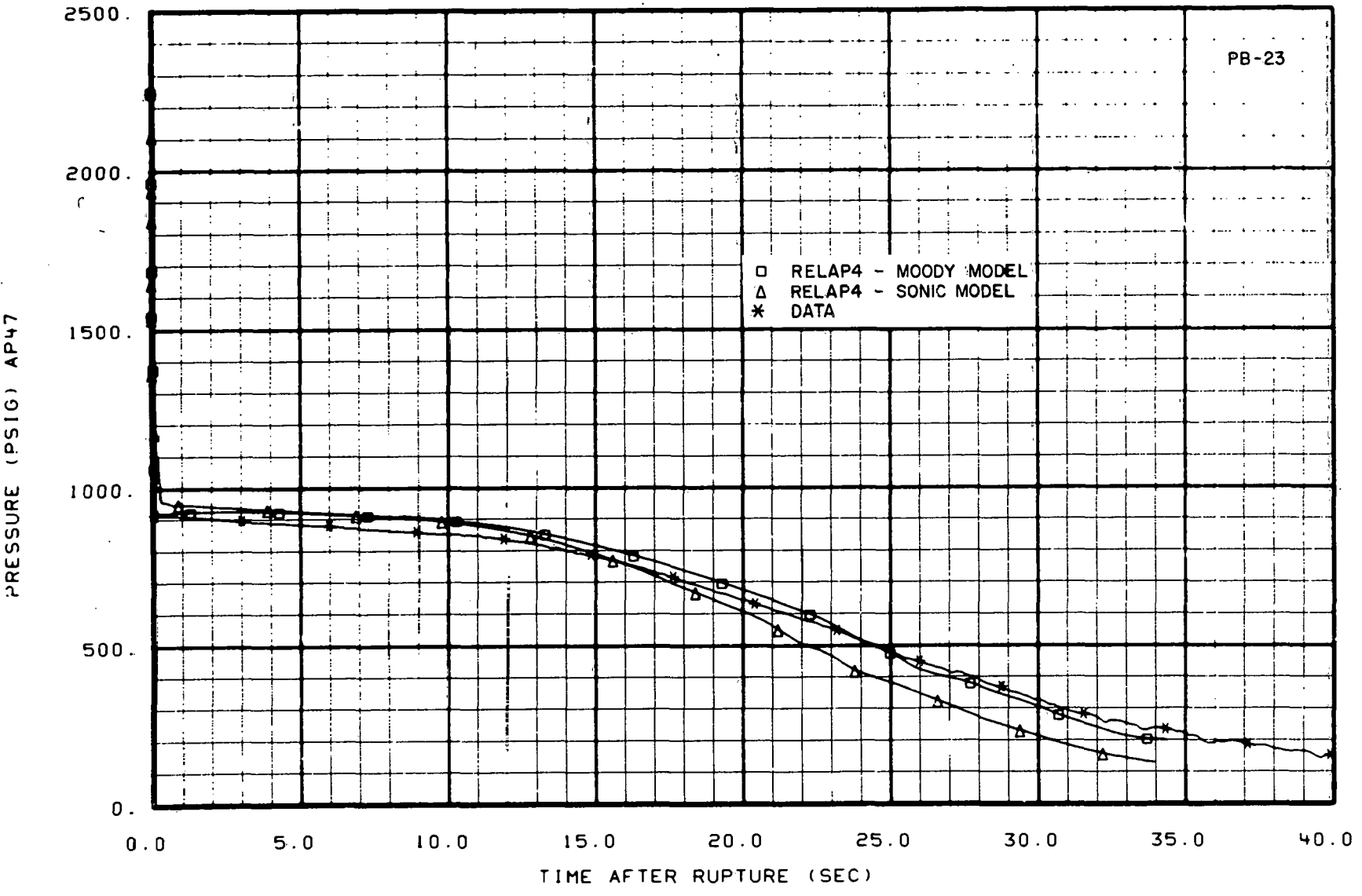

Fig. 11 Comparison of experimental and calculated saturated blowdown pressures at vessel side of break – Test S-01-4A.

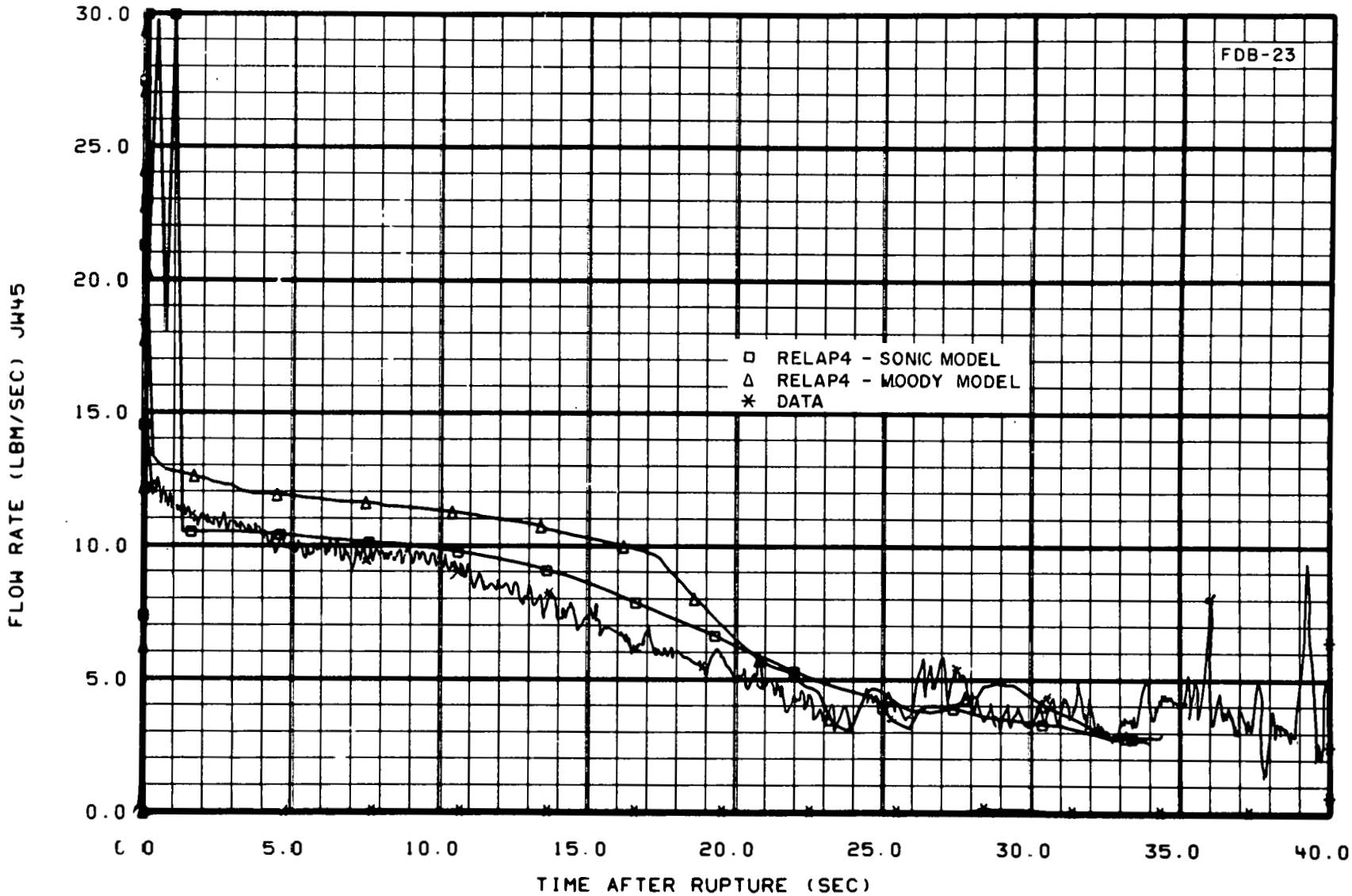

Fig. 12 Comparison of experimental and calculated saturated blowdown flow rates at vessel side of break – Test S-01-4A.

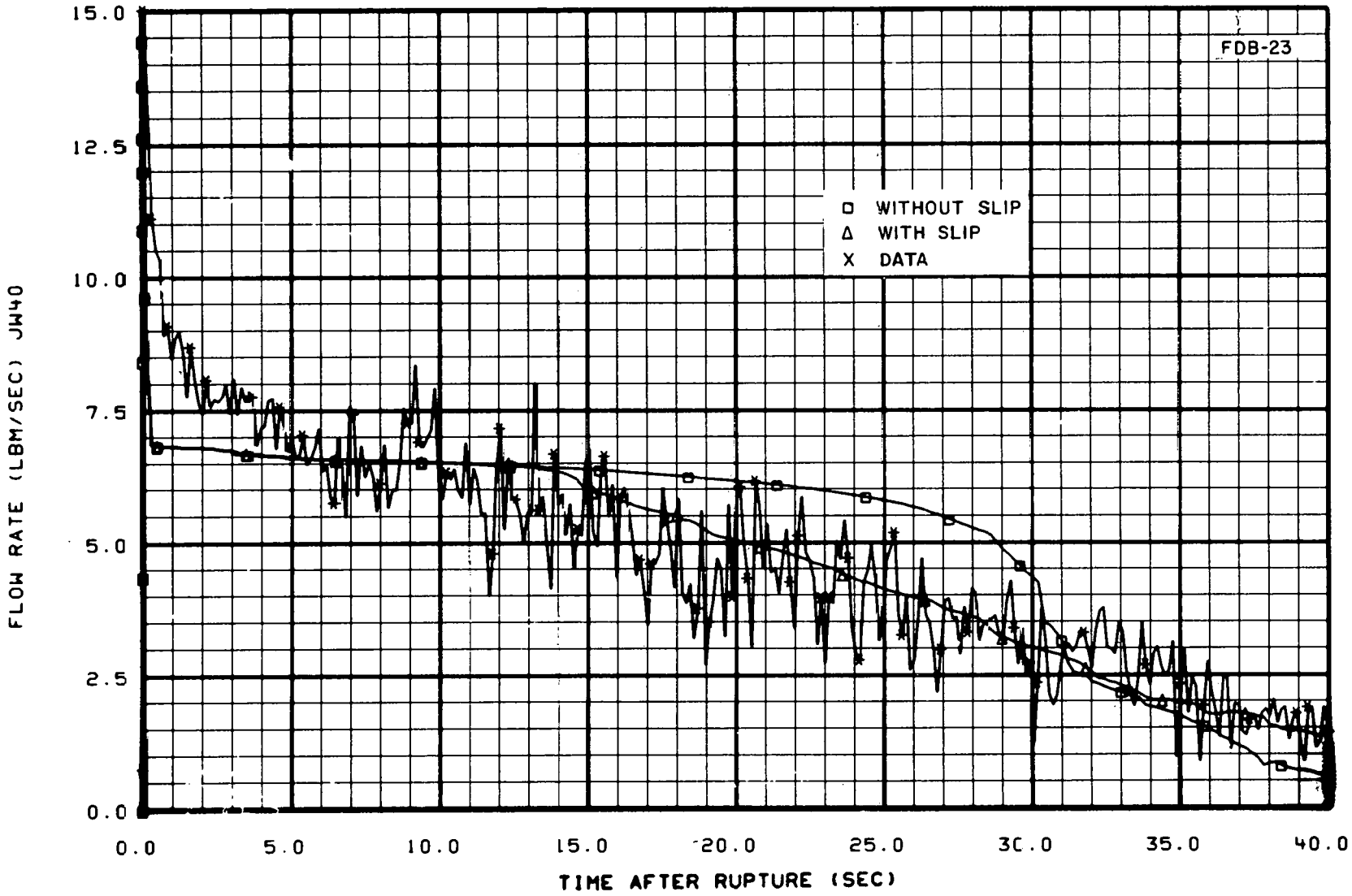

Fig. 13 Flow rate at vessel side of break – comparison of calculations with and without slip (Test S-01-1B).

improves in RELAP4, thus improving the density calculation of the fluid coming into the pipe leading to the break[a].

The principal difference in flows from the vessel side of the break for the 100% hot leg versus the 200% cold leg break is shown in Figure 14. As expected, the smaller break test exhibited a lower flow rate during the blowdown process until about 45 seconds at which time a negative flow occurred in Test S-01-4A. The back flow (reverse flow) through the vessel side of the break lasted from 45 to 62 seconds after rupture. For several tests with ECC injected into the cold leg of the intact loop (Tests S-01-4, S-01-4A, and S-01-5), the large amounts of condensation taking place in the broken loop cold leg and inlet annulus caused the pressure to be lower than that existing within the pressure suppression tank. Condensation resulted from the ECC passing from the intact loop cold leg into the inlet annulus and bypassing directly to the broken loop cold leg rather than proceeding down the downcomer. The downcomer and intact loop cold leg vessel inlet instrumentation shows very little reverse flow during this time, indicating that the reverse flow of fluid through the vessel side of the break is principally condensed within the inlet annulus.

The principal influence of the break fluid conditions on system response during saturated blowdown occurs within the core region. Knowledge of core fluid properties during blowdown is important to blowdown analysis in that high core flow rates and low fluid qualities result in high energy removal from the core.

The general response of the core flow for saturated blowdown during several of the 200% cold leg break isothermal tests is shown in Figure 15. The core flow data from the 200% cold leg break tests (with the exception of those from Test S-01-2 which had a high intact loop flow resistance) are negative by 5 seconds after rupture and flow stagnation occurs at about 15 seconds and is followed by a further negative flow until the end of blowdown. The core flow direction during blowdown was influenced by the conditions at the breaks. Although this influence cannot be shown directly from the data, a study of RELAP4 calculations aids in an understanding of the influence of the break conditions on core flow. The RELAP4 calculation using the sonic critical break flow model indicated, as shown in Figure 16, negative flow through the core early in time (less than 1 second). However, the data in Figures 15 and 16 show the flow to be positive for the same time interval, with negative flow not evident until after 4 seconds. The RELAP4 calculation obtained through use of the Henry and Moody critical break flow models for subcooled and saturated blowdown, respectively, not only gave the desired positive flow during saturated blowdown but fairly closely matched the test data. The results presented in Figure 16 show that the calculation of core flow is very sensitive to the critical break flow model used in RELAP4, which implies that the break conditions have significant influence on core fluid behavior.

---

[a] The slip model was also tried in a 200% cold leg break RELAP4 calculation, but a similar improvement in the density calculation was not observed for the large break, indicating that the more rapid depressurization and the larger flow rates resulted in a generally more homogeneous fluid in the broken legs.

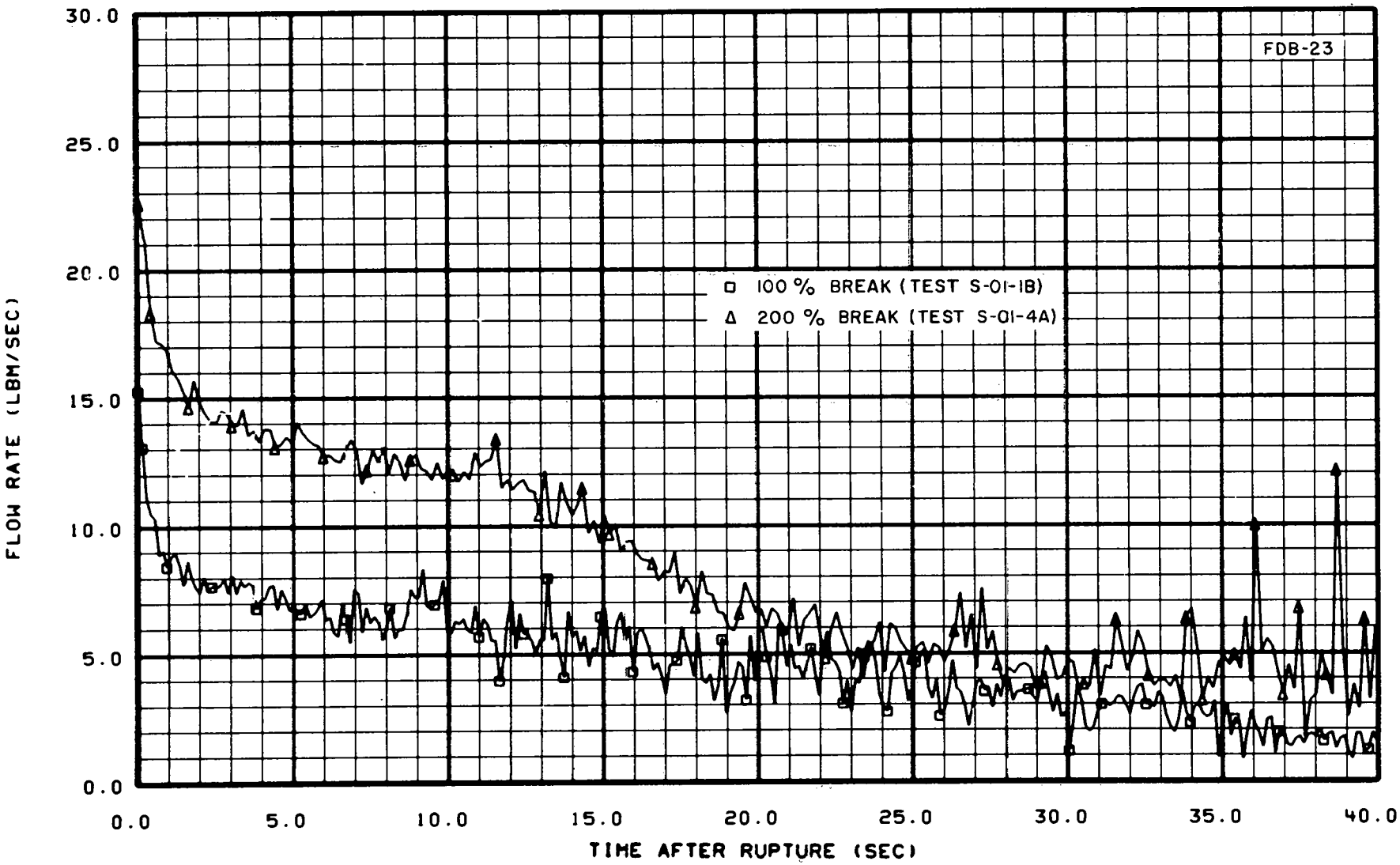

Fig. 14 Flow rate at vessel side of break – comparision of results of 100% break (Test S-01-1B) and of 200% break (Test S-01-4A)

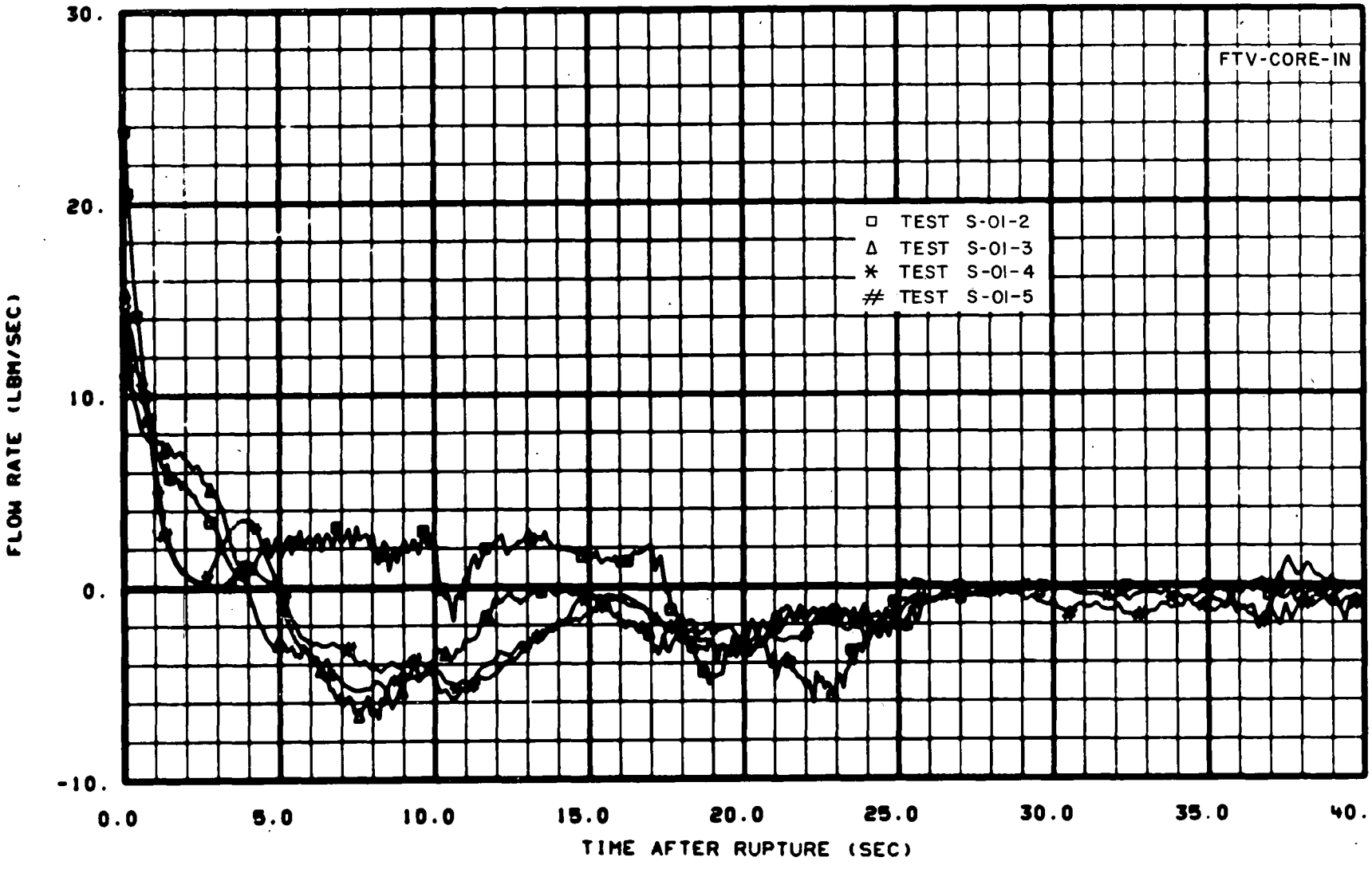

Fig. 15 Flow rate at entrance to core – Test S-01-2, S-01-3, S-01-4, and S-01-5.

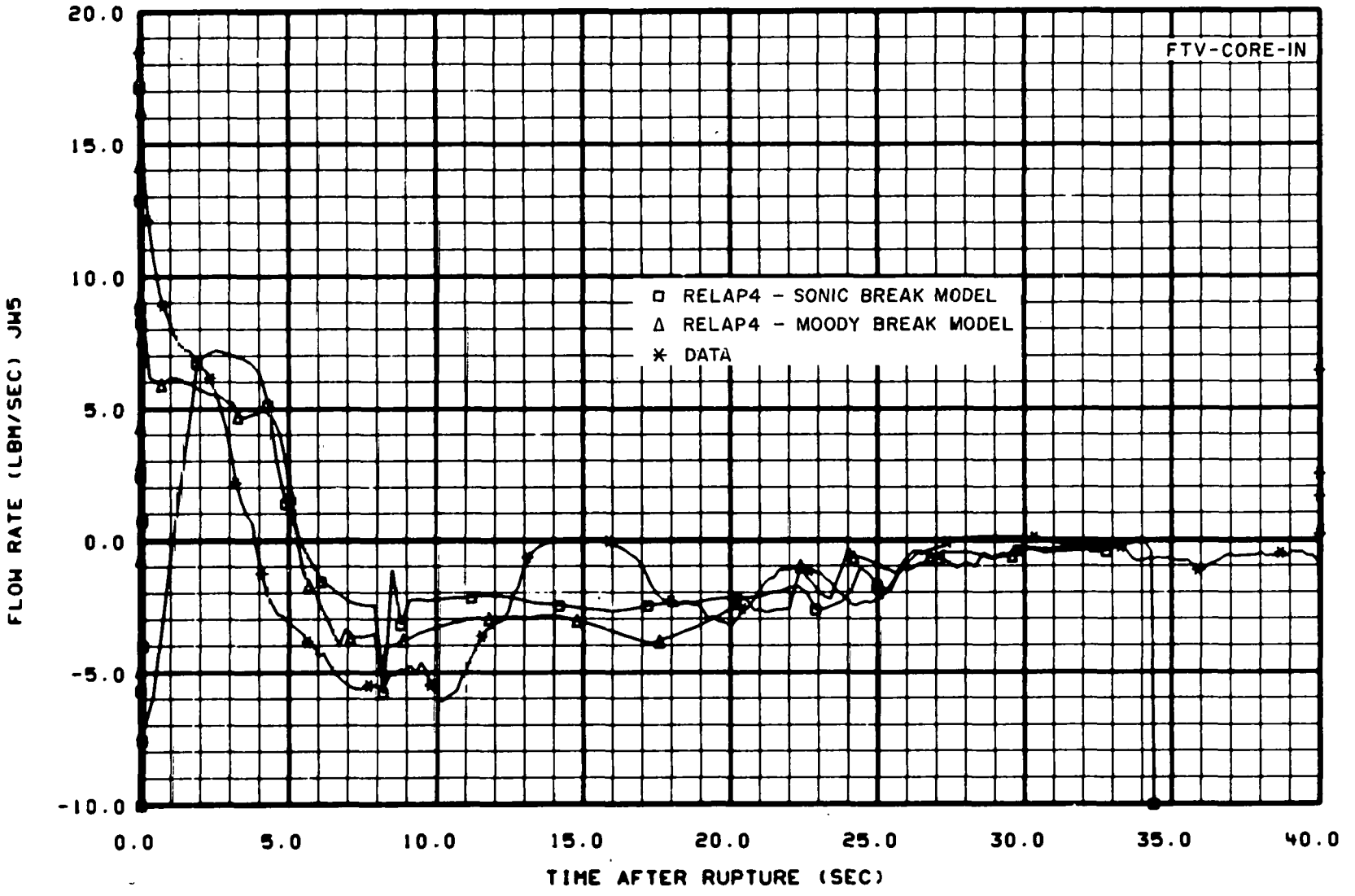

Fig. 16 Flow rate at entrance to core – comparison of RELAP4 results with test S-01-4A data.

The influence of the break conditions on core flow was also studied for the hot leg break configuration. The core fluid flow direction for the 100% small break was positive for the entire blowdown period as shown in Figure 17. The fact that relative to the 200% break tests, Test S-01-1B employed a hot leg break configuration with a smaller break size resulted in break conditions which caused a slower discharge rate from the downcomer through the broken loop cold leg which in turn resulted in a higher pressure in the downcomer region than in the core. In addition to the break influencing core behavior, the pump also aided significantly in causing the continued positive flow through the core. Furthermore, the resistive path from the core through the vessel side of the break was much smaller than that which existed for the cold leg break tests, allowing a strong positive flow through the core during the early stages of blowdown.

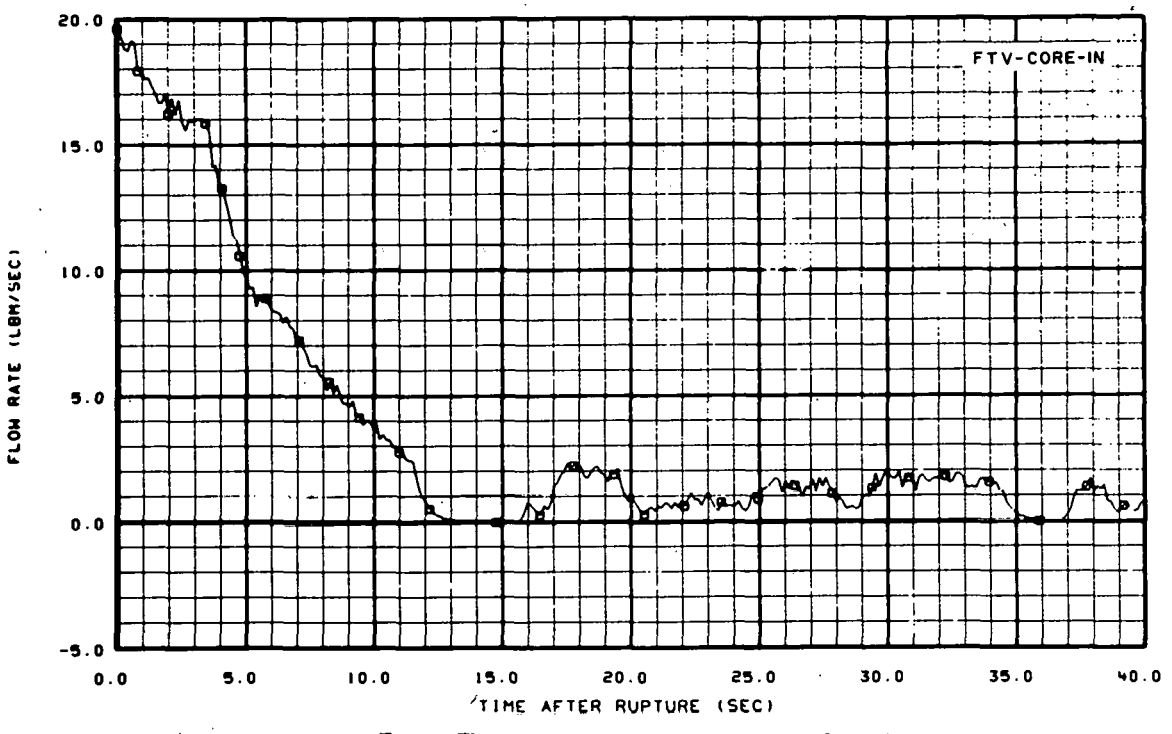

Fig. 17 Flow rate at entrance to core – Test S-01-1B.

1.1.3 Break Flow Summary. Analysis of the phenomena occurring at the simulated breaks lead to the conclusion that the break fluid conditions control the depressurization rate and directly influence the core fluid response during blowdown.

The core fluid behavior is very sensitive to the critical break flow model used during subcooled blowdown, indicating that the fluid conditions at the break strongly influence the core fluid behavior during subcooled blowdown. A more nearly accurate determination of the fluid density at the breaks, resulting from a closer evaluation of the depressurization rate, accounts for the fact that the Henry subcooled critical flow model calculates values closer to the data than does the other models used.

The saturated fluid flow at the breaks was determined to be homogeneous as it passed through the break nozzles, accounting for the fact that the RELAP4 sonic critical break flow model most closely matched the data for saturated blowdown.

1.2 Pump Phenomena

A thorough discussion of the pump performance data is included in Reference 10. This section summarizes the results of that analysis with respect to the effect of the pump on system fluid response.

During a simulated LOCA, the head generated by the intact loop pump affects loop and vessel flow directions and flow rates early in the blowdown. However, the capability of the pump to force fluid around the intact loop and core in the prerupture flow direction declines as blowdown progresses, principally due to the increasing influence of flow rates at the breaks and to the degradation of the pump head which results from the increasing void fraction at the pump inlet. Therefore, an understanding of the pump performance is necessary in an analysis of the core fluid behavior. Although the fluid phenomena occurring in and around the pump for the isothermal test series may not be typical of the pump fluid phenomena in a test in which a temperature difference exists across the core, an analysis of the pump performance for the isothermal tests is useful for comparing the transient behavior of the pump with steady state pump data taken during earlier tests. In addition, the pump performance data for this test series provide a data base for checking the pump models used in the analytical codes.

An example of the influence of the pump on system response early in blowdown is shown in Figure 18, which compares the flow rate through the core for Test S-01-1 with the pump inlet flow rate. The trend in flow occurring at the pump inlet at about 2 seconds in Figure 18 is shown to be reflected shortly thereafter within the core, indicating that the occurrences at the pump strongly affect phenomena at other locations within the system.

The influence of the pump on the system from about 5 seconds throughout the rest of blowdown is very limited partially due to the degraded pump head and partially due to the influence of the break flows on the system response.

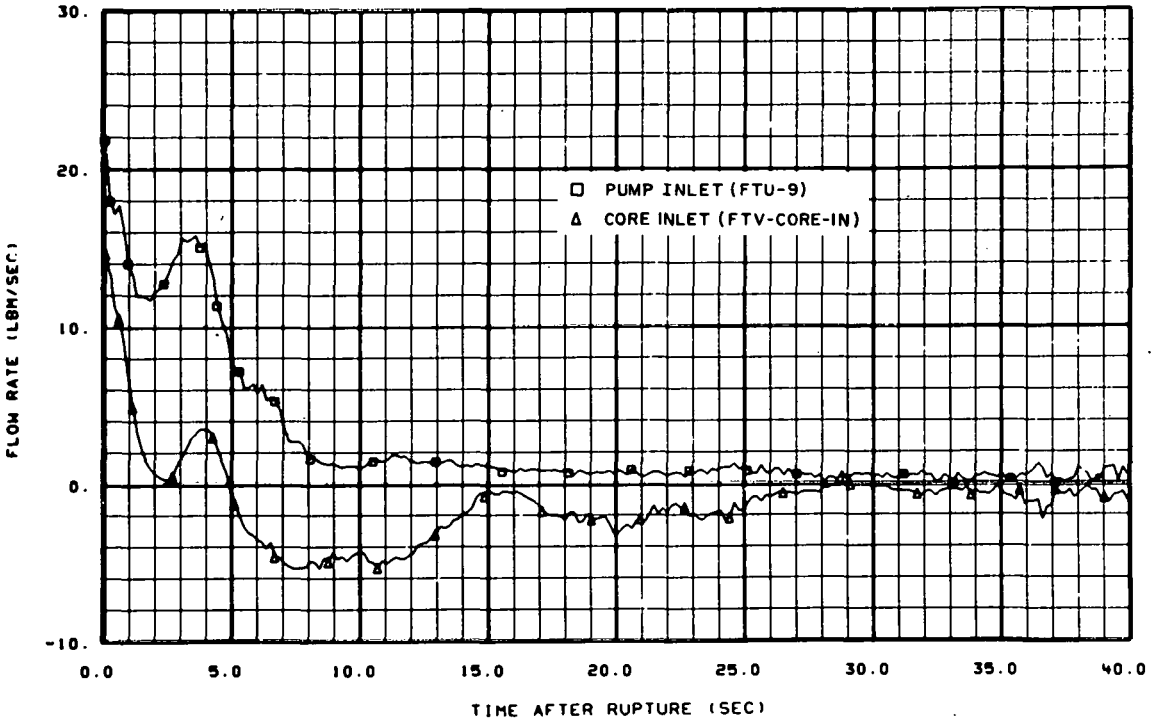

Fig. 18 Core flow rate versus pump inlet flow rate – Test S-01-4A.

Pump performance data from the Semiscale Mod-1 isothermal test series were analyzed and compared with previous pump performance data. The previous tests included single- and two-phase steady state testing[15,16] on the Semiscale Mod-1 pump and a test from the Semiscale 1-1/2-loop isothermal blowdown test series (Test 1010)[14].

Comparison of the Mod-1 isothermal series pump performance data with data obtained on the same pump during steady state two-phase pump tests indicates that more pump head degradation occurred during the Mod-1 series tests than during the steady state tests. Also, the initial operating point for Mod-1 data does not agree with the single-phase homologous head curves which were developed during the steady state testing.

The pump model for the Semiscale Mod-1 system contained in the RELAP4 code appears to predict the trends of the data reasonably well, as indicated in Figure 19, although the magnitudes were poorly predicted early in the blowdown period.

In summary, analysis of data and the RELAP4 pump model leads to the conclusion that the intact loop pump has major influence on system response for the first several seconds of blowdown. On the basis of comparisons with previous pump data, the two-phase pump head degradation is greater in the Mod-1 system than experienced in the previous test system. In addition, the data from the Mod-1 isothermal tests do not fit the homologous pump curves as well as expected. The RELAP4 code calculates the trends of the data well but not the magnitudes.

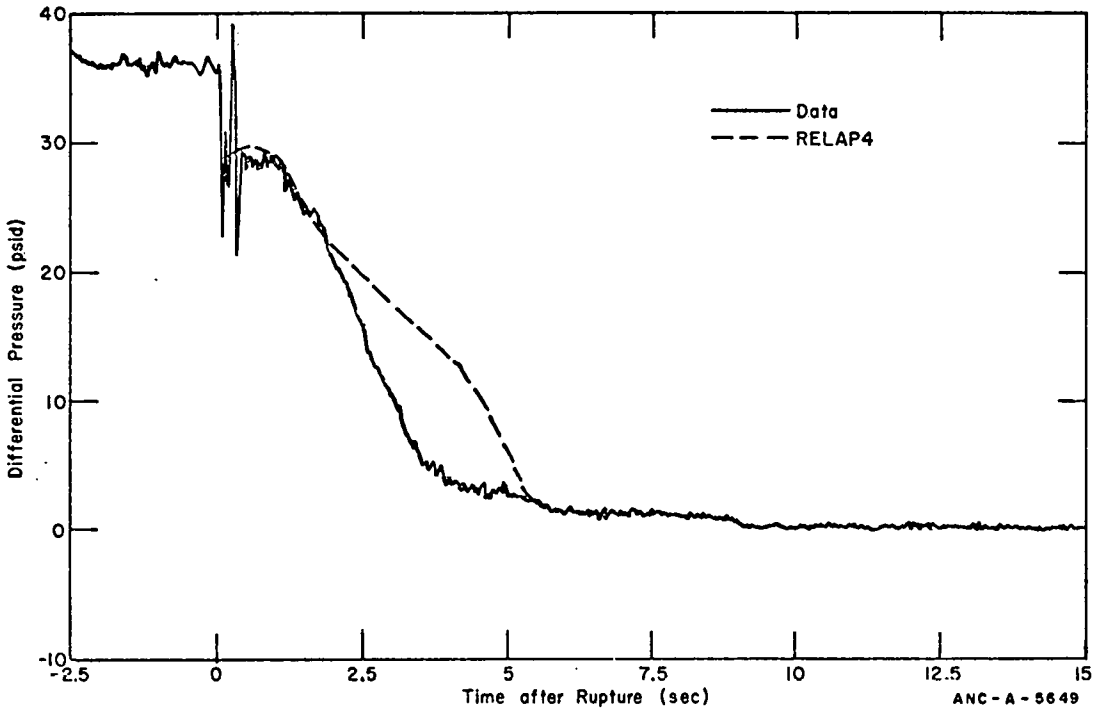

Fig. 19 Pump differential pressure – comparison of RELAP4 calculation with Test S-01-4A data.

1.3 Emergency Core Coolant Influence

An extensive investigation of ECC performance during previous Semiscale 1-1/2-loop isothermal blowdown tests has been documented[17]. Analysis of the data provided in that document has provided an understanding of the phenomena controlling ECC behavior in the Semiscale geometry. The Semiscale Mod-1 isothermal test series is similar to the previous test series, and therefore the results discussed in this section only treat ECC test results which have provided further contribution to the understanding of such phenomena. In addition, the discussion in this section represents a synopsis of an analysis of ECC performance in the Semiscale Mod-1 isothermal test program presented in Reference 11.

1.3.1 Fluid Oscillations Near the Injection Point The data from the Semiscale Mod-1 isothermal tests were analyzed to determine the steam-water mixing phenomena occurring in the cold leg during ECC injection. The density values from the densitometers located upstream and downstream of the ECC injection point for Test S-01-1B, shown in Figure 20, clearly indicate that oscillatory flow existed within the intact loop cold leg during ECC injection. The density measurement upstream of the injection point (GU-13) shows the principal oscillation. The interface of the primary coolant steam and the ECC liquid oscillates about the injection point, being periodic in nature. This interface approaches the vessel inlet and is eventually forced out of the intact loop cold leg completely. Data from two thermocouples located about 3 inches upstream and downstream of the ECC injection

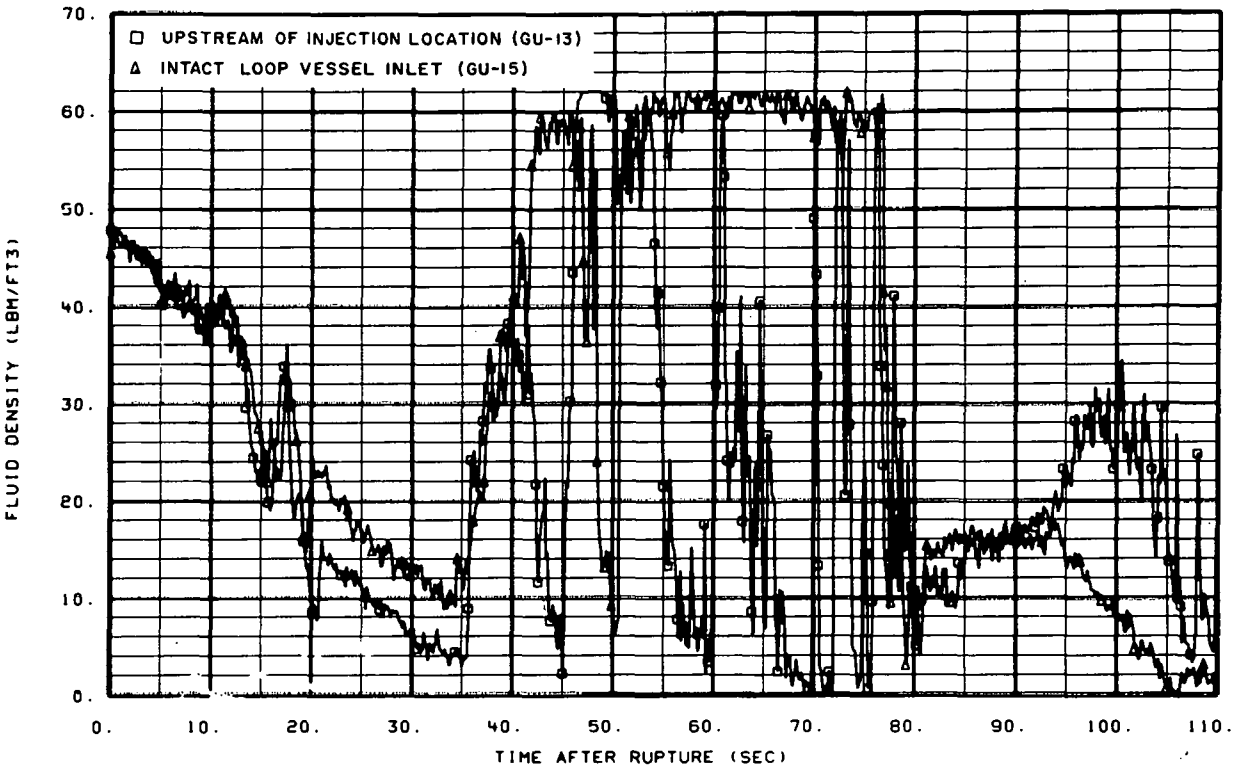

Fig. 20 Fluid densities near ECC injection point in intact loop – Test S-01-1B.

point are used in obtaining an understanding of the nature of the flow oscillations. The results shown in Figure 21 indicate that significant condensation occurs near the injection location which is the cause for the establishment of the oscillatory flow pattern existing within the intact loop cold leg. The degree of condensation is somewhat evident considering that the downstream measurement shows the fluid to be as much as 130°F cooler than the upstream measurement.

The oscillatory phenomena experienced in the Semiscale Mod-1 isothermal tests is consistent with results of tests conducted by Wallis et al[18] at CREARE, Inc. Their efforts have culminated in the development of a mathematical model capable of describing oscillatory cold leg pressure and flow phenomena during ECC injection at a constant system pressure. The Semiscale ECC data are expected to be valuable in the verification process of their model.

The oscillatory data obtained during ECC injection exhibited basically the same phenomena for both 200% cold leg break and 100% hot leg break tests. The flow oscillated at a frequency of approximately 1.0 Hz with a maximum peak-to-peak amplitude of approximately 1.5 psid. The steam-water mixing process caused system pressure fluctuations of about ±20 psia during the ECC injection period.

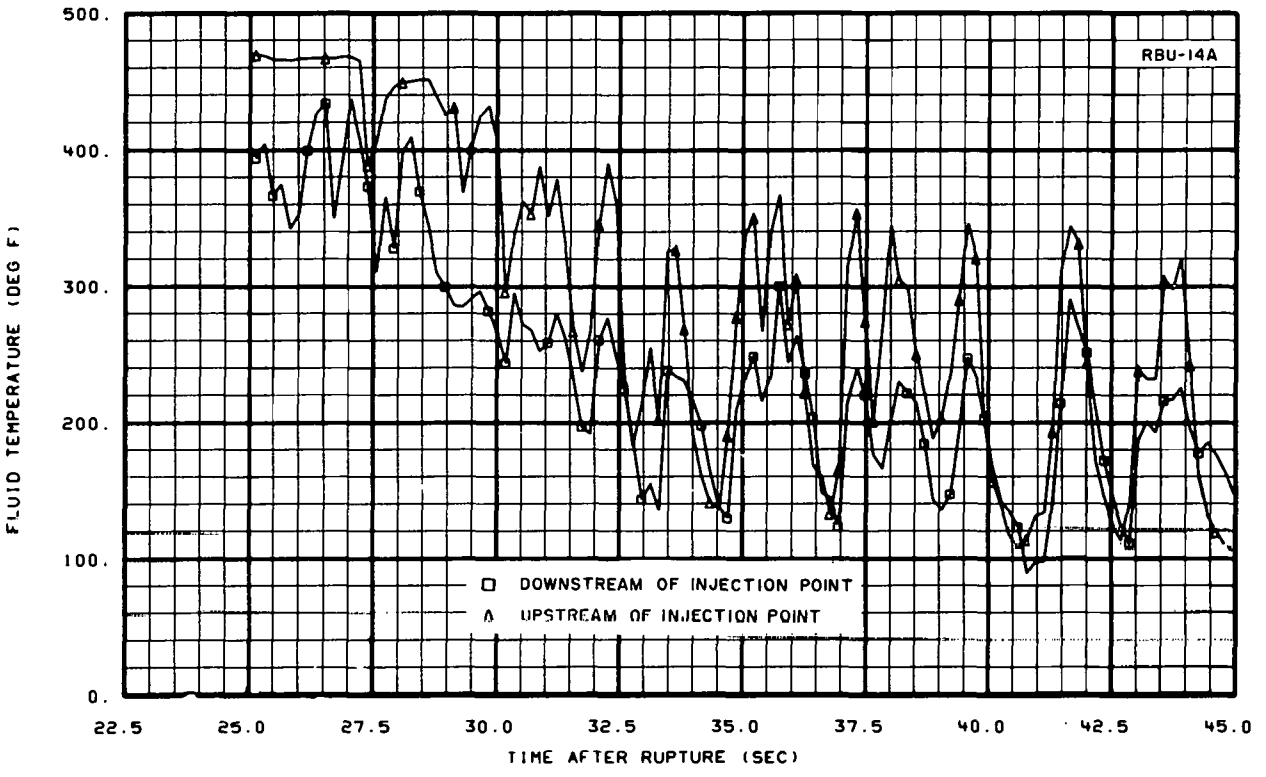

Fig. 21 Fluid temperatures on each side of ECC injection point in intact loop – Test S-01-4A.

1.3.2 Downcomer Countercurrent Phenomena. The complex phenomena that occurred in the downcomer region during the Semiscale Mod-1 isothermal tests influenced the time of delivery and the rate of delivery of ECC to the lower plenum. Downcomer countercurrent flow, bypass flow, and heat transfer phenomena controlled the time ECC reached the lower plenum.

The effect of the countercurrent flow process on delivery of water to the lower plenum is demonstrated in Figure 22. Results from Test S-01-4A indicate that significant flow bypassed the downcomer starting at 30 seconds after rupture and flowed out the vessel-side break until about 60 seconds after rupture. The downcomer turbine flowmeters (turboprobes) indicated negative flow (flow upward through the downcomer) for this same time interval, thus supporting the bypass phenomena. In addition to countercurrent flow upward through the downcomer causing the injected ECC to bypass out the vessel-side break, steam generation on the hot downcomer walls enhances high velocity steam flow up the downcomer, further retarding the ECC coolant from proceeding downward. A method was developed for the Semiscale system to calculate the delay in delivery of water to the lower plenum that was caused by the hot downcomer walls. This method is based on the results from the coordinated test program to investigate the ECC performance in the Semiscale geometry. The method predicts the delay in delivery to the lower plenum in the Semiscale system with reasonable accuracy. The fraction of the time delay in lower plenum delivery attributable to steam generation on hot downcomer walls during Test S-01-4A is

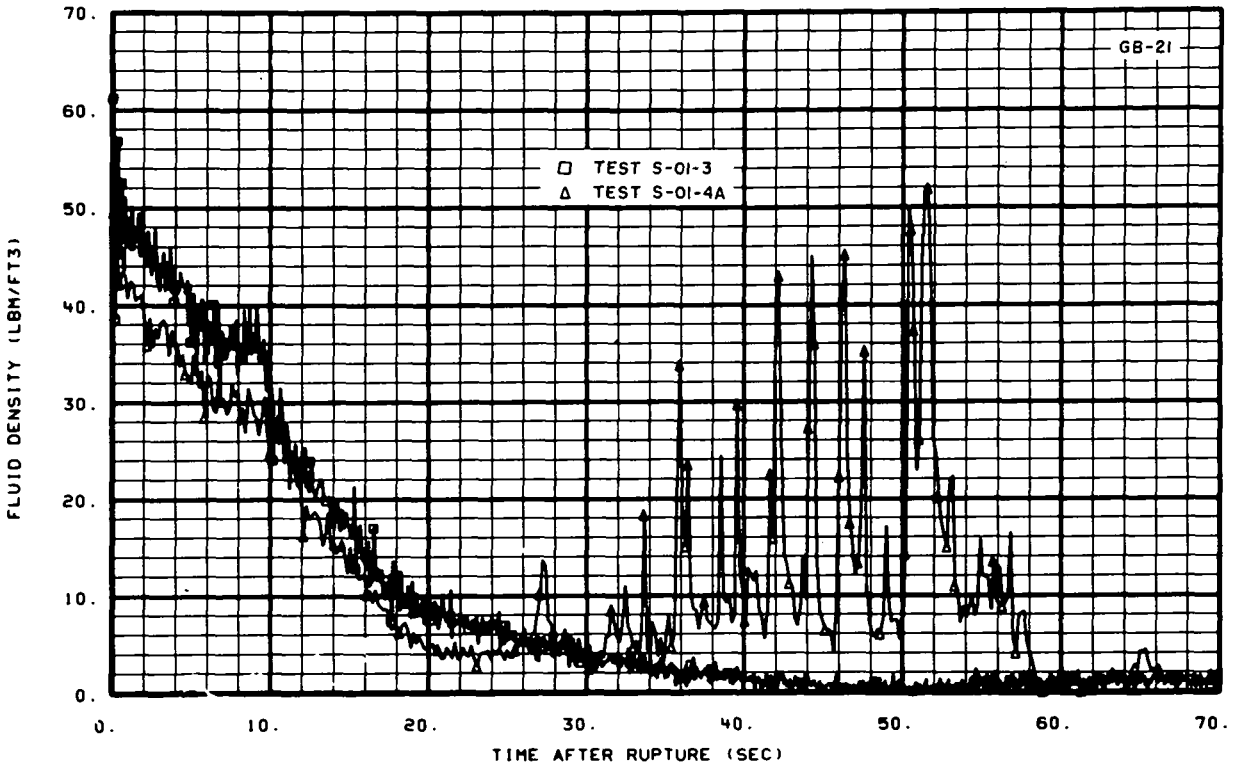

Fig. 22 Fluid density at broken loop cold leg vessel inlet – Tests S-01-3 and S-01-4A.

calculated to be about 10 seconds. This lengthy hot-wall delay time is much longer than the hot-wall delay times calculated for systems that are many times larger than the Semiscale Mod-1 system. The rapid rate of increase in lower plenum density at about 62 seconds after rupture is equivalent to an ECC delivery rate of about 36 gpm. Since this delivery rate is much larger than the water injection rate, some of the injected water must have been from storage in the downcomer during the hot-wall countercurrent flow period.

1.3.3 ECC Injection Location. The effect upon system response following ECC injection caused by the location of the injection is discussed in this section. Comparison of results from Test S-01-3 (lower plenum injection) and Test S-01-4A (intact loop cold leg injection) for the cold leg break configuration indicates that the core phenomena following ECC injection is definitely affected by the location of the injection. Figure 23 shows the core inlet density for Tests S-01-3 and S-01-4A. ECC injection started at about 22 seconds for both tests. The lower plenum ECC injection test (Test S-01-3) exhibits ECC at the core barrel inlet 14 seconds after injection, as the density rapidly rises to that of liquid water at 38 seconds after rupture. However, the cold leg ECC injection test (Test S-01-4A) exhibits a density that is very small until 62 seconds after rupture. Lower plenum injection thus would provide 26 seconds of additional cooling for the core as compared to cold leg injection. The difference in cooling time is caused primarily by the countercurrent flow and hot-wall process existing within the downcomer for cold leg injection mentioned in the previous section.

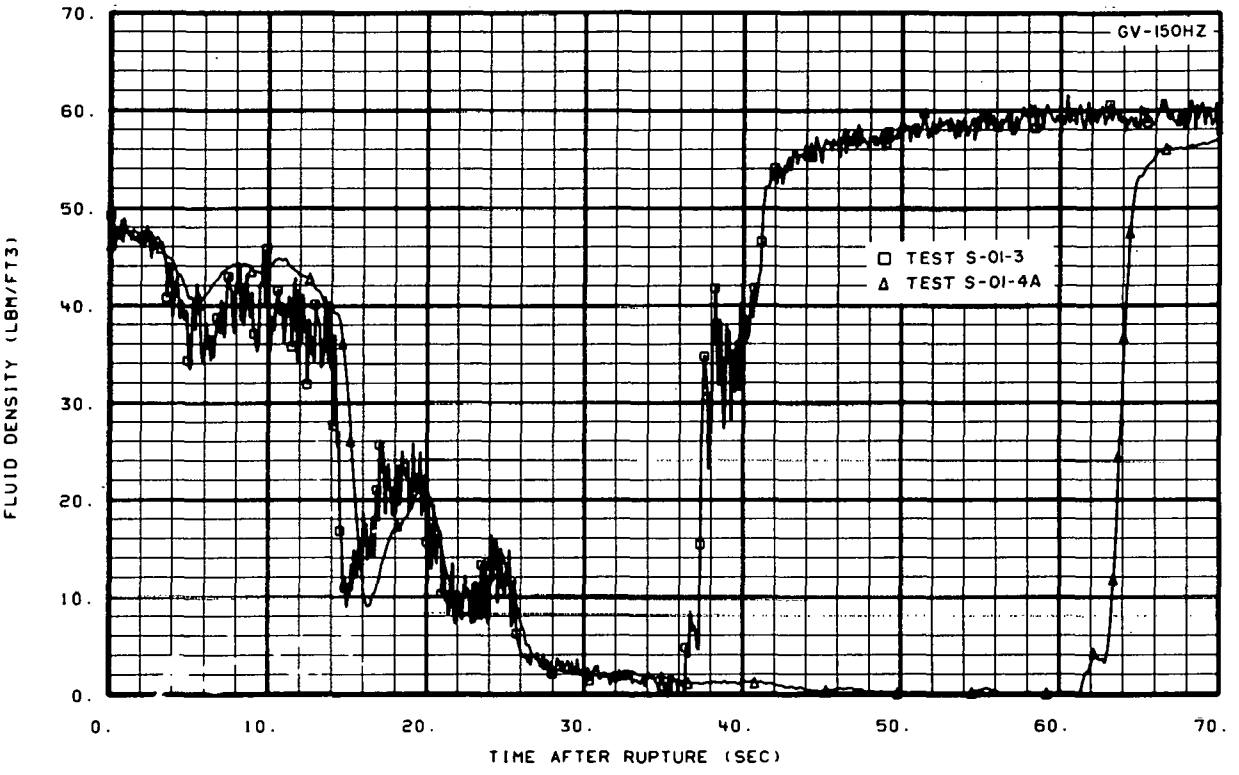

Fig. 23 Fluid density at core entrance showing ECC delivery time – Tests S-01-3 and S-01-4A.

Comparison of the results of Test S-01-1 (upper annulus ECC injection) and Test S-01-1B (intact loop cold leg ECC injection) shows very little effect of this change in injection location. The times of ECC injection and the rates of injection were similar for both tests, with the initiation of accumulator injection occurring about 33 seconds after rupture. Figure 24 shows the density measured at the core flow mixer box for both tests. The results from Test S-01-1 indicate a slightly earlier delivery of significant amounts of ECC to the mixer box. As with the results from the cold leg injection Test S-01-3, the delay in ECC delivery to the core region appears to be caused by the combined effects of downcomer countercurrent flow and steam generation in the hot downcomer walls. The density measurement at the broken loop cold leg vessel outlet indicated a slightly later initiation of downcomer bypass for Test S-01-1B. This later bypass initiation with cold leg injection appears to result from ECC partially filling the intact loop cold leg before flowing to the annulus-downcomer region, and therefore does not signify an improvement in delivery to the downcomer. The difference in the time of delivery to the core flow mixer box may be due to the time required for the ECC to partially fill the cold leg.

1.4 Piping Heat Transfer and Steam Generator Performance

Piping and steam generator heat transfer affects the quality, velocity, and temperature of the primary fluid during the semiscale Mod-1 blowdown transient. For example, piping and steam generator heat transfer in the intact loop adds energy to the primary fluid which

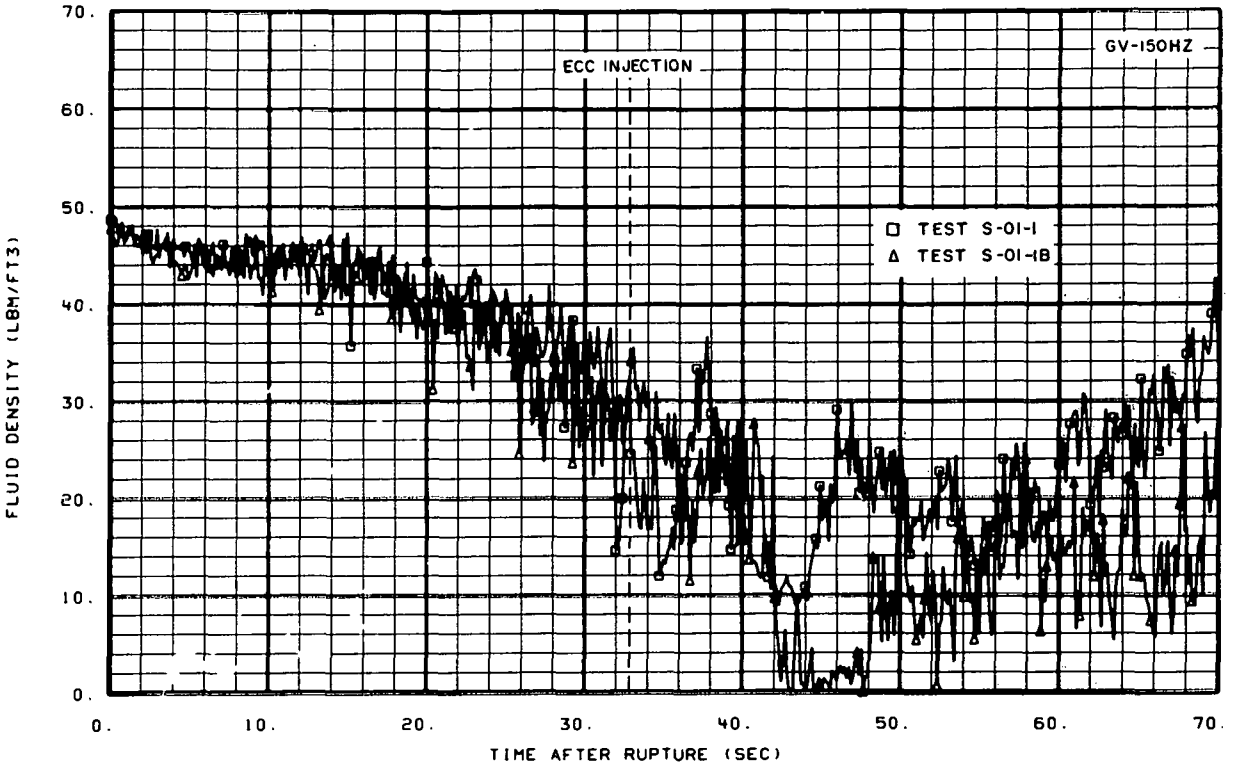

Fig. 24 Fluid density at core entrance showing ECC delivery time – Tests S-01-1 and S-01-1B.

can result in increased fluid velocity and quality at the vessel cold leg inlet, which can in turn affect core performance. The piping heat transfer during the Semiscale Mod-1 isothermal test series was evaluated to determine its sensitivity to azimuthal position in the pipe section, general location of the pipe section in the intact and broken loops, and broken loop break location and size. The piping wall heat fluxes were determined for the isothermal tests from the observed temperature history provided by thermocouples installed within the material of the piping walls in both the intact and broken loops. Selected experimental data pertinent to piping heat transfer and steam generator heat transfer obtained during the Semiscale Mod-1 isothermal blowdowns were analyzed and are presented in a separate test results report on piping heat transfer and steam generator performance[9]. The following discussion summarizes the major results obtained from that study.

The results of the analysis indicate that the intact and broken loop piping heat transfer is sensitive to azimuthal location in a given pipe, location of the pipe in both the intact and broken loops, and the broken loop break characteristics. Typical of the results from the analysis are the heat transfer rates calculated from thermocouple output obtained during Test S-01-1, which are presented in Figure 25. These thermocouples were located in the top, side, and bottom of the pipe in the intact loop hot leg (Spool 1 – about 25 inches from the vessel outlet). As shown in the figure, the maximum heat transfer rates occurred in the bottom of the pipe and decreased toward the top. This phenomenon is attributable to phase separation of the blowdown fluid. The trend of larger heat fluxes toward the bottom of the pipe is consistent with the nonhomogeneous structure of the flow which was

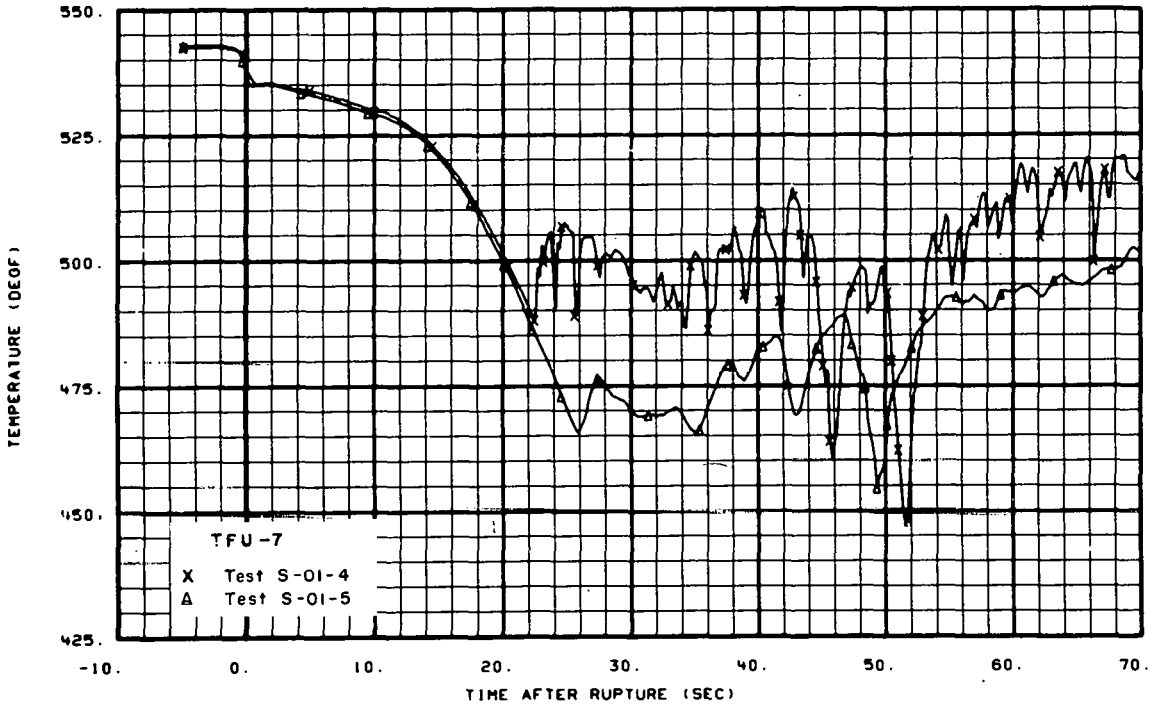

Fig. 25 Azimuthal variations in piping heat transfer at intact loop hot leg vessel outlet – Test S-01-1.

indicated by the horizontal and vertical density measurements at this location. This sensitivity of piping heat transfer to azimuthal locations was noted in all horizontal pipe sections during the Semiscale Mod-1 isothermal test series.

The sensitivity of piping heat transfer to location in the intact loop is relatable to the location of the primary fluid stagnation point in the intact loop. The sensitivity to location in the broken loop is caused by unequal division of break flows and the presence of bypassed ECC at the broken loop vessel inlet side of the break. The broken loop break characteristics (location and size) were shown to significantly affect the piping heat transfer at all locations in both loops due to differences in fluid velocity and wall-to-blowdown fluid temperature differential. Maximum piping heat transfer of about 105,000 Btu/hr-ft^2 occurs in the intact loop cold leg when ECC is injected into the cold leg of the intact loop.

Since the amount of heat transferred from the metal into the system fluid is greater in the Mod-1 system than in larger systems, a reasonably accurate calculation of the amount of heat transferred to the fluid from the structure is desirable. Comparison of RELAP4 results with test data showed that RELAP4 predicted the pipe-to-primary-fluid heat flux rates and average heat transfer coefficients during blowdown reasonably well. Differences between the measured and calculated heat fluxes result primarily from two sources: (a) the use of the homogeneous flow model in RELAP4, and (b) differences in the predicted system primary fluid quality and velocity response to the blowdown transient. In general, RELAP4

predicted the piping heat transfer response for the 200% cold leg break configuration tests better than for the 100% hot leg break configuration tests.

An evaluation of the isothermal test data indicate that heat transfer from the steam generator did not significantly affect the overall behavior of the Semiscale Mod-1 system. The total steam generator heat transfer to the primary fluid was about 3,000 Btu for each isothermal blowdown test with the steam generator maintained in a hot standby condition. This value (3,000 Btu) represents less than 2% of the inital total system energy.

RELAP4 also predicted relatively little effect of steam generator heat transfer on system response. However, comparison of the RELAP4 calculated values of heat transfer with the actual test data indicates that the value of the RELAP4 heat transfer coefficient for the secondary side of the steam generator was too small. Additional RELAP4 calculations were conducted for Test S-01-4 in which the heat transfer coefficient was increased from the previously used 5 Btu/hr-ft^2-^{o}F to 300 Btu/hr-ft^2-^{o}F. However, the effect of the increased heat transfer value upon system response was found to be minimal outside the region of the steam generator, even though these calculations did improve the secondary side heat transfer and metal temperature results as shown in Figure 26. For a more thorough discussion of the effect of the secondary side of the steam generator on system performance, the reader is referred to Reference 9.

1.5 Influence of Simulators

The pump and steam generator simulators in the broken loop have a series of orifice plates which are designed to be geometrically similar to the LOFT simulators. The orifice plates are used to obtain a scaled flow resistance representative of the LOFT counterparts. Since the Semiscale simulators were designed directly from their LOFT counterparts, information on the simulator pressure drops as well as an evaluation of the calculated pressure loss across these components will aid the LOFT Program in evaluating their broken loop pressure drops.

The pressure drop across the pump simulator represented the principal pressure drop in the Semiscale Mod-1 system during blowdown, and an accurate calculation of the pressure drop across this component is necessary in order for correct broken loop blowdown predictions to be made. A comparison of a RELAP4 calculation of the differential pressure across the pump simulator with the data for Test S-01-4A is presented in Figure 27. The data show an initial sharp rise in the pressure drop caused by the accelerating fluid. A relatively high two-phase pressure drop occurs from 1 to 14 seconds after rupture, after which the high quality fluid combined with low velocities results in a gradual decline of the pressure drop until the end of blowdown. The response of the pump simulator during blowdown was predicted fairly well by RELAP4 for the cold leg break configuration; however, the RELAP4 calculations of pressure drop are slightly lower than the data. This lower pressure drop could be caused by the RELAP4 program using only three junctions to represent the total resistance across nine orifice plates.

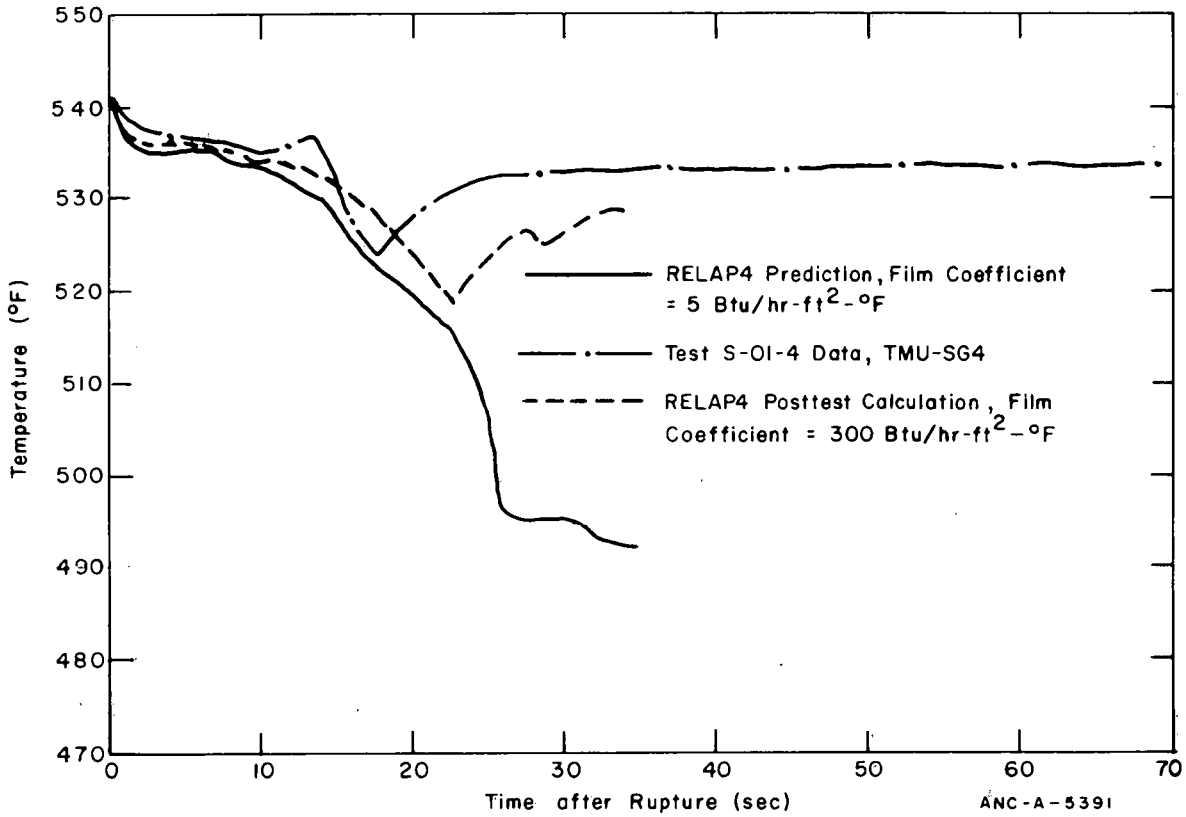

Fig. 26 Surface metal temperature – secondary side of steam generator – Test S-01-4.

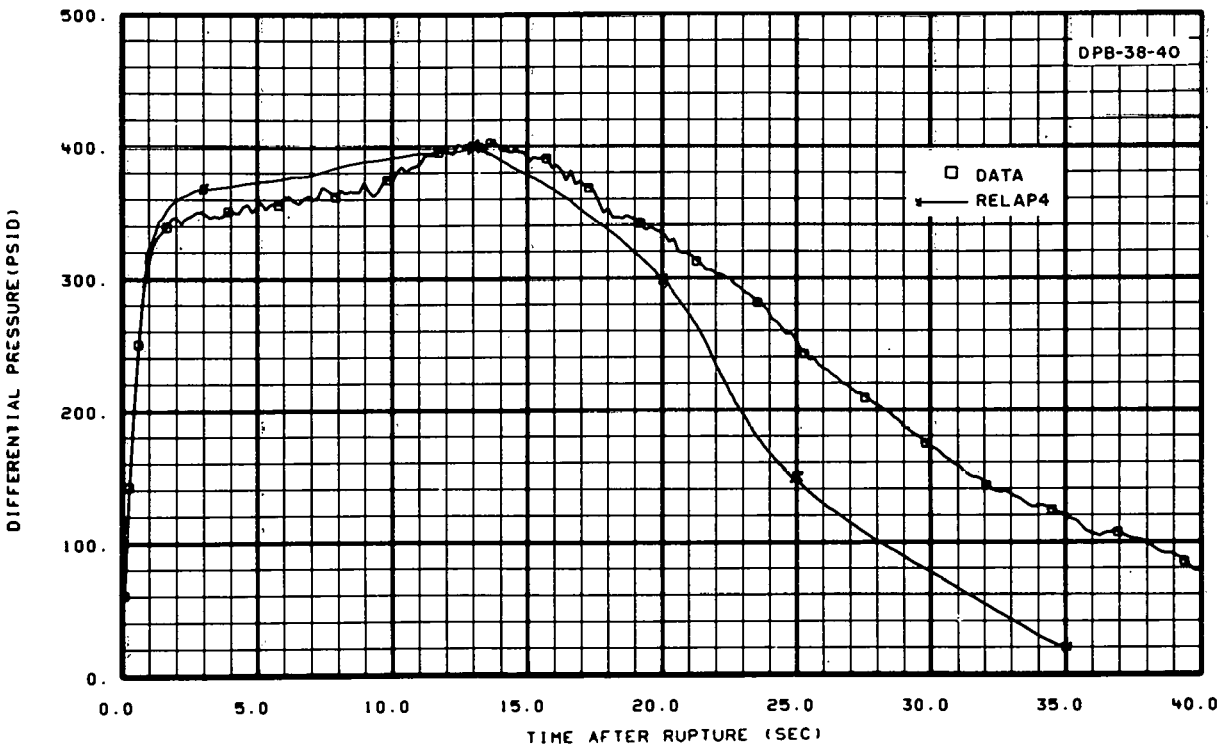

Fig 27. Differential pressure across pump simulator – Test S-01-4A.

The general response of the steam generator simulator was quite similar to that of the pump simulator. The steam generator simulator consisted of 14 orifice plates constituting an orifice assembly, an inlet nozzle, and an outlet nozzle and was instrumented such that pressure drops across the inlet and outlet nozzles and across just the orifice assembly could be measured as a check against the measurement across the entire steam generator simulator assembly. Good agreement between the pressure drop across the entire simulator assembly and the sum of the respective pressure drops across the nozzles and orifice assembly was obtained. The RELAP 4 calculation of the same measurements indicate that the pressure drop across the outlet nozzle is considerably underpredicted, thereby contributing to the RELAP4 underprediction of the pressure drop across the entire steam generator assembly. The RELAP4 underprediction of the pressure drop across the outlet nozzle resulted from a reverse loss coefficient which was too small for the nozzle configuration.

The transient response of the simulators provides a check on the applicability of steady state pressure drop correlations being used in a transient situation. The pressure drops across both simulators previously discussed were calculated by RELAP4 using a modification of the Barcozy[19] correlation. The resistance values used with this correlation are based on steady state single-phase flow resistance calculations rather than a transient two-phase mixture flow resistance (which actually exists during a blowdown).

The pressure drop across both simulators was also calculated using a two-phase flow correlation developed by Thom[20]. As in the Baroczy correlation, Thom's correlation uses measured steady state flow resistances as input to the correlation. The results, shown in Figures 28 and 29, indicate that the use of steady state single-phase resistances do an adquate job when used to calculate two-phase phenomena. A curve showing the RELAP4 calculations for the two-phase pressure drop is included for comparison purposes. The large oscillations in the Thom's calculated values after 25 seconds result from the two-phase multiplier which is principally a function of the actual density measurements.

1.6 Pressurizer Performance and Intact Loop Hot Leg Fluid Response

Flow in the hot leg of the intact loop was influenced by the break, the pump, and the pressurizer. The interaction of these components during the blowdown process determined the hot leg fluid response and the possible subsequent effect that the hot leg fluid had on core fluid behavior. The response of the intact loop hot leg was studied during and after the pressurizer emptied of water. Analysis of the measurements in the hot leg while the pressurizer was voiding indicates that the pump had the most significant influence on the hot leg fluid for about the first 4 seconds, after which the vessel-side break conditions apparently controlled the remainder of the intact loop hot leg fluid response.

The effect of the transition from water to steam (from the pressurizer) on the hot leg fluid response was evaluated. The high velocity steam flowing from the pressurizer literally swept out all liquid remaining in the hot leg and left a very low density fluid. This phenomenon is shown in the plot of fluid densities within the hot leg at Stations 1 and 5 included as Figure 30. Note should be taken of the magnitudes of the densities between 10

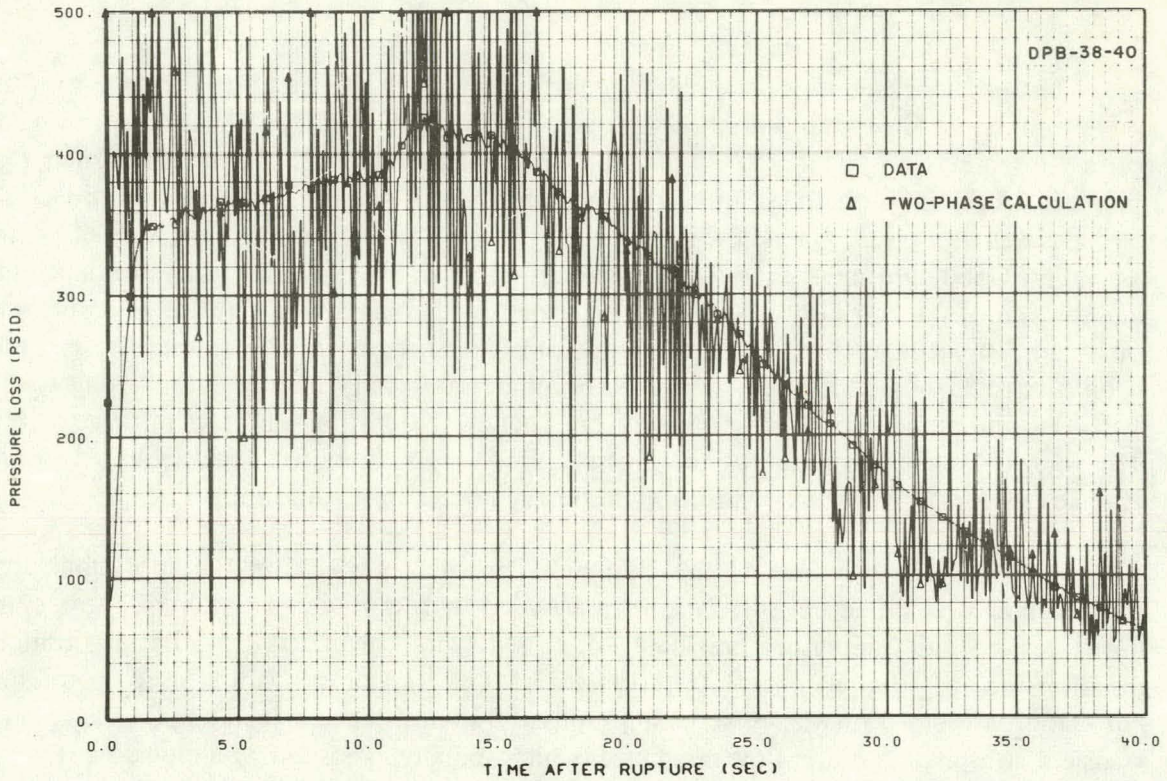

Fig. 28 Two-phase pressure drop across pump simulator — Thom's correlation versus data from Test S-01-3.

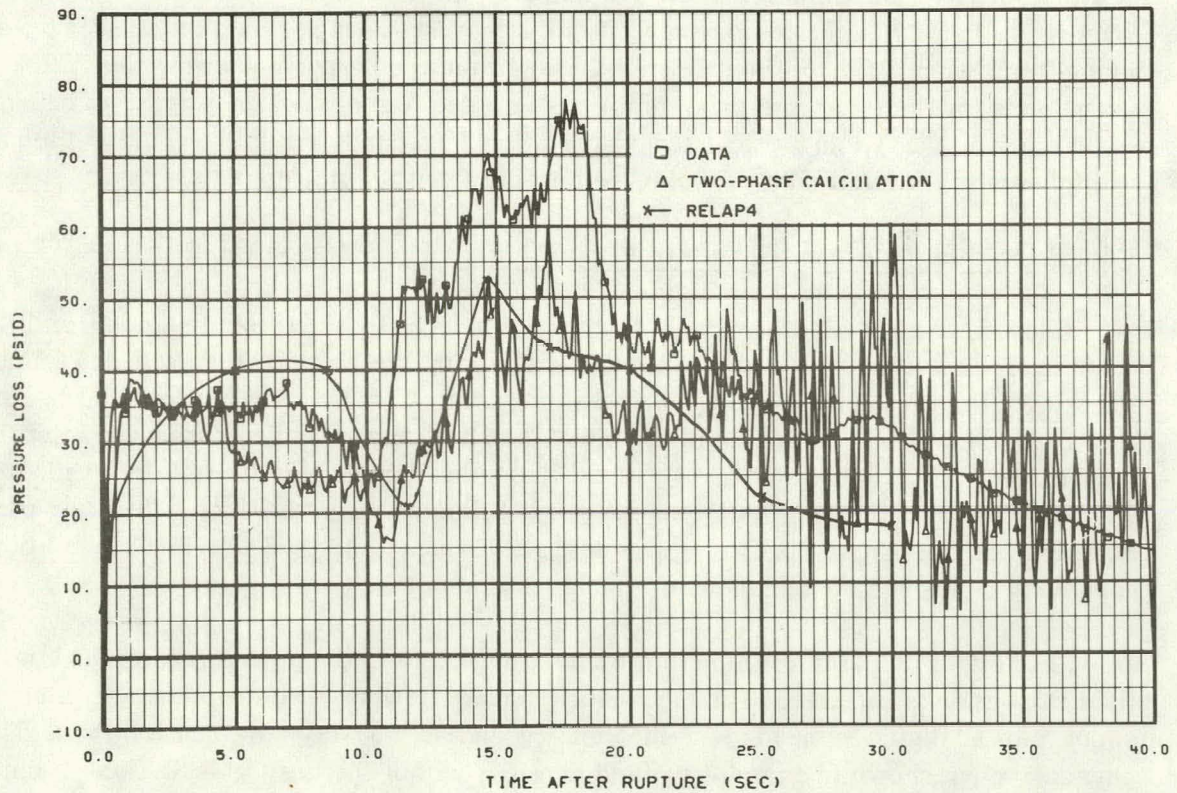

Fig. 29 Two-phase pressure drop across steam generator simulator – Thom's correlation versus data from Test S-01-3.

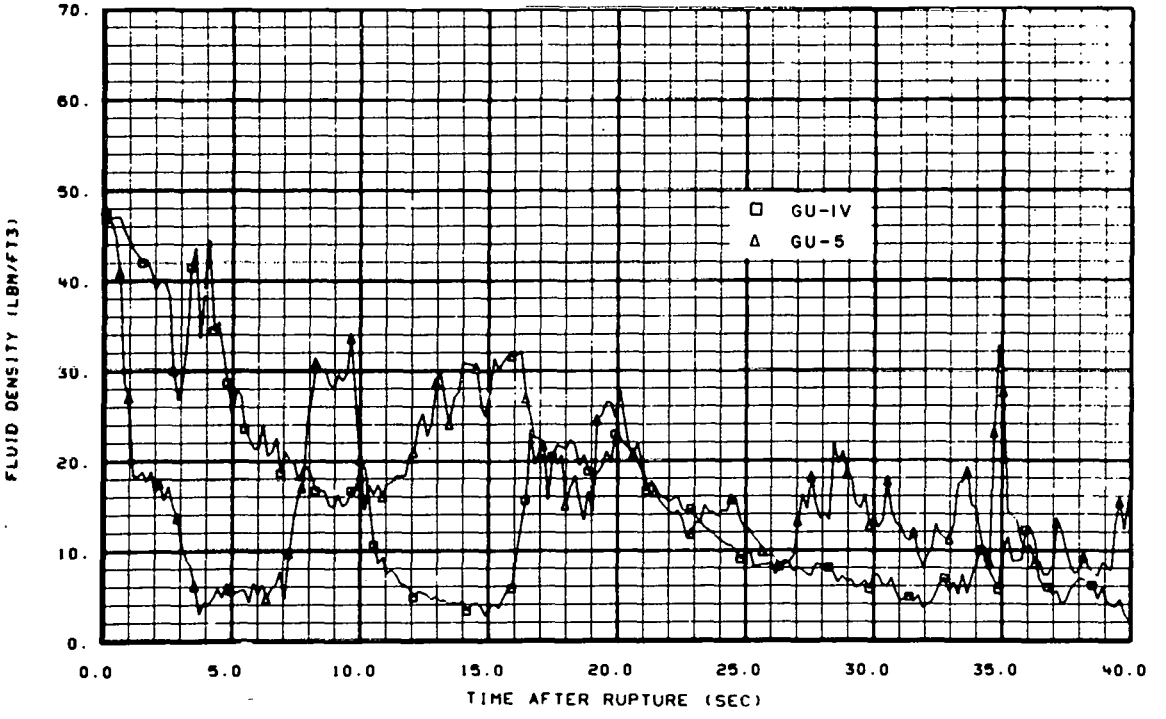

Fig. 30 Fluid densities within intact loop hot leg – Test S-01-4A.

and 20 seconds after rupture. The fluid during this interval appears to have come from the steam generator. The steam flow from the pressurizer terminates at about 20 seconds, causing a decrease in both flow and density within the hot leg. This phenomenon of the pressurizer "sweeping the high density fluid from the hot leg" would not be expected to occur in a commercial PWR because only one of the three intact hot leg loops in a PWR has a pressurizer attached.

2. REPEATABILITY OF RESULTS

Experimental data from the isothermal test program provide information on the repeatability of the complex phenomena occurring in the Semiscale system when that system is subjected to similar blowdown environments. Determination of the repeatability of phenomena is important because many of the objectives for the current Semiscale tests are related to comparing results from two or more differential tests. In these differential tests, either the initial conditions or configuation is changed to determine the effect of the change on overall system response. The repeatability of the Semiscale system with respect to measuring repeated phenomena under similar conditions during various blowdown tests was determined for the isothermal test series. This section discusses the repeatability of the results for the Semiscale Mod-1 isothermal test series. However, in certain cases, the repeatability of results was affected by unexpected differences in the preblowdown initial conditions. When such differences occur, they are noted.

In general, the two hot leg break tests (Tests S-01-1 and S-01-1B) provided data which were in excellent agreement up to the time of ECC injection from the accumulator system. The general performance (that is, trends of the data) was also repeatable after initiation of ECC injection even though magnitudes varied somewhat. The close similarity of the initial conditions for Tests S-01-1 and S-01-1B provides an excellent basis for assessing repeatability of results. The only significant difference between these two tests was the ECC injection location, which did not affect the system until 31 seconds after rupture. Figure 31 shows excellent repeatability of flow rate for the two tests during the first 30 seconds of blowdown. Although the density measurements within the core did not exhibit quite as good agreement, Figure 32 indicates the results were repeatable with respect to general trends. The differential pressure measurements within the system likewise showed repeatable results as evidenced by the pressure drop across the pump simulator and the pressure rise across the intact loop pump, shown in Figures 33 and 34, respectively.

Results from the large doubled-ended cold leg breaks were also examined. With the exception of the secondary side of the steam generator (containing water and steam for Test S-01-4 and nitrogen for Test S-01-5), the inital conditions for Tests S-01-4 and S-01-5 were also very similar. A comparison of the results for these tests is reasonable because the secondary side of the steam generator had little effect on system response. As for the hot leg break tests, the core fluid responded in an almost identical manner during Tests S-01-4 and S-01-5, as shown in Figure 35. In fact, up to the time of ECC injection, almost all of the fluid response within the Semiscale Mod-1 isothermal test system (with the exception of the intact loop cold leg) performed in a very repeatable manner. Figures 36 and 37 show the flow rates at the vessel side of the break and the intact loop hot leg, respectively, for the cold leg break Tests S-01-4 and S-01-5. The differences in flow rate that existed within the intact loop involved magnitudes and were caused by the difference in the pump head degradation experienced between 2 and 4 seconds after rupture for the two tests. In general, however, the results of Tests S-01-4 and S-01-5 exhibit excellent agreement.

From the test comparisons previously discussed, the conclusion is reached that the repeatability of the thermal-hydraulic response of the system during the isothermal test series was good. Agreement between system reponse phenomena for the hot leg break configuration and between system response phenomena for the cold leg break configuration was excellent prior to ECC injection. The phenomena are not as repeatable after ECC injection principally because of condensation phenomena and the associated flow processes resulting from ECC injection.

3. COMPARISON OF RESULTS FROM DIFFERENTIAL TESTS

The differences in the results from the various isothermal tests in which the initial conditions were changed are discussed in this section. Included in this section is a discussion and comparison of the effect of changes in the system configuration on system response during blowdown. The changes in system configuration consisted of: (a) changing intact loop flow resistance, (b) changing break location and size, (c) changing from water to nitrogen in the steam generator secondary, and (d) having the 40-rod core installed rather than the core simulator.

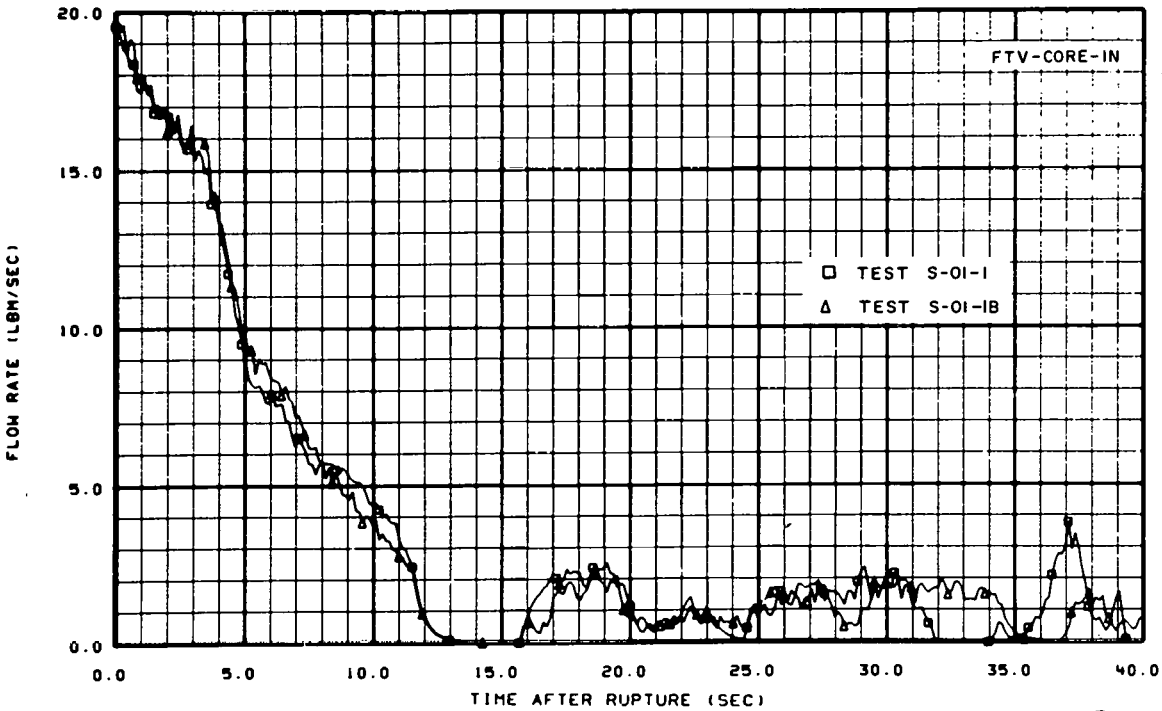

Fig. 31 Flow rate at entrance to core – showing repeatability of results – Tests S-01-1 and S-01-1B.

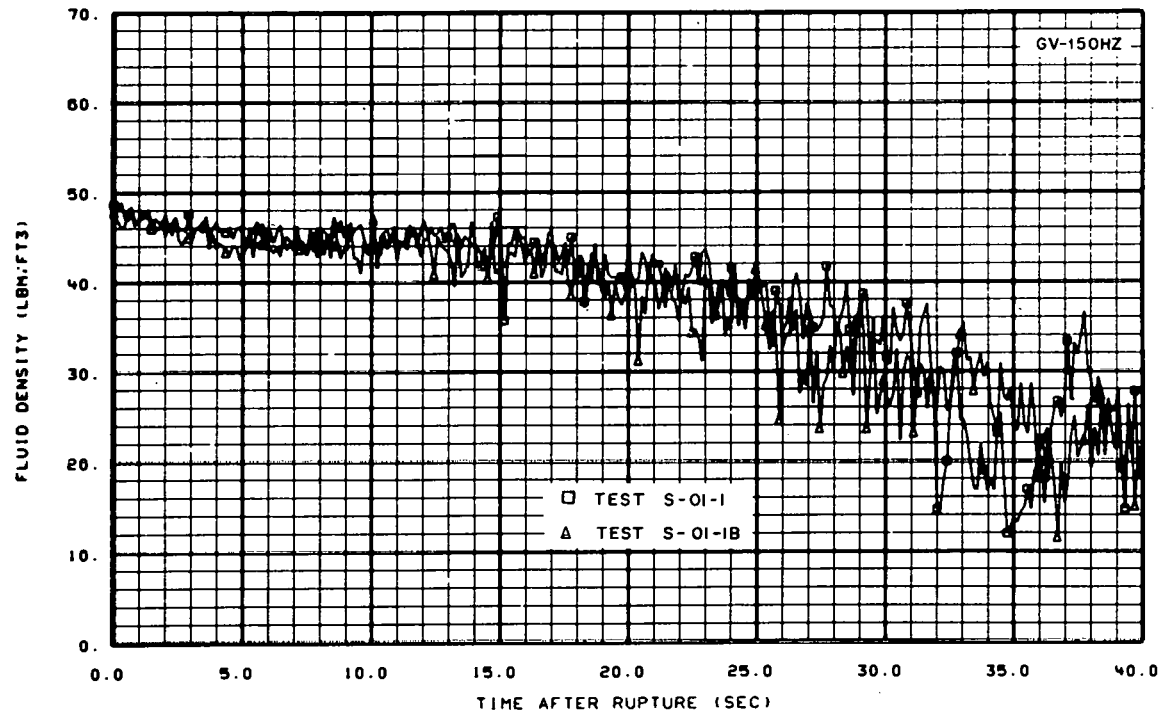

Fig. 32 Fluid density at entrance to core – showing repeatability of results – Tests S-01-1 and S-01-1B.

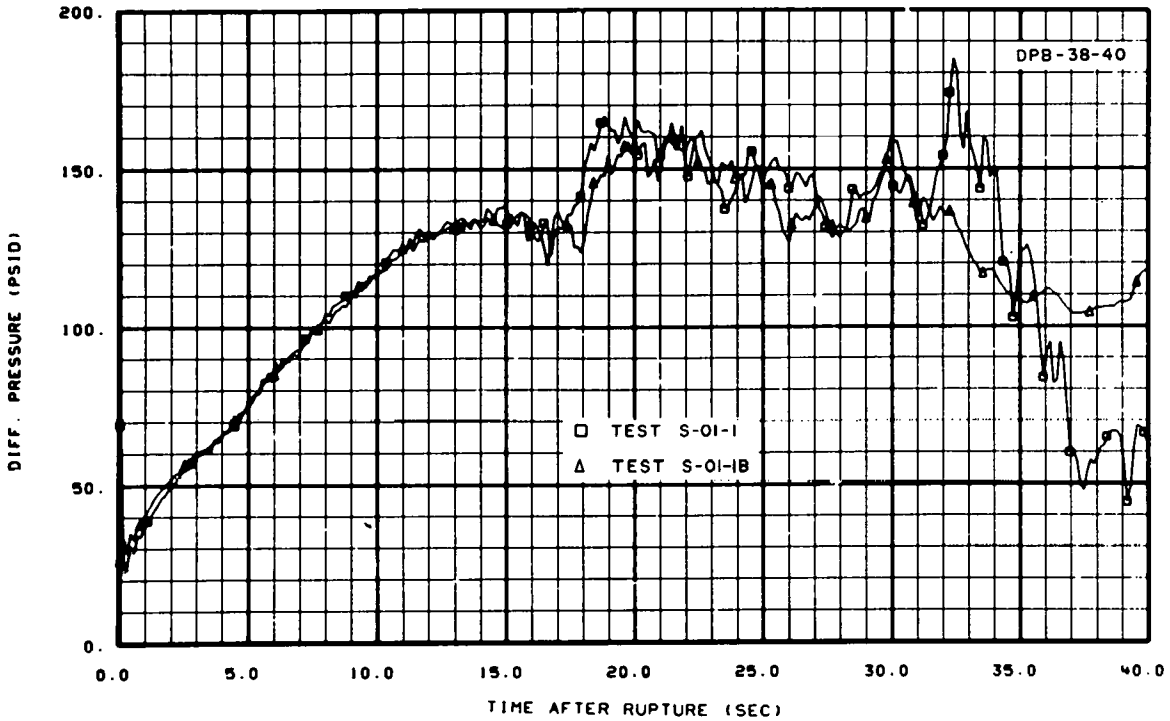

Fig. 33 Differential pressure across pump simulator – showing repeatability of results – Tests S-01-1 and S-01-1B.

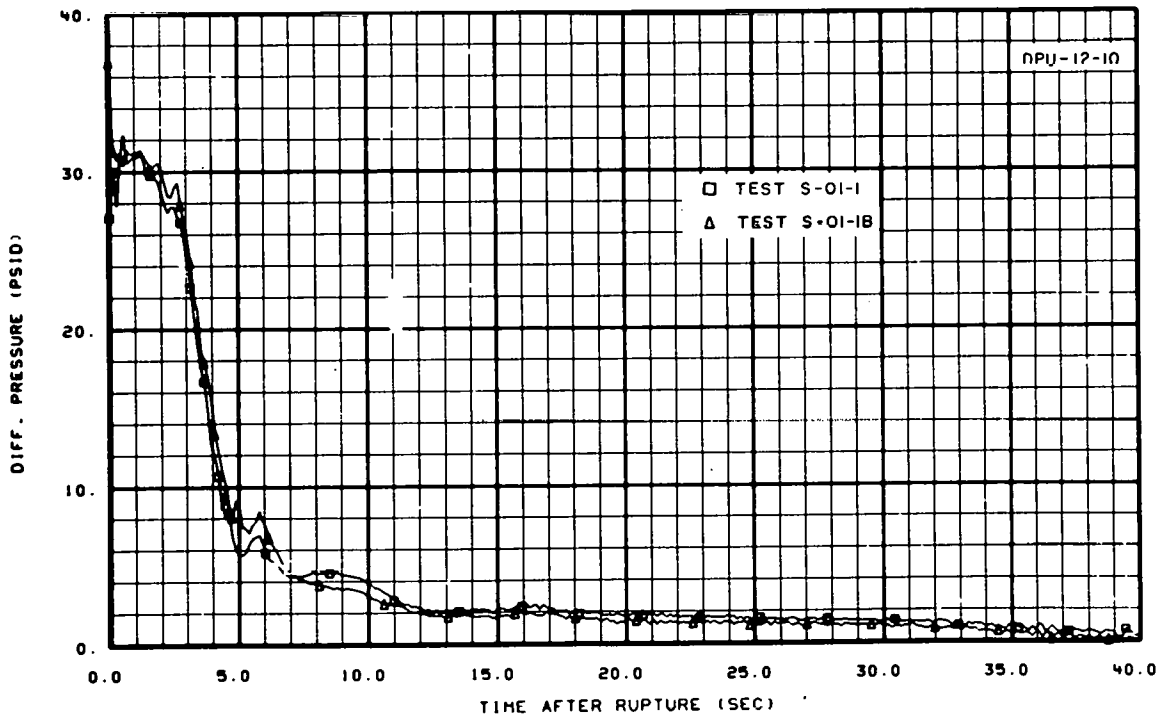

Fig. 34 Differential pressure across intact loop pump – showing repeatability of results – Tests S-01-1 and S-01-1B.

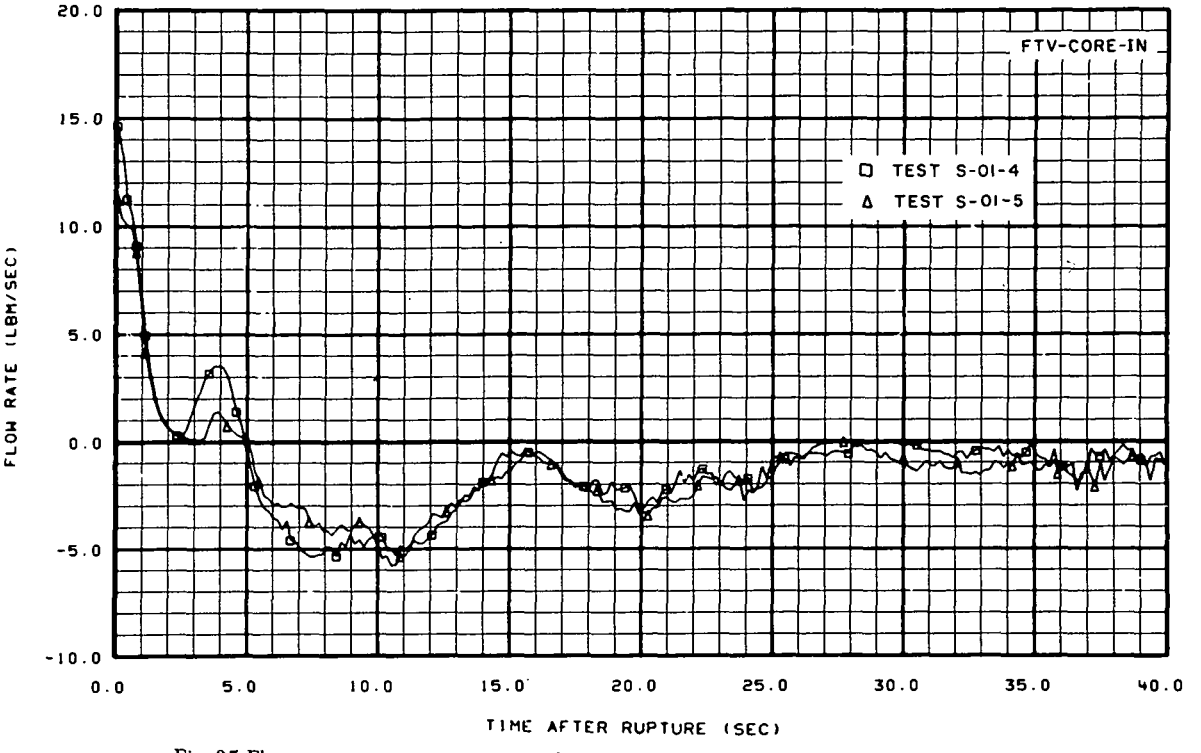

Fig. 35 Flow rate at entrance to core – showing repeatability of results – Tests S-01-4 and S-01-5.

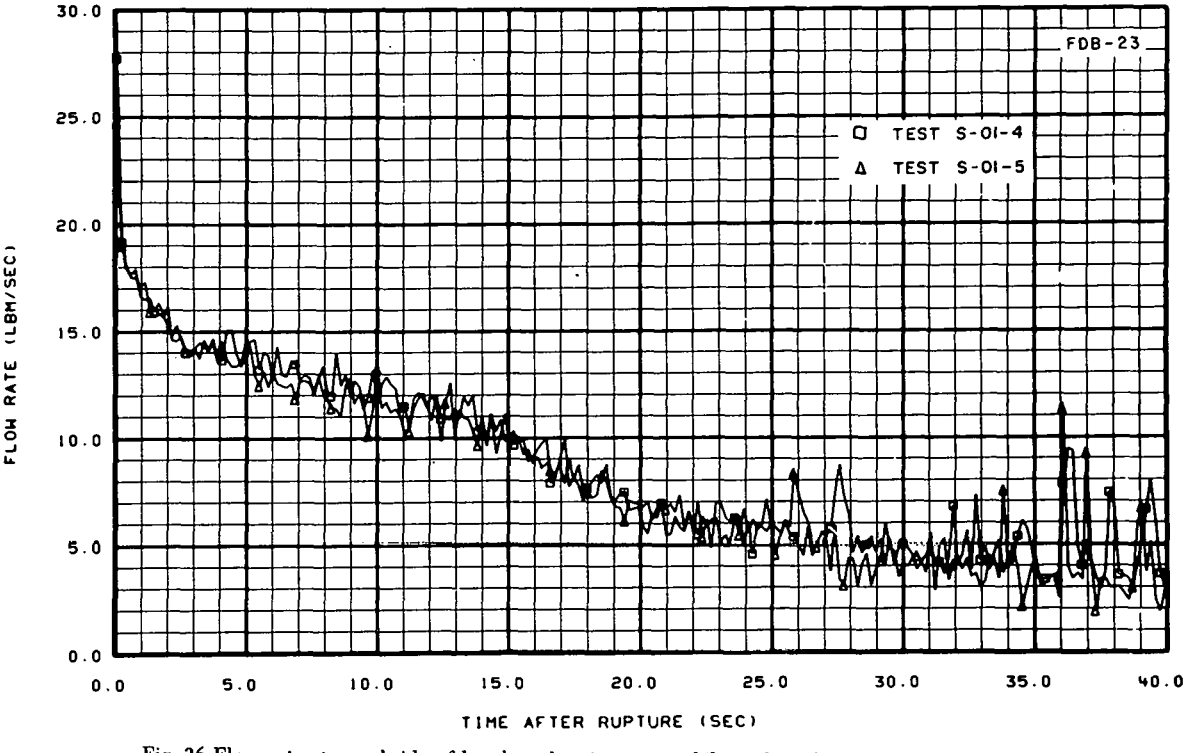

Fig. 36 Flow rate at vessel side of break – showing repeatability of results – Tests S-01-4 and S-01-5.

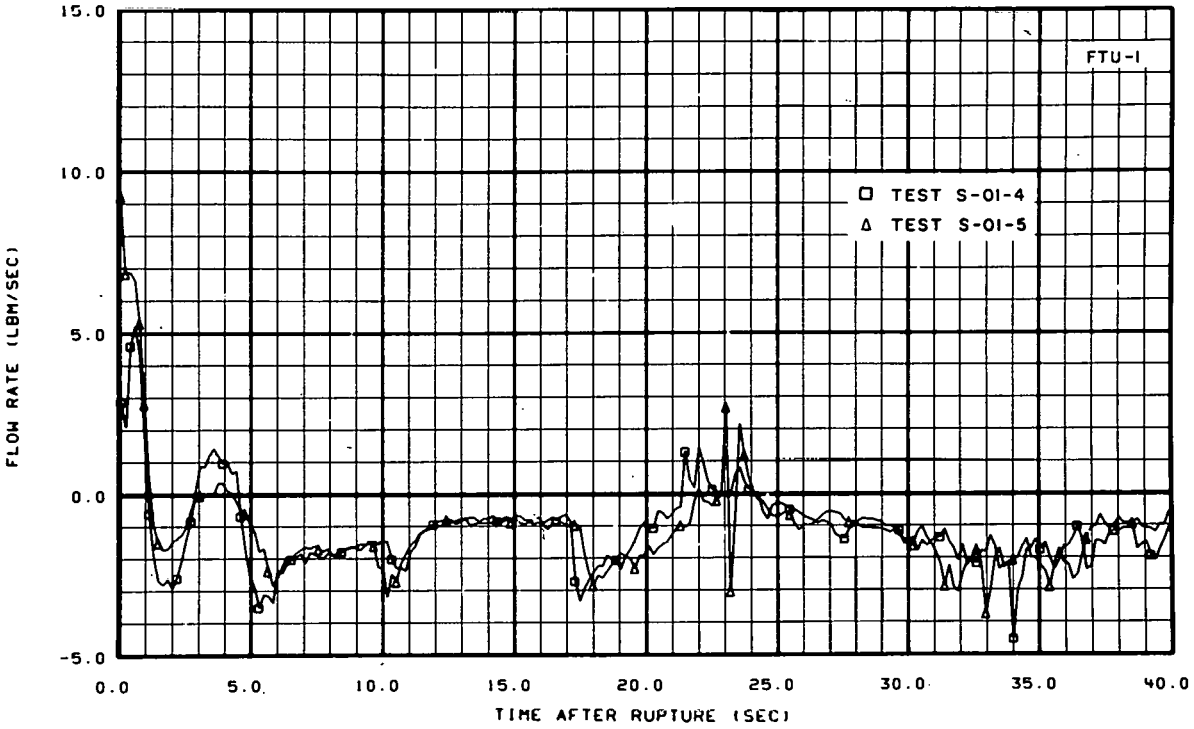

Fig. 37 Flow rate at intact loop hot leg – showing repeatability of results – Tests S-01-4 and S-01-5.

3.1 High Versus low Intact Loop Resistance

In order to establish the importance of operating loop resistances on system response during blowdown, Tests S-01-2 and S-01-4A were conducted with different intact loop flow resistances. The intact loop resistance for Test S-01-2 was relatively large (based on volumetric scaling), whereas that for Test S-01-4A was smaller (based on core area scaling). The change in flow resistance was made by using different size orifice plates at the inlet and outlet to the intact loop steam generator.

The effect of intact loop flow resistance on system performance was studied prior to ECC injection (during the first 20 seconds of blowdown) at measurement locations throughout the system. Areas of interest included the pump, the core region, and the break. Slight differences in measured response occurred at the intact loop pump and the core inlet. The pump performance for the two tests is presented in Figure 38. The difference in the initial pressure rise across the pump created by the difference in flow resistance within the intact loop accounts for the major difference in pump degradation shown to exist in the figure. RELAP4 calculations (not shown) exhibited the difference in pump degradation fairly well for the first few seconds of blowdown. Other than the pump phenomena, the effect upon intact loop response due to the two different resistances appears to have been a local phenomenon, causing minor changes in density and flow rates in the pump suction leg. The experimental results are consistent with the RELAP4 calculations which indicated no appreciable differences in intact loop response between the two tests.

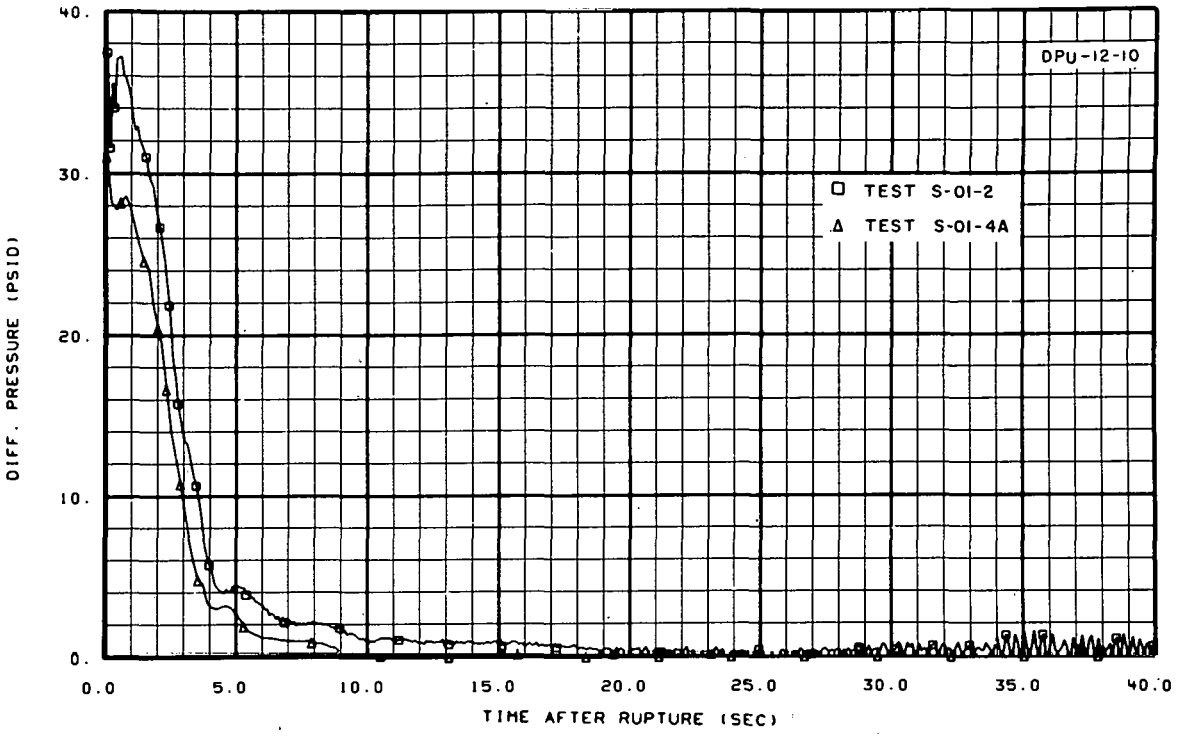

Fig. 38 Differential pressure across intact loop pump – Tests S-01-2 and S-01-4A.

The largest difference in system response due to change intact loop flow resistance existed within the core region. Figure 39 shows a much higher density for Test S-01-2 between 16 and 24 seconds after rupture relative to that for Test S-01-4A. Results from other cold leg break tests are consistent with the results of Test S-01-4A, indicating that the core density during this time interval is affected by the intact loop flow resistance. However, the RELAP4 calculations for the two resistance cases show no difference in core density with the calculations agreeing reasonably well with Test S-01-4A results. Another core region measurement which might be used for comparing the results of the two tests is that from the core turbine flowmeter as shown in Figure 40. The Turbine flowmeter measurements at the core inlet for the two tests show different results. The turbine flowmeter measurement shows positive flow through the core between 4 and 17 seconds after rupture for the high resistance case (Test S-01-2), whereas the turbine flowmeter measurement for the low resistance test indicates negative flow through the core during the same time interval. RELAP4 calculations (not shown) were studied to determine whether consistency existed between the data and the calculations. RELAP4 indicates that negative flow should exist for both Tests S-01-2 and S-01-4A from 6 seconds after rupture until the end of blowdown. A thorough evaluation of the experimental phenomena occurring within and near the vessel region was performed for Test S-01-2. Of the nine measurements studied within or around the vessel region, six indicated negative flow should have occurred through the core between 4 and 18 seconds after rupture, whereas the other three measurements, including the density and turbine flowmeter measurements indicated positive flow. The

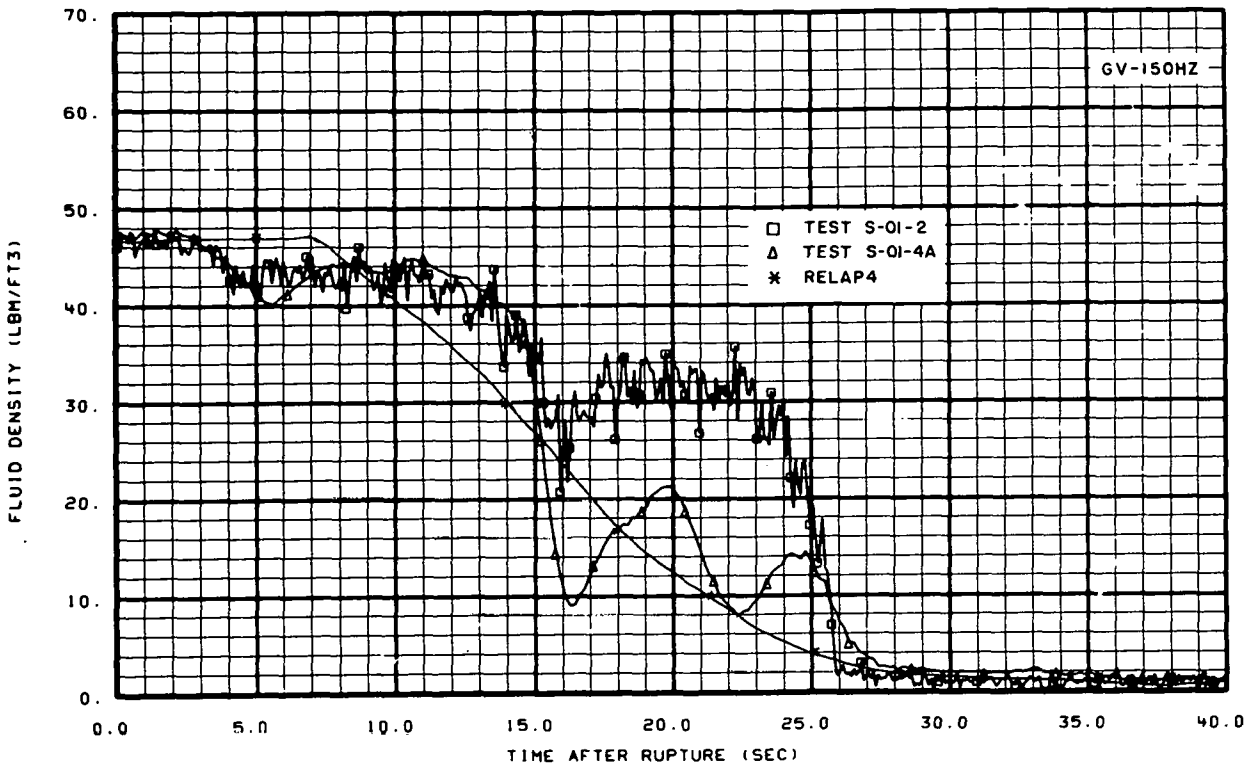

Fig. 39 Fluid density at entrance core – Tests S-01-2 and S-01-4A.

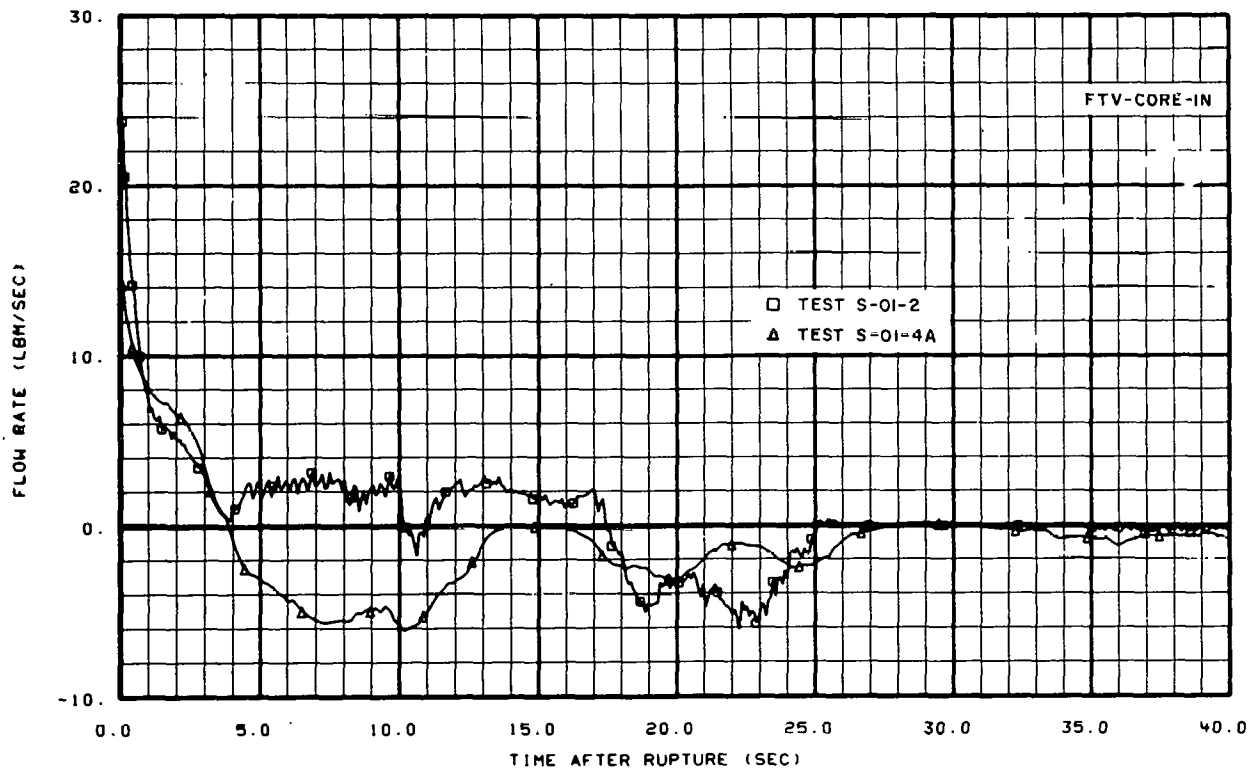

Fig. 40 Flow rate at entrance to core – Tests S-01-2 and S-01-4A.

conclusion was reached that the core turbine flowmeter may not have been functioning properly but evidence is not sufficient to definitely prove this conclusion. A detailed presentation of the nine measurements studied is presented in Appendix B.

Since break flow conditions strongly influence the core behavior, the fluid response at the breaks was studied with respect to high versus low intact loop resistance. Both the flows and densities at the break for the two tests indicate no appreciable effect on break fluid response due to the different intact loop resistances. Figures 41 and 42 show this close similarity of results.

In summary, a change in intact loop flow resistance during blowdown changes the fluid behavior near the intact loop pump and, more significantly, within the core region. The fluid density at the inlet to the core was significantly changed, although the change was not consistent with RELAP4 calculations. The turbine flowmeter measurement at the core inlet also showed a difference of results for the two tests, although the turbine flowmeter measurement for Test S-01-2 is in question. In view of the inconsistency between measured and calculated fluid densities, and the questionable turbine flowmeter measurements, the conclusion is reached that the effect on core performance of high versus low intact loop resistance is uncertain.

3.2 Cold Leg Versus Hot Leg Break Configuration

The effect on system response of a 100% hot leg break, rather than a 200% cold leg break, is demonstrated through an analysis and comparison of results from Tests S-01-1B and S-01-4A. The effect of break size and location of break on system response is large. The depressurization rate for the two tests of interest is presented in Figure 43. The slower depressurization rate of Test S-01-1B (as compared to that of Test S-01-4A) corresponds to a pronounced difference in flow rate out the vessel-side break as shown in Figure 44. The differences in break flow rate from the side of the break which includes the broken loop simulators are not as pronounced, as indicated in Figure 45. However, the actual distribution of break flows was significantly different for Test S-01-1B as compared to Test S-01-4A. The 100% hot leg break test (Test S-01-1B) had an almost equal distribution of break flow out each side of the break, whereas the 200% cold leg break test (Test S-01-4A) resulted in about 65% of the system fluid leaving the vessel side of the break (least resistive path) and 35% leaving the pump side of the break.

The strongest differences in behavior between the hot leg and the cold leg break tests occurred within the core region. The fluid response at the entrance to the core is shown in Figure 46. The equal break flow distribution of Test S-01-1B resulted in positive flow through the core for the entire blowdown period. The continued positive flow through the core resulted directly from large flow rates in the hot leg combined with the parallel influence of the pump. The positive flow through the core resulted in a much higher density within the core for Test S-01-1B (shown in Figure 47) than existed for Test S-01-4A. The higher density fluid for Test S-01-1B indicates better cooling characteristics existed within the core region for the 100% hot leg break configuration than for the 200% cold leg break configuration.

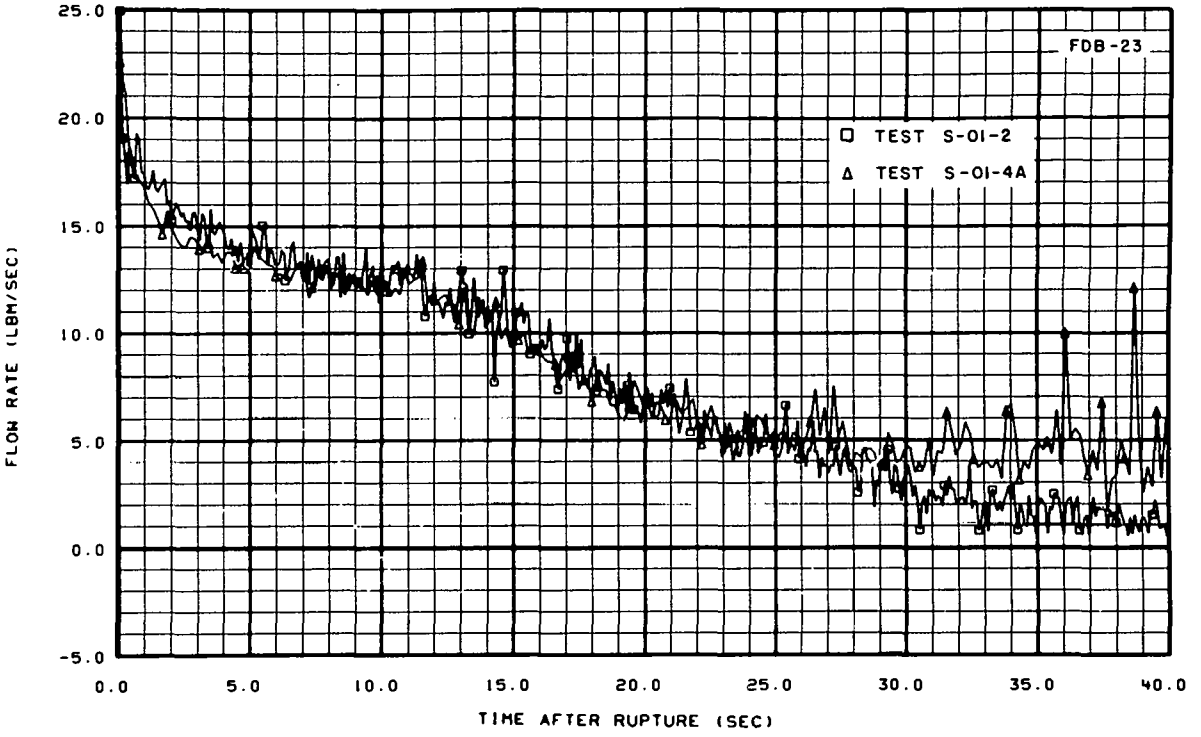

Fig. 41 Flow rate at vessel side of break – Tests S-01-2 and S-01-4A.

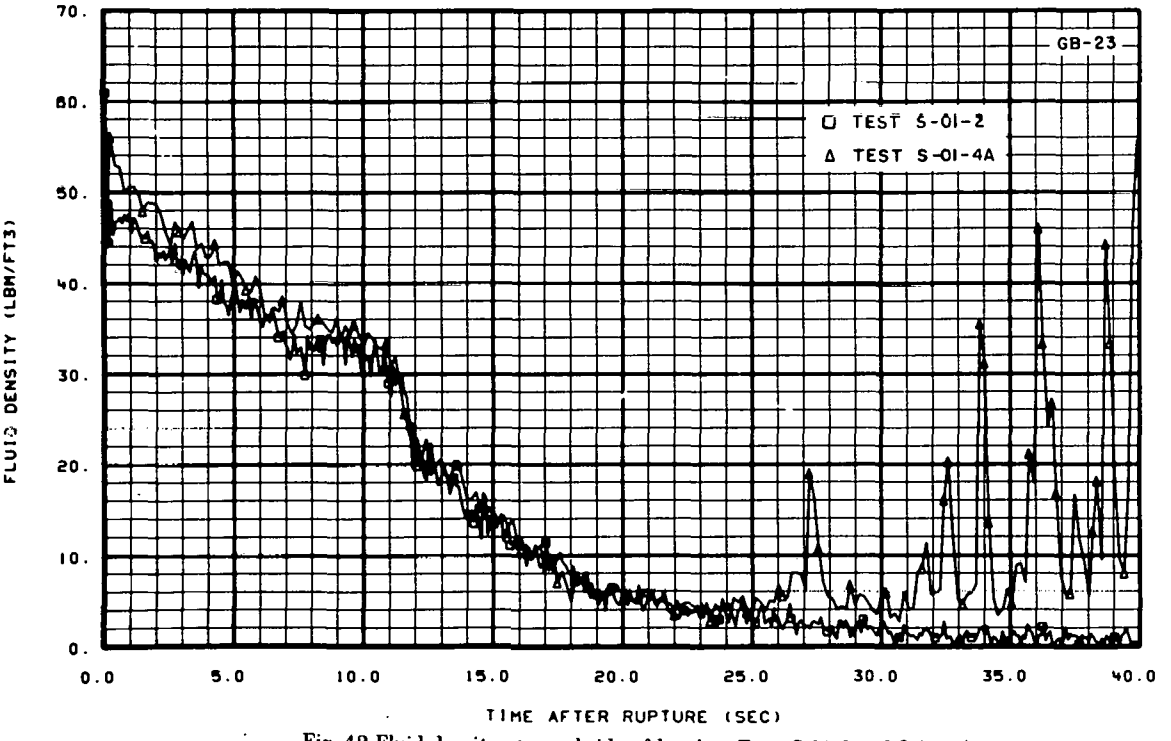

Fig. 42 Fluid density at vessel side of break – Tests S-01-2 and S-01-4A.

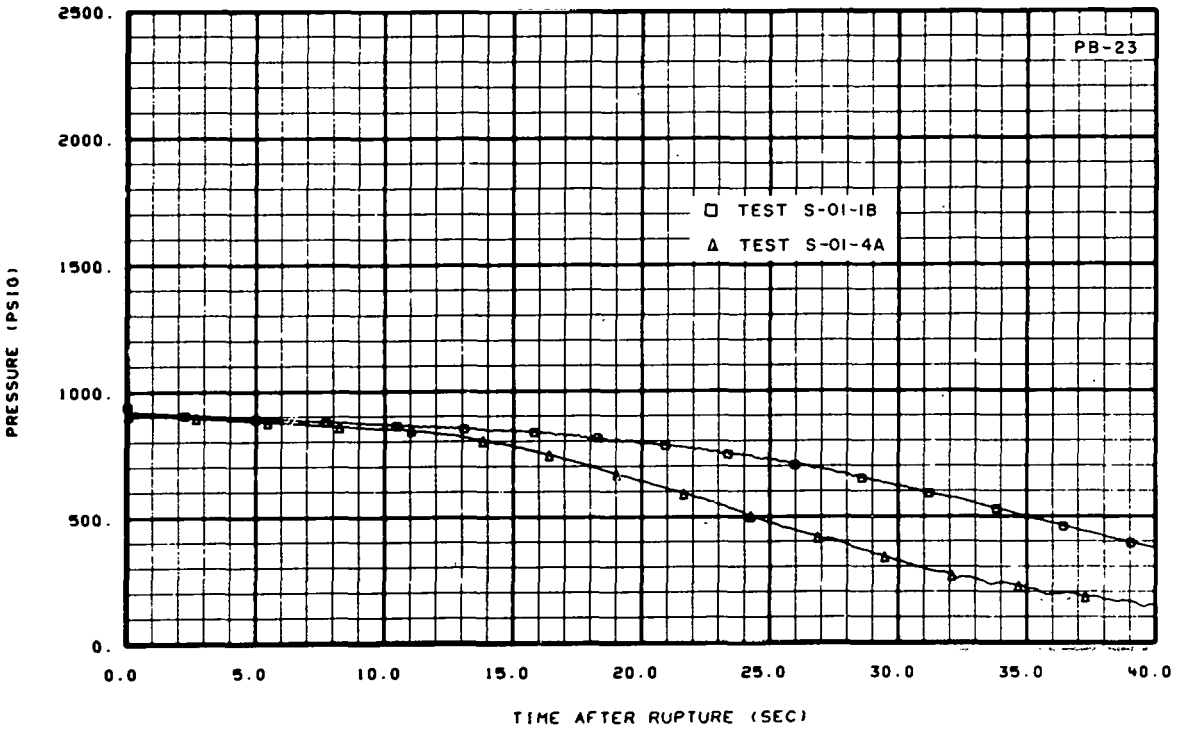

Fig. 43 Pressure at vessel side of break – Tests S-01-1B and S-01-4A.

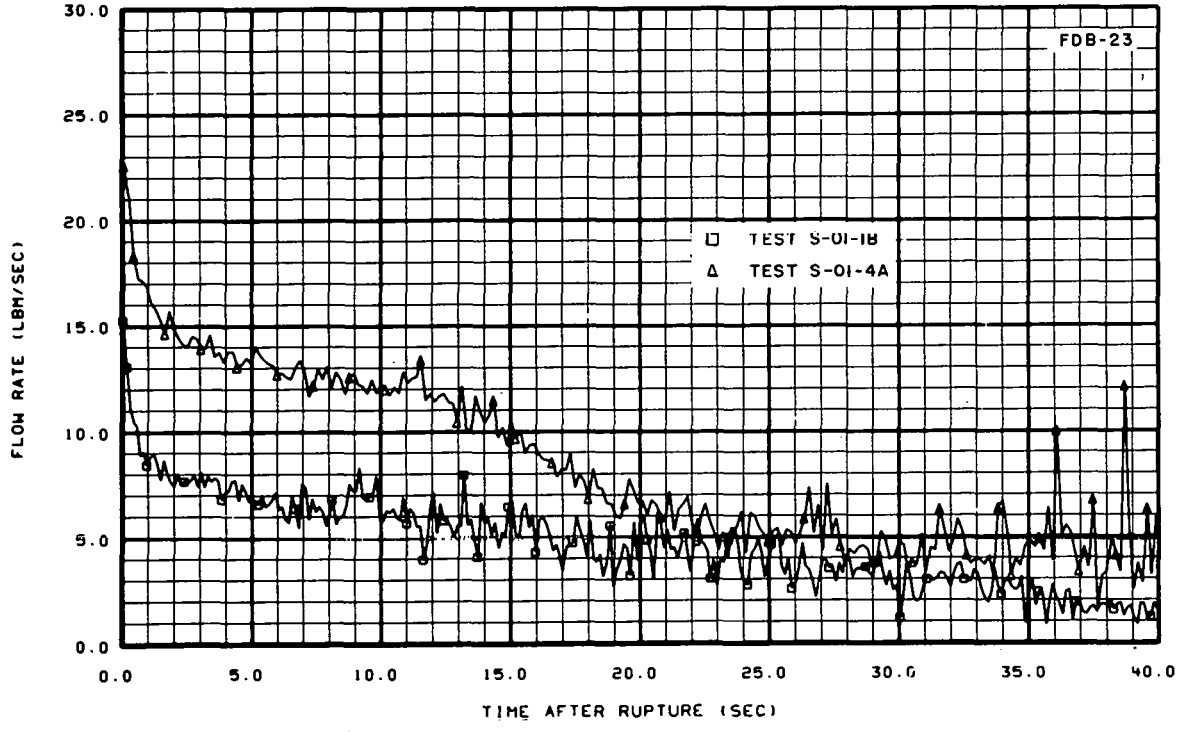

Fig. 44 Flow rate at vessel side of break – Tests S-01-1B and S-01-4A.

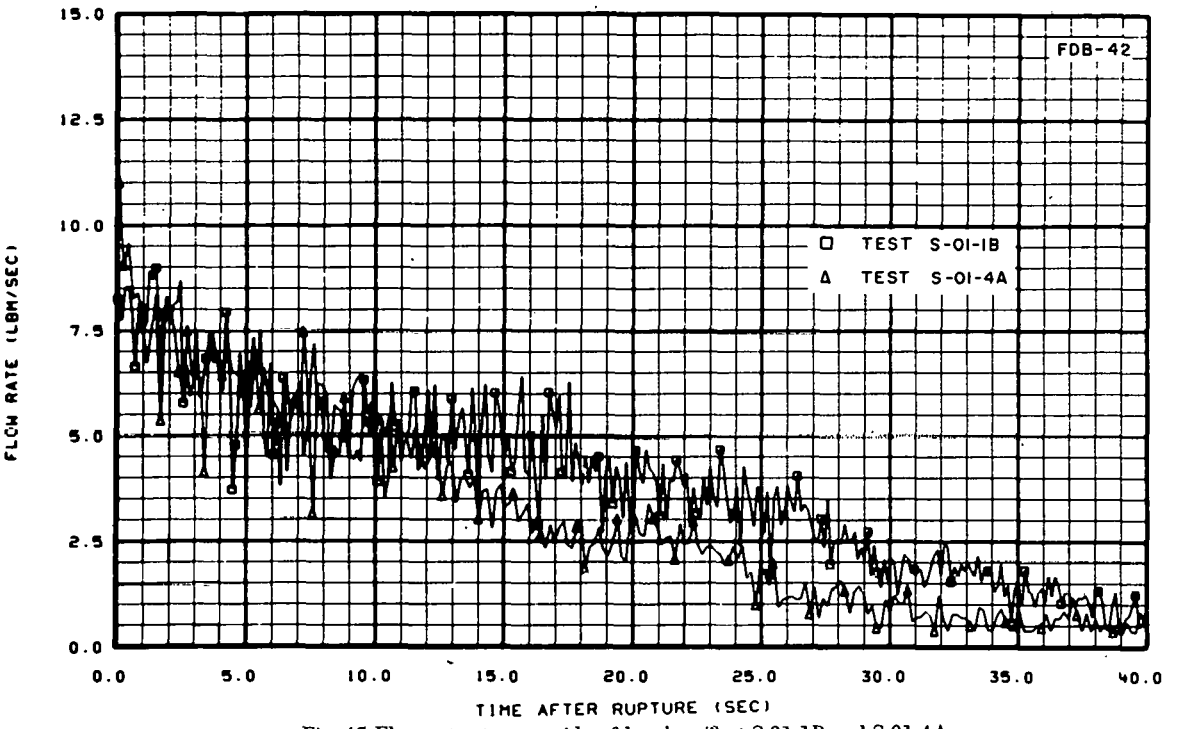

Fig. 45 Flow rate at pump side of break – Test S-01-1B and S-01-4A.

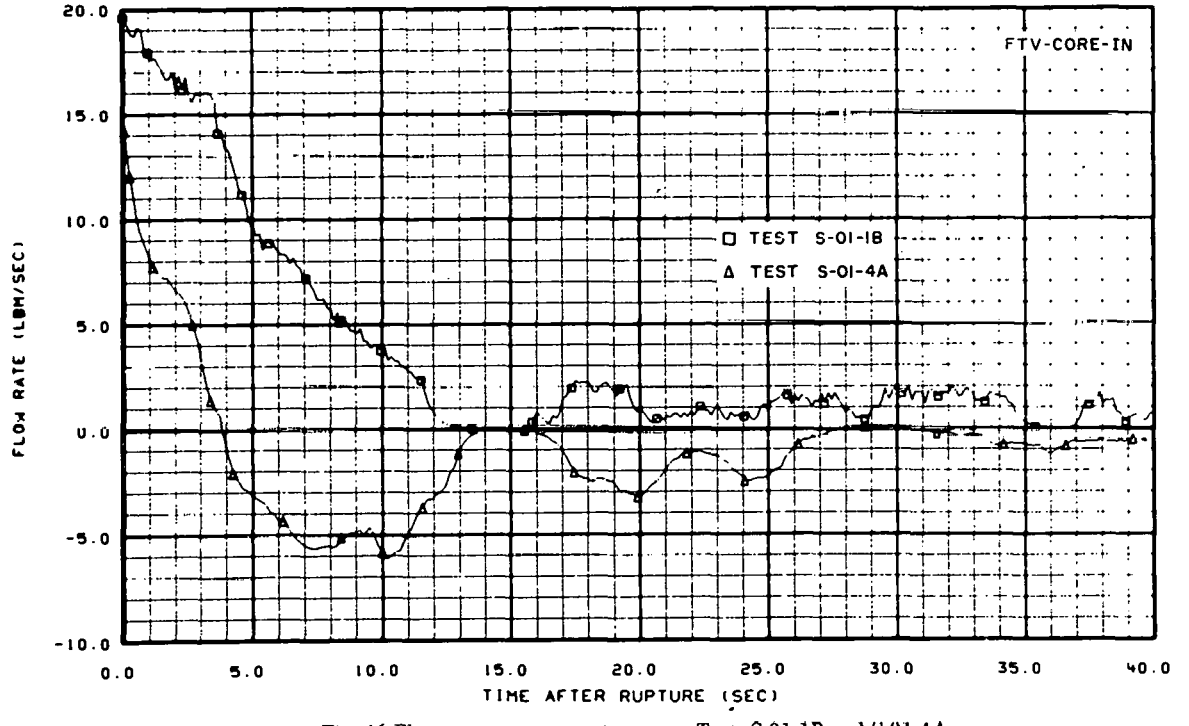

Fig. 46 Flow rate at entrance to core – Tests S-01-1B and S-01-4A.

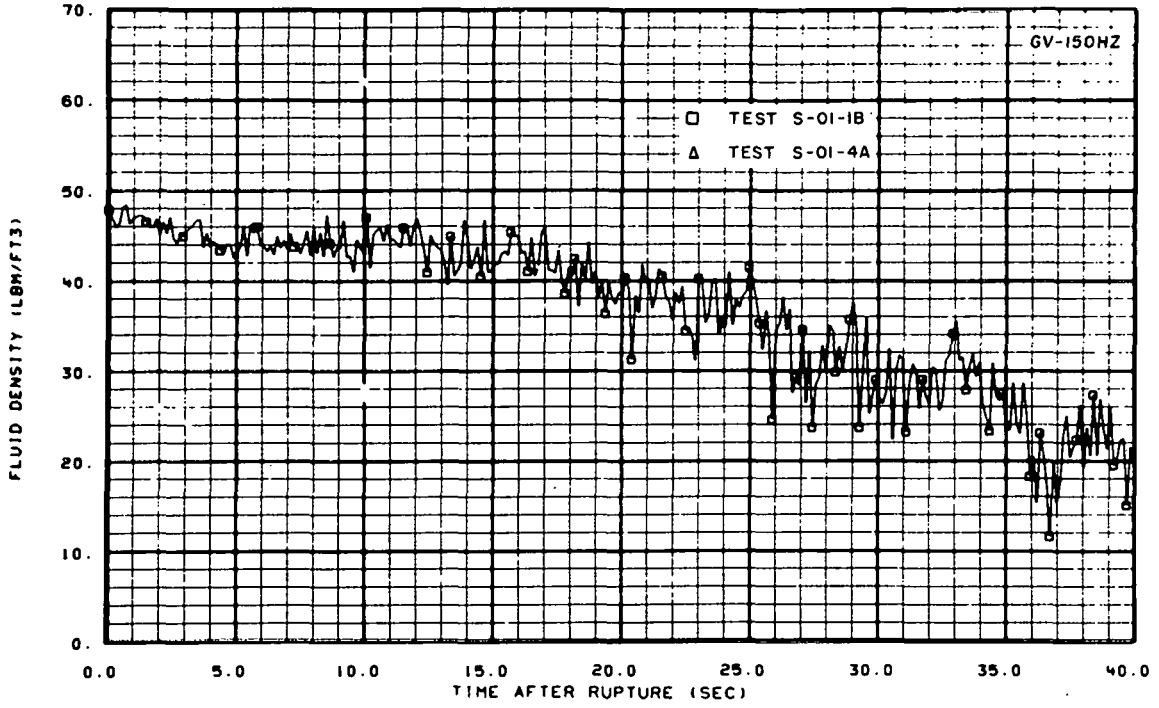

Fig. 47 Fluid density at entrance to core – Tests S-01-1B and S-01-4A.

3.3 Nitrogen Versus Water in Steam Generator

The effect upon system response caused by the energy transfer from the secondary side of the steam generator is demonstrated through an analysis and comparison of results from Tests S-01-4 and S-01-5. Both tests were 200% offset shear cold leg break tests with ECC injection into the cold leg of the intact loop. Test S-01-4 employed an intact loop steam generator maintained in a hot standby condition. Test S-01-5 was an exact repeat of Test S-01-4 with the exception that the steam generator secondary was filled with nitrogen gas maintained at the corresponding hot standby condition. The steam generator was instrumented with four metal and four secondary fluid thermocouples paired to provide an indication of the heat transfer to the primary fluid during blowdown.

Intact loop secondary to primary steam generator heat transfer was found to have little, if any, effect on overall system performance during the blowdown transient. Local effects were noted to occur primarily between the steam generator outlet and the vessel cold leg inlet. However, the local variations in blowdown response noted in comparing the two tests had very little effect on overall system performance. Calculations indicate that the total steam generator heat transfer to the primary fluid was about 3,000 Btu for both Tests S-01-4 and S-01-5 with the steam generator maintained in a hot standby condition. Although no secondary water was used for Test S-01-5, about 1,500 Btu of energy was removed from the steam generator tubes.

The model used in RELAP4 to predict steam generator heat transfer consists of four control volumes on the primary side, each with a two-dimensional heat slab, and one control volume on the secondary side containing the secondary fluid. In general, the RELAP4 code did an adequate job of modeling the intact loop steam generator performance for Tests S-01-4 and S-01-5. RELAP4 predicted no appreciable difference in system response due to the two different steam generator secondary side fluids.

2.4 40-Heater-Rod Core Versus Core Simulator

The system configuration and initial conditions for Test S-01-6 were basically identical to those of Test S-01-4A except that the 40-heater-rod core was used for Test S-01-6, whereas a core resistance simulator was used for Test S-01-4A. The 40-rod core had less resistance ($R' = 0.815$ $sec^2/in.^2\text{-}ft^3$) than the core simulator ($R' = 1.77$ $sec^2/in.^2\text{-}ft^3$), with the resistance being distributed more uniformly over the length of the core region for the 40-rod core. Because of the existence of the 40 rods, the liquid volume in the core region of the vessel was also less for Test S-01-6 than for those tests which used the core simulator.

Comparison of system response between Tests S-01-4A and S-01-6 has revealed very little difference between the two tests, except at measurement stations near the core region. Core inlet flow for these two tests is shown in Figure 48. For about 5 seconds, the flows for the two tests are identical. The lower fluid density at the core entrance shown in Figure 49 and the lower flow rate shown in Figure 48 for Test S-01-6 indicate the fluid voided the core in a shorter time.

Two possible causes for these differences in core response are the influence of the break conditions on the core, and the influence of having a different core configuration and resistance distribution. Previous isothermal tests within this series indicate a strong influence on the core response of the break flow conditions. Figures 50 and 51 show that the broken loop break flow rates for Tests S-01-6 and S-01-4A are very similar. Since the system configuration and initial conditions for Test S-01-6 were basically identical to those of Test S-01-4A except for the 40-heater-rod core, and since the break conditions of the two tests were similar, the conclusion reached is that the major difference in core response is due to the difference in core configuration and resistance distribution.

In summary, data evaluation of Tests S-01-6 and S-01-4A indicates that the presence of the 40-rod core during Test S-01-6 did not appreciably alter the phenomena occurring in the intact and broken loops. However, the density and volumetric flow at the core inlet were affected with the density dropping to a low value early in Test S-01-6 and the volumetric flow increasing sharply over this same time period. The Test S-01-6 mass flow at the core inlet, which is the combination of the density and volumetric flow, was similar to that of other isothermal tests even though the core inlet density and volumetric flows were different.

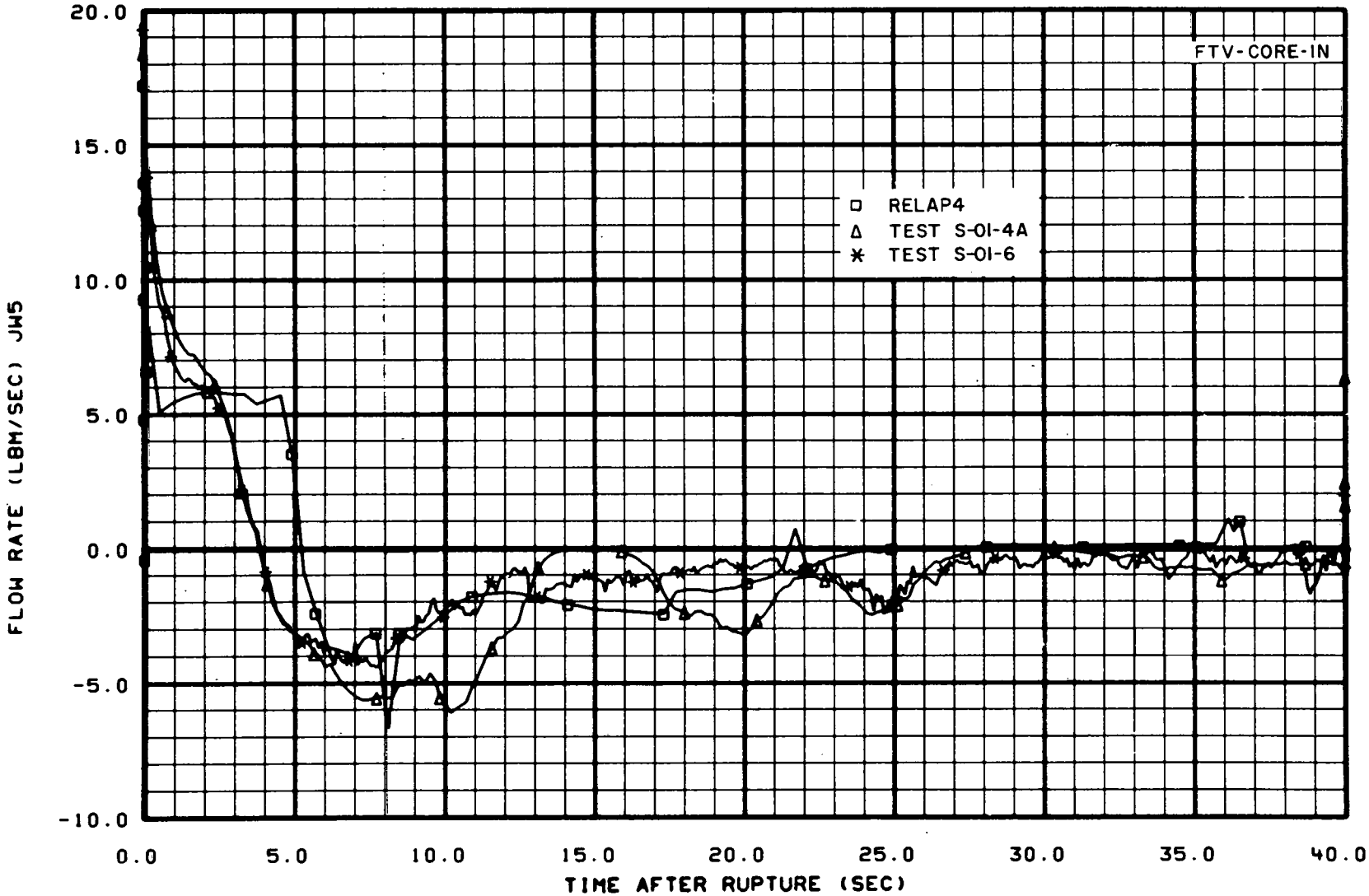

Fig. 48 Flow rate at entrance to core – Tests S-01-4A and S-01-6.

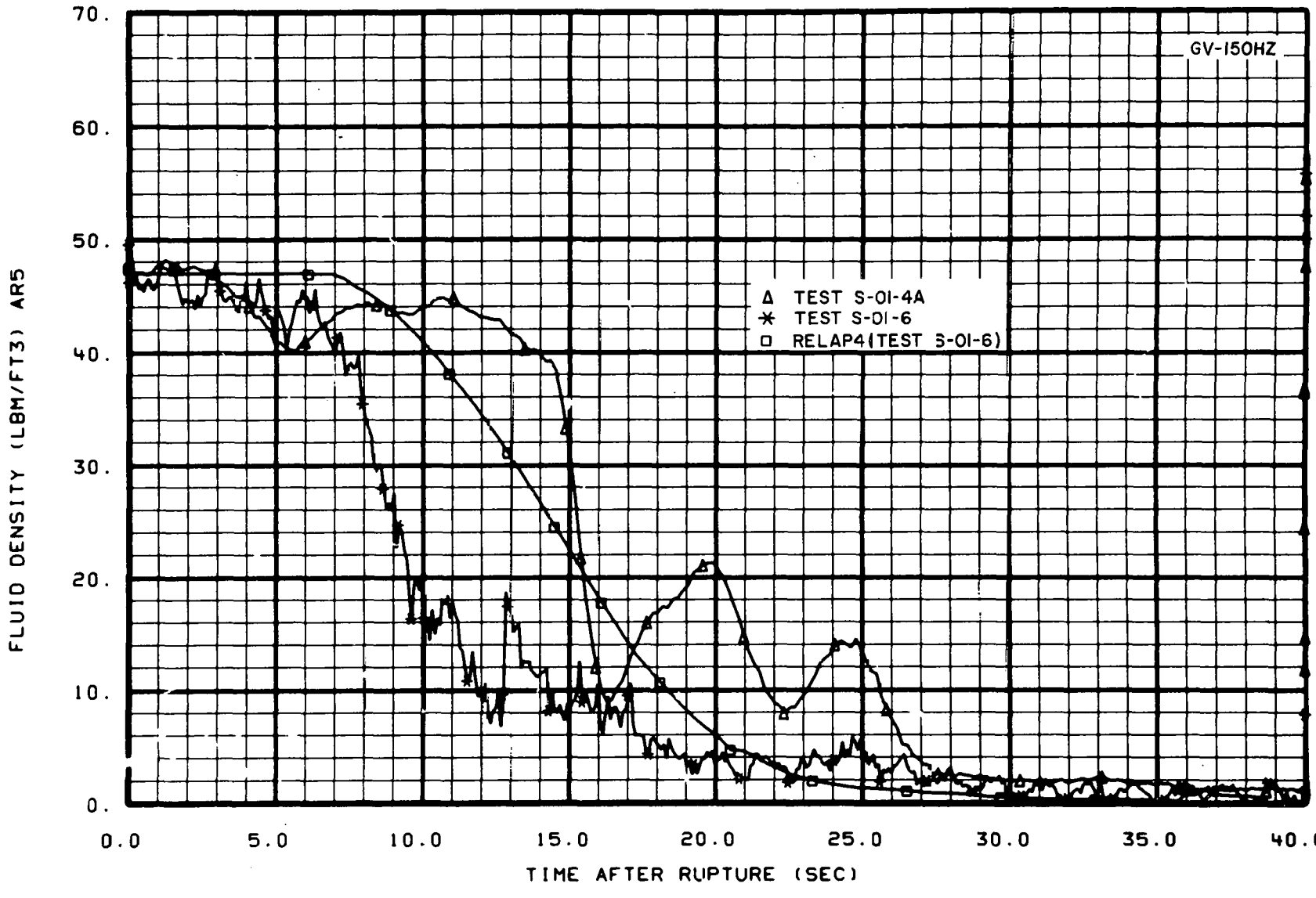

Fig. 49 Fluid density at entrance to core – Tests S-01-6.

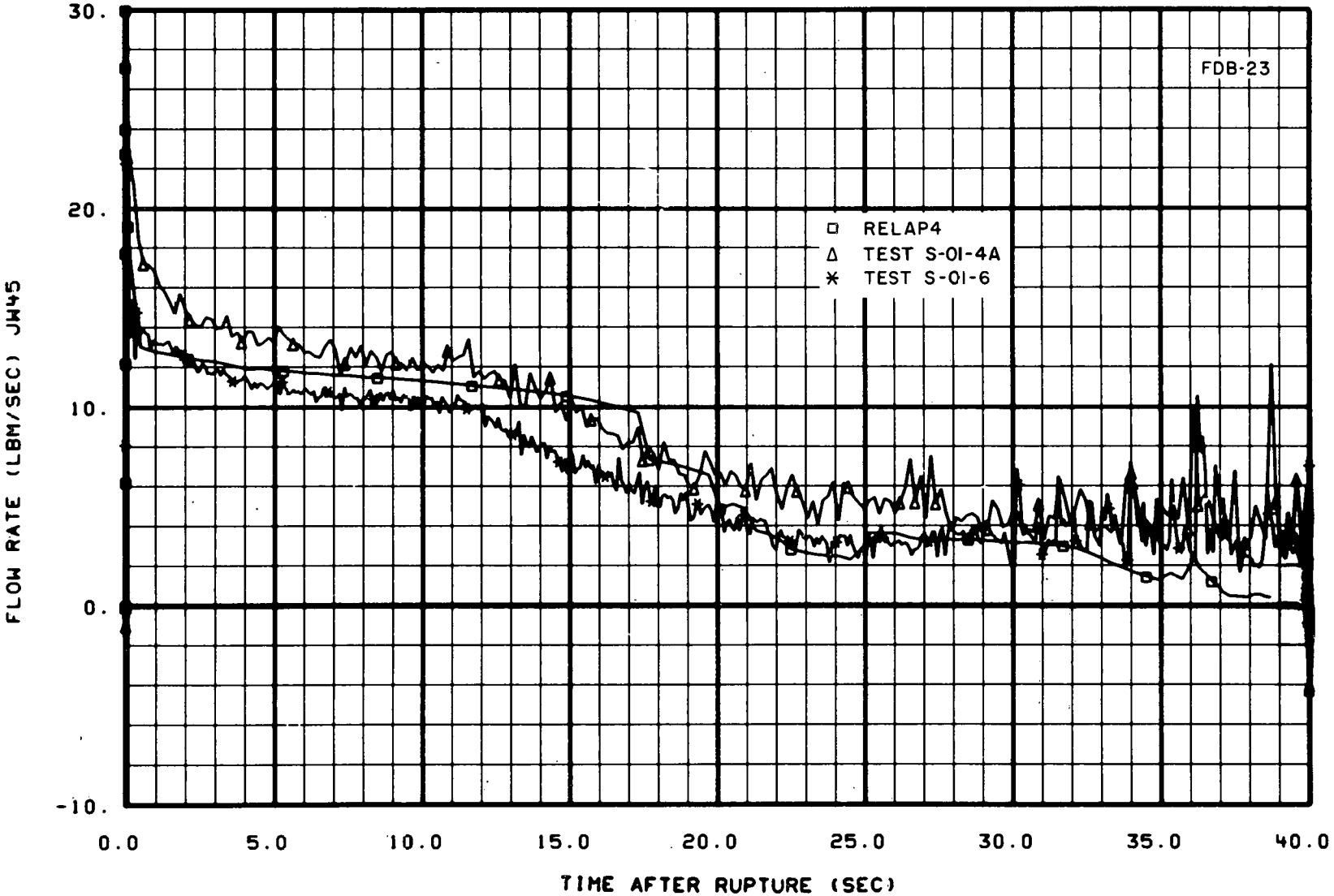

Fig. 50 Flow rate at vessel side of break – cold leg break Tests S-01-4A and S-01-6.

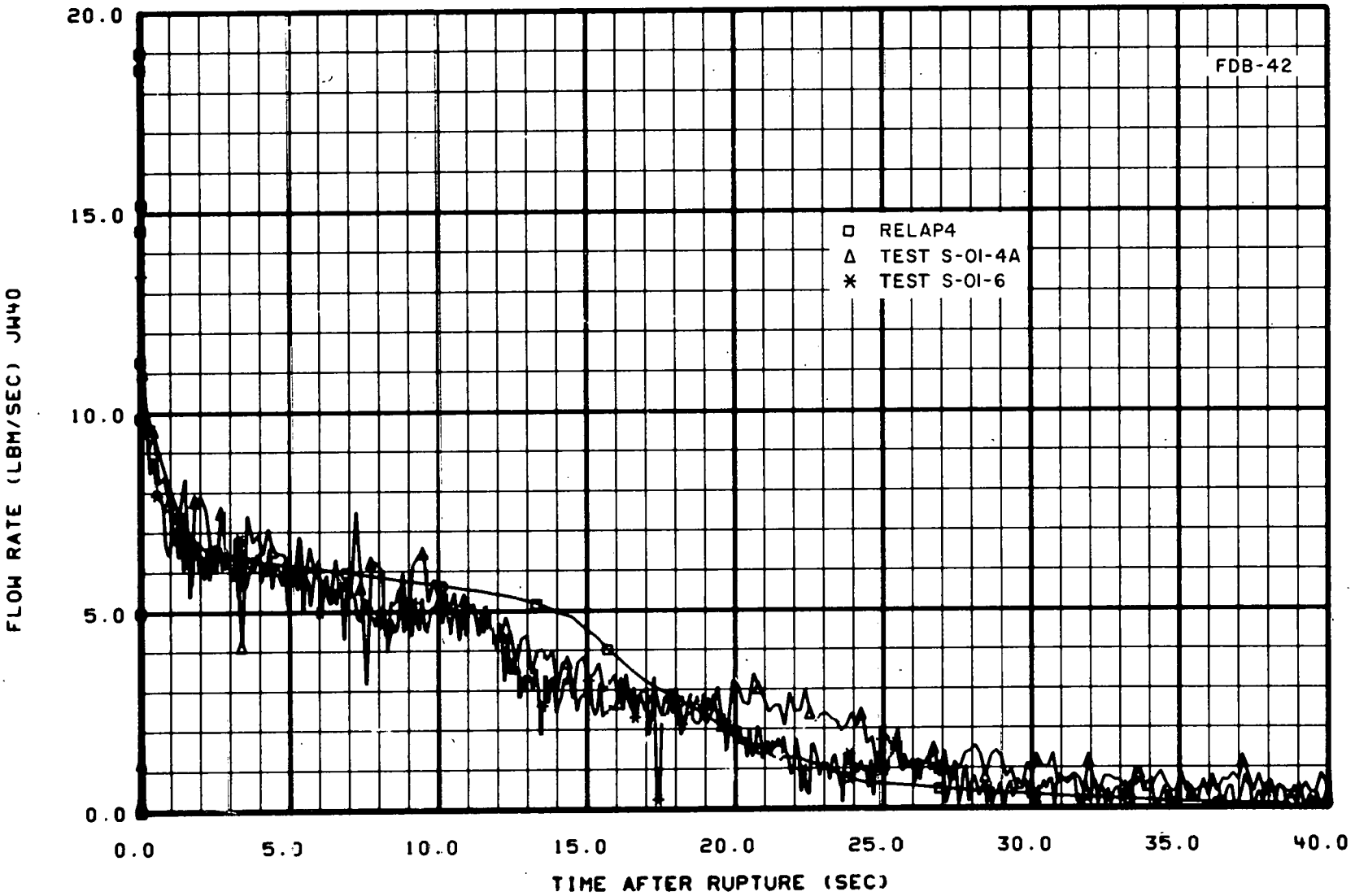

Fig. 51 Flow rate at pump side of cold leg break Tests S-01-4A and S-01-6.

IV. CONCLUSIONS

The thermal-hydraulic response of the Semiscale Mod-1 system during an isothermal blowdown has been investigated. The results from the isothermal tests have led to an increased understanding of the heat transfer and flow processes that occur throughout the Semiscale Mod-1 system during a loss-of-coolant test and are valuable for evaluating the adequacy and improving the predictive capability of analytical models developed to predict system response and ECC behavior during an LOCA.

The author has reached the following conclusions from the results of the Semiscale Mod-1 isothermal test series data analysis.

1. PHENOMENA WHICH STRONGLY INFLUENCE SYSTEM BEHAVIOR

During blowdown, the system fluid response is principally a function of the break and pump conditions. The break and pump conditions compete with each other in determining the magnitudes and direction of fluid flow through the Semiscale Mod-1 system during the first few seconds of the blowdown. However, the pump head rapidly degrades and after the first several seconds the system response is primarily determined by the break flow. The principal influence of the break flow rates and fluid conditions on system response occurs within the core region, causing the core flow rate to approach zero between 10 and 15 seconds after rupture.

An analysis of the emergency core coolant influence on the system indicated that periodic oscillatory flow existed about the injection point within the intact loop cold leg during ECC injection. Downcomer countercurrent flow, bypass flow, and heat transfer phenomena were the variables controlling when ECC reached the lower plenum.

Analyses of the piping heat transfer and steam generator performance have led to the conclusion that the intact and broken loop piping heat transfer is sensitive to azimuthal location in a given pipe, location of the pipe in both the intact and broken loops, and the broken loop break characteristics. Maximum heat transfer has been shown to occur in the bottom of horizontal pipe sections. Heat transfer from the steam generator, operating in the hot standby condition, did not significantly affect the overall behavior of the Semiscale Mod-1 system.

2. REPEATABILITY OF RESULTS

In general, the results for the isothermal test series provided data which were quite repeatable up to the time of accumulator ECC injection. The general performance with respect to the trends of the data was also repeatable after inititation of ECC injection; however, magnitudes varied somewhat.

3. COMPARISON OF RESULTS FROM DIFFERENTIAL TESTS

The effect on system response of having different intact loop flow resistances during blowdown was to change the fluid behavior near the intact loop pump and, more significantly, within the core region. The fluid density at the inlet to the core was quite different. The turbine flowmeter measurement at the core inlet also showed a difference of results for these two tests, although other measurements around the core region indicate the turbine flowmeter measurement for Test S-01-2 may be questionable. Due to the questionable turbine flowmeter measurement, the effect on core performance of high versus low intact loop resistance cannot be conclusively stated.

Intact loop secondary to primary steam generator heat transfer was found to have little, if any, effect on overall system performance during the blowdown transient. Local effects were noted to occur primarily between the steam generator outlet and the vessel cold leg inlet. However, the local variations in blowdown response noted in comparing the two tests had very little effect on overall system performance.

The effect of break size and location on system response was demonstrated to be large when results from a 100% hot leg break test were compared with data from a 200% cold leg break test. The most significant difference occurred within the core region. The positive flow through the core throughout blowdown for the hot leg break resulted in a much higher density within the core than existed for the cold leg break, leading to the conclusion that better cooling characteristics existed within the core for the 100% hot leg break configuration than for the 200% cold leg break configuration.

The presence of the 40-heater-rod core during Test S-01-6 did not appreciably alter the phenomena occurring in the intact and broken loops. However, the density and volumetric flow at the core inlet were affected, with the density dropping to a low value early in the test and the volumetric flow increasing sharply over this same time period. The mass flow at the core inlet, which is the combination of the density and volumetric flow, was similar to that of other isothermal tests even though the core inlet density and volumetric flows were different.

V. REFERENCES

1. K. V. Moore and W. H. Rettig, *RELAP4 – A Computer Program for Transient Thermal-Hydraulic Analysis,* ANCR-1127 (December 1973).

2. S. N. Zender, *Experiment Data Report for Semiscale Mod-1 Test S-01-2 (Isothermal Blowdown with Core Resistance Simulator),* ANCR-1194 (February 1975).

3. S. N. Zender, *Experiment Data Report for Semiscale Mod-1 Test S-01-3 (Isothermal Blowdown With Core Resistance Simulator),* ANCR-1195 (March 1975).

4. S. N. Zender, M. F. Jensen K. E. Sackett, *Experiment Data Report for Semiscale Mod-1 Tests S-01-4 and S-01-4A (Isothermal Blowdown with Core Resistance Simulator),* ANCR-1196 (March 1975).

5. S. N. Zender, H. S. Crapo, M. F. Jensen, K. E. Sackett, *Experiment Data Report for Semiscale Mod-1 Test S-01-5 (Isothermal Blowdown with Core Resistance Simulator),* ANCR-1197 (April 1975).

6. S. N. Zender, H. S. Crapo, M. F. Jensen, K. E. Sackett, *Experiment Data Report for Semiscale Mod-1 Test S-01-1 (Isothermal Blowdown with Core Resistance Simulator),* ANCR-1198 (April 1975).

7. S. N. Zender, H. S. Crapo, M. F. Jensen, K. E. Sackett, *Experiment Data Report for Semiscale Mod-1 Test S-01-1B (Isothermal Blowdown with Core Resistance Simulator),* ANCR-1199 (May 1975).

8. H. S. Crapo, M. F. Jensen, K. E. Sackett, *Experiment Data Report for Semiscale Mod-1 Test S-01-6 (Isothermal Blowdown with 40-Rod Heater Core),* ANCR-1253 (September 1975).

9. R. T. French, *An Evaluation of Piping Heat Transfer, Piping Flow Regimes, and Steam Generator Heat Transfer for the Semiscale Mod-1 Isothermal Tests,* ANCR-1229 (August 1975).

10. G. G. Loomis *Intact Loop Pump Performance During the Semiscale Mod-1 Isothermal Test Series,* ANCR-1240 (November 1975).

11. D. J. Hanson, R. T. French, C. J. Shaffer, *An Evaluation of ECC Related Phenomena During Semiscale Mod-1 Isothermal Tests,* ANCR-1239 (December 1975).

12. R. E. Henry and H. K. Fauske, *"The Two-Phase Critical Flow of One-Component Mixtures in Nozzles, Orifice, and Short Tubes", Journal of Heat Transfer,* Trans. ASME (May 1971).

13. F. J. Moody, *"Maximum Flow Rate of a Single Component, Two-Phase Mixture", Journal of Heat Transfer,* Trans. ASME (February 1965).

14. R. S. Alder, E. M. Feldman, P. A. Pinson, *Experiment Data Report for 1-1/2-Loop Semiscale System Isothermal Tests 1008 and 1010,* ANCR-1145 (March 1974).

15. D. J. Olson, *Single- and Two-Phase Performance Characteristics of the Mod-1 Semiscale Pump Under Steady State and Transient Fluid Conditions,* ANCR-1165 (October 1964).

16. D. J. Olson, *Experiment Data Report for Single- and Two-Phase Steady State Tests of the 1-1/2-Loop Mod-1 Semiscale System Pump,* ANCR-1150 (May 1974).

17. D. J. Hanson, C. E. Cartmill, K. R. Perkins, C. J. Shaffer, D. M. Snider, *ECC Performance in the Semiscale Geometry* ANCR-1161 (June 1974).

18. G. B. Wallis, J. A. Block, S. R. Johnson, *An Analysis of Cold Leg ECC Flow Oscillations* CREARE TN-196 (August 1974).

19. C. J. Barcozy, *A Systematic Correlation for Two-Phase Pressure Drop,* NAA-SR-MEMO-11858 (March 1966).

20. J. R. S. Thom et al, *"Boiling in Subcooled Water During Flow Up Heated Tubes or Annuli", Proc. Instsn. Mech. Engrs.,* 180 Part 3C (1966) pp 226-246.

APPENDIX A

RELAP4 COMPUTER CODE AS APPLIED

TO SEMISCALE MOD-1 THERMAL-HYDRAULIC ANALYSIS

THIS PAGE

WAS INTENTIONALLY

LEFT BLANK

APPENDIX A

RELAP4 COMPUTER CODE AS APPLIED TO SEMISCALE MOD-1 THERMAL-HYDRAULIC ANALYSIS

The RELAP4 computer program[A-1] was developed primarily to describe the transient behavior of water-cooled nuclear reactors subjected to postulated accidents such as those resulting from loss of coolant, pump failure, or nuclear power variations. Since features of the program that describe the nuclear reactor are optional, the program can be applied to experimental water-reactor simulators such as the Semiscale Mod-1 system.

The Semiscale Mod-1 system is modeled in RELAP4 as a set of fluid control volumes connected by flow junctions. Numerical methods calculate the fluid conditions within the control volumes during an assumed depressurization, such as would occur from a double-ended offset shear of a primary coolant pipe.

The geometric and thermodynamic features of the system to be analyzed are input to the program. Geometric features necessary to describe the volumes are fluid volume, elevation, flow area, hydraulic flow resistance, and surface areas and volumes of hardware which exchange energy with the fluid. Power generation in the components, thermal properties of the components, and initial conditions of the fluid are input thermodynamic features. Other required inputs include junctions connecting the fluid volumes, pump models, bubble rise models, and choices of heat transfer correlations and flow choking models. Given the mechanical and thermodynamic features and initial conditions of the system, RELAP4 then solves an integral form of the one-dimensional momentum, energy, and mass conservation equations of each control volume.

The RELAP4 model of the Semiscale Mod-1 system includes 55 control volumes interconnected with 57 junctions including the junctions for ECC injection. Junctions occur at the approximate location of the experimental measurements to facilitate comparisons between calculations and data. The RELAP4 model of the Semiscale Mod-1 system in the 200% cold leg break configuration is shown in Figure A-1 and that for the 100% hot leg break configuration is shown in Figure A-2. Table A-1 gives a description of the control volumes corresponding to Figure A-1. A description of the control volumes corresponding to Figure A-2 can be obtained by referring to the corresponding volume difference between Figures A-1 and A-2.

Included in the RELAP4 Semiscale Mod-1 isothermal system model is the best-estimate pump head and torque models for the Semiscale pump. The best-estimate pump head model option used in RELAP4 has been improved by changing the head multiplier function which has been updated following recent evaluation of isothermal blowdown data. The best-estimate torque model has been improved by use of a simple torque multiplier function dependent upon average void fraction, which was determined from Semiscale isothermal blowdown data.

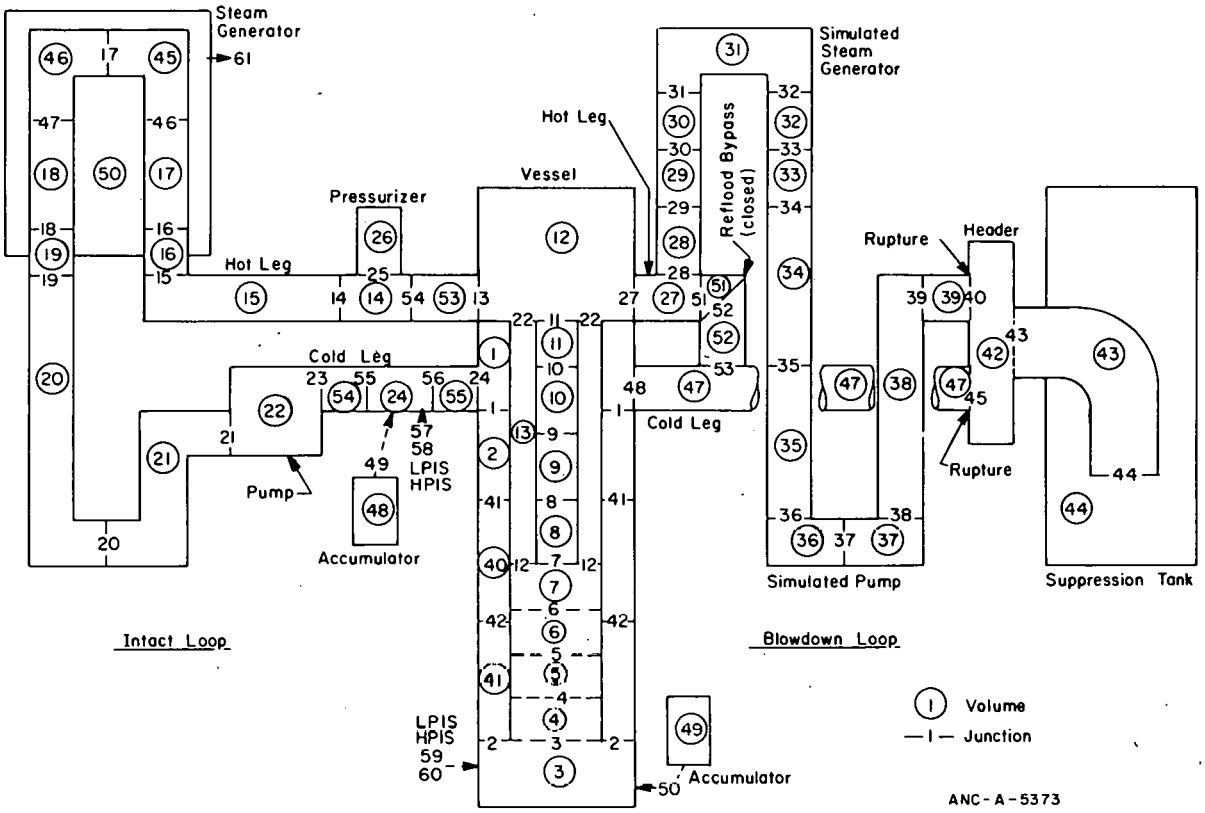

Fig. A-1 RELAP4 Semiscale Mod-1 flow diagram – 200% cold leg break configuration.

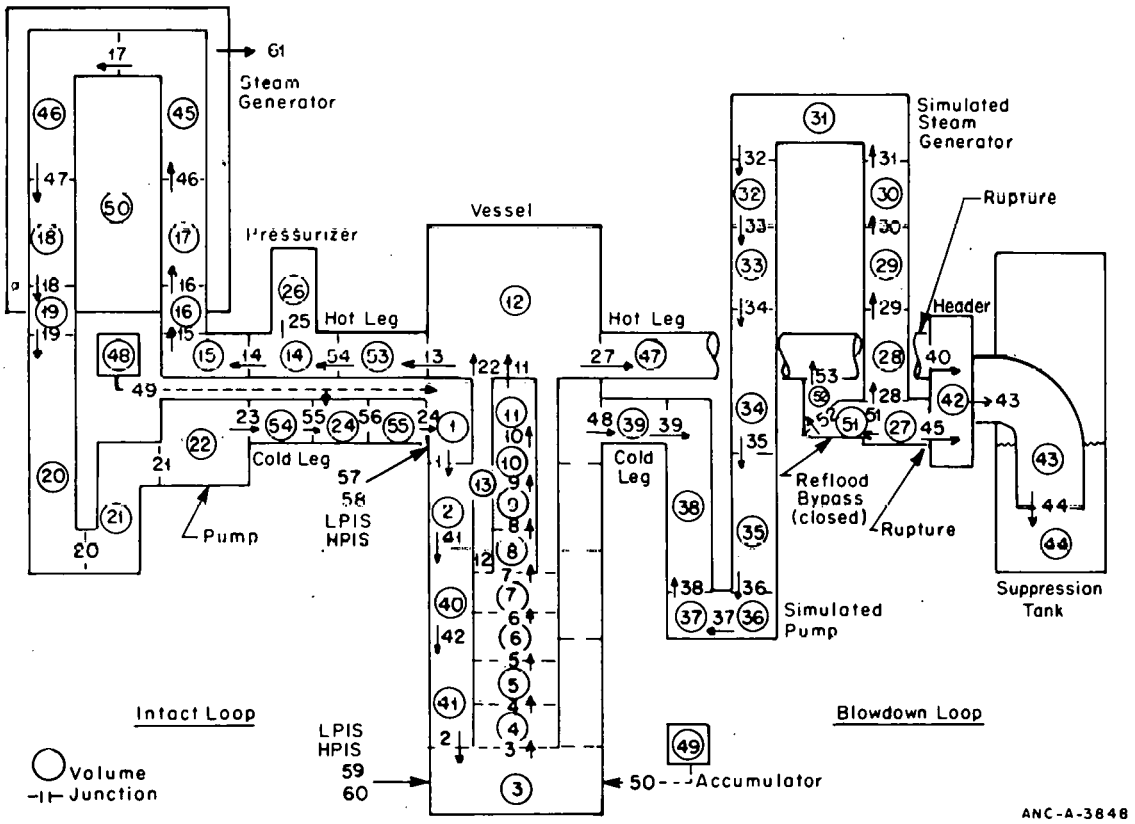

Fig. A-2 RELAP4 Semiscale Mod-1 flow diagram -- 100% hot leg break configuration.

TABLE A-1

RELAP4 SEMISCALE MOD-1 MODEL
FOR 200% COLD LEG BREAK CONFIGURATION[a]

Volume	Description
1	Inlet Annulus
2	Top Third of Downcomer
3	Lower Plenum
4	Mixer Region and Lower Instrumentation
5	
6	Lower Core Barrel
7	
8	Main Flow of Core Simulator
9	
10	
11	
12	Upper Plenum
13	Core Simulator Bypass
14	Center Third of Operating Hot Leg
15	Last Third of Operating Hot Leg
16	Inlet Chamber of Steam Generator
17	First Fourth of U-Tubing of Steam Generator
18	Last Fourth of U-Tubing of Steam Generator
19	Outlet Chamber of Steam Generator
20	3-inch Pipe of Steam Generator Outlet to Bottom of U-Bend
21	3-inch Pipe of Bottom of U-Bend to Pump Inlet
22	Pump
23	Not used
24	Center Third of Operating Cold Leg
25	Surge Line
26	Pressurizer
27	Blowdown Cold Leg to Bottom of Simulated Steam Generator
28	Bottom of First Orifice

TABLE A-1 (contd.)

Volume	Description
29, 30	All Orifices on Upstream Side of Simulated Steam Generator
31	Top Piping in Simulated Steam Generator
32, 33	Include all Orifices on Downstream Side of Simulated Steam Generator
34	Simulated Steam Generator -- Last Orifice Outlet to Piping Neck Down
35	Simulated Pump Inlet Piping
36, 37	Simulated Pump Orifices
38	Simulated Pump Outlet Piping
39	Simulated Cold Leg Pump to Break
40	Middle Third of Downcomer
41	Lower Third of Downcomer
42	Header -- Pressure Suppression System
43	Downcomer -- Pressure Suppression System
44	Pressure Suppression Tank
45	Second Fourth of Steam Generator
46	Third Fourth of Steam Generator
47	Blowdown Cold Leg
48	Cold Leg Accumulator
49	Lower Plenum Accumulator (also used for blowdown side)
50	Secondary Side of Steam Generator
51	First Half (hot leg side) of Blowdown Bypass
52	Second Half (cold leg side) of Blowdown Bypass
53	First Third of Intact Loop Hot Leg
54	First Third of Intact Loop Cold Leg
55	Last Third of Intact Loop Cold Leg

[a] For system with core resistance simulator.

In modeling the Semiscale Mod-1 isothermal system for the isothermal test series, several compromises were necessary. The header and downcomer of the pressure suppression system had to be considered as containing saturated steam at 32.1 psia (244^{o}F) because RELAP4 cannot accommodate air flow through a junction. Also the pressurizer surge line had to be eliminated from the model due to numerical instability encountered when the flow from the pressurizer changed from liquid to steam. This instability appeared to be caused by the small volume of the pressurizer surge line (the surge line volume was five times smaller than any other volume in the model). The surge line volume was eliminated from the RELAP4 model, and the equivalent resistance of the line was placed at the junction between the pressurizer and the hot leg piping. The resulting solution was stable throughout blowdown.

REFERENCE

A-1. K. V. Moore and W. H. Rettig, *RELAP4 – A Computer Program for Transient Thermal-Hydraulic Analysis*, ANCR-1127 (December 1973).

APPENDIX B

HIGH VERSUS LOW INTACT LOOP RESISTANCE

THIS PAGE

WAS INTENTIONALLY

LEFT BLANK

APPENDIX B

HIGH VERSUS LOW INTACT LOOP RESISTANCE

In order to establish the importance of operating loop resistance during blowdown, Tests S-01-2 and S-01-4A were conducted with different intact loop flow resistances. The effect of the use of these two resistance values on system performance was studied during the first 20 seconds of blowdown (prior to ECC injection) at measurement locations throughout the system. The most marked difference in measured response occurred at the core inlet. However, the measurements at the core inlet for Test S-01-2 are in question as to accuracy. The purpose of this appendix is to present the results of measurements within and near the core region which were studied in arriving at the previous conclusion concerning the accuracy of the measurements for Test S-01-2.

The principal measurement of concern was that provided by the turbine flowmeter at the inlet to the core. Figure B-1 presents the flow rate calculated from the turbine flowmeter at the core barrel inlet for Tests S-01-2 and S-01-4A. The discrepancy arises because the measurement for Test S-01-2 incicates positive flow between 4 and 17 seconds after rupture, whereas the majority of the measurements studied within or around the vessel region during this time period indicate the measured flow should have actually been negative. This concept is supported through a study of the differential pressure across the vessel. Since differential pressure is the driving potential for liquid flow, the direction of flow should be determinable through a differential pressure measurement. Figure B-2 represents the pressure drop across the vessel from the cold leg to the hot leg outlet of the intact loop for both tests. From 4 seconds on, the figure indicates the pressure at Station 1 is higher than that at Station 15, implying an increasing negative flow for both tests until 10 seconds. Figure B-3 further supports this concept by showing negative flow upward through the downcomer for both tests during this time interval. For the flow rate into the vessel from the intact loop cold leg, Figure B-4 shows an almost exact overlay of results for the two tests up to about 20 seconds after rupture, indicating that the vessel inlet conditions and the downcomer performance for both tests were essentially the same for the first 20 seconds of blowdown.

If the flow rates through the core region were in opposite directions for the two tests, the hot leg fluid behavior should be significantly different for the two tests, provided the intact and broken loop phenomena were the same. Figures B-5 and B-6 show the hot leg fluid densities at Stations 1 and 5, respectively, for the two tests. Although fluid density itself does not specifiy flow direction, the close similarity of results at both stations would imply that the flow direction through the hot leg should be the same for these two tests. However, the drag disc momentum flux measurement at Station 1, shown in Figure B-7, indicates a positive flow rate for Test S-01-2, supporting positive flow through the core. The inconsistency of results could have been clarified if the turbine flowmeter at Station 1 or the drag disc within the core had functioned properly. But the turbine flowmeter was

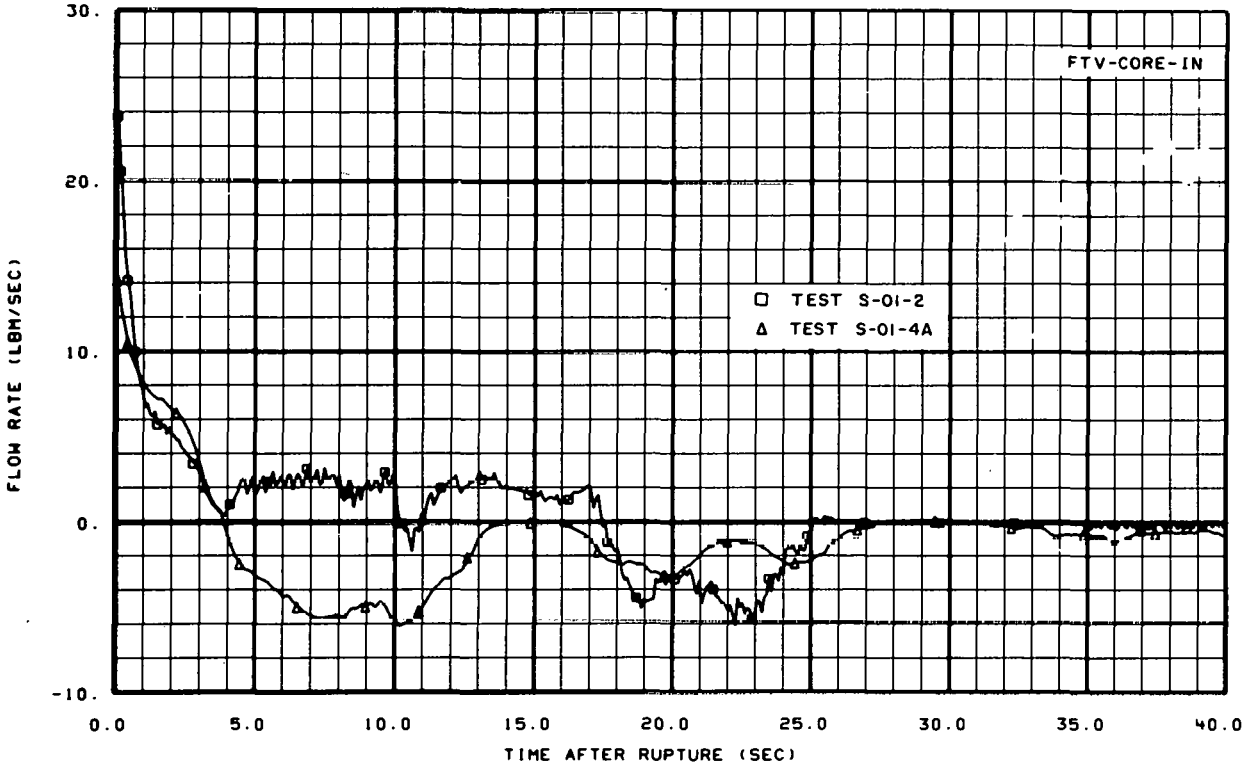

Fig. B-1 Flow rate at entrance to core – Tests S-01-2 and S-01-4A.

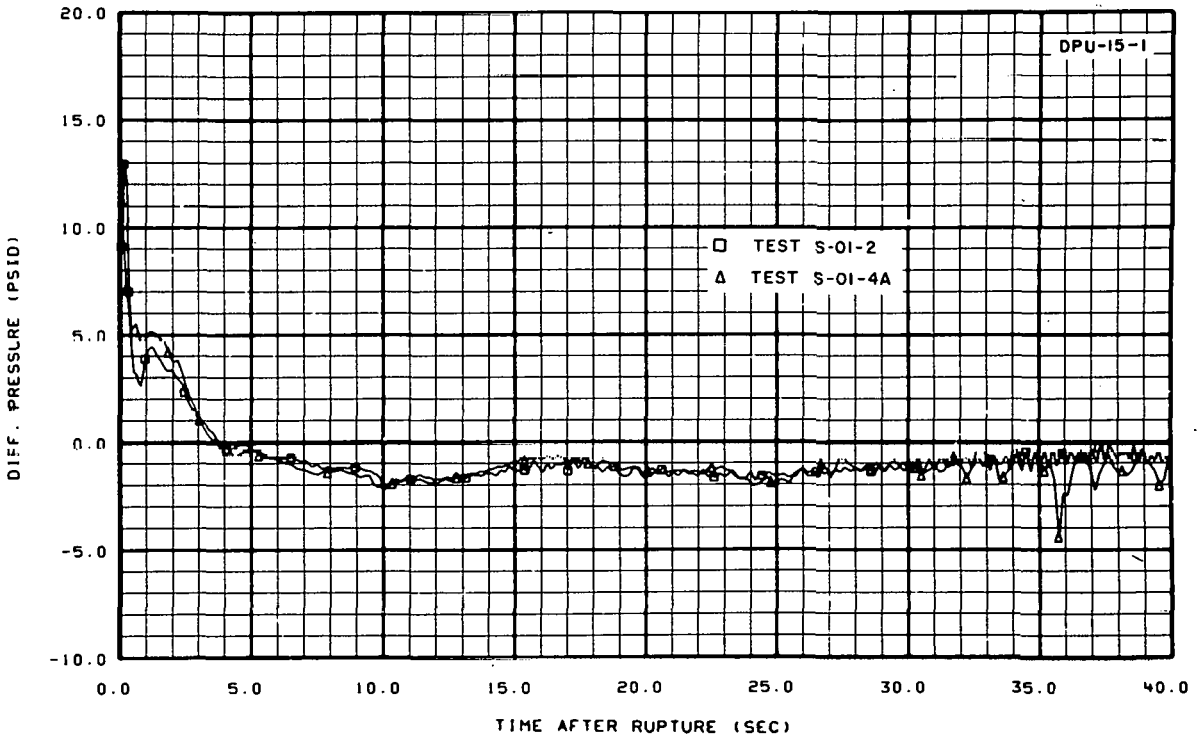

Fig. B-2 Differential pressure across vessel – Tests S-01-2 and S-01-4A.

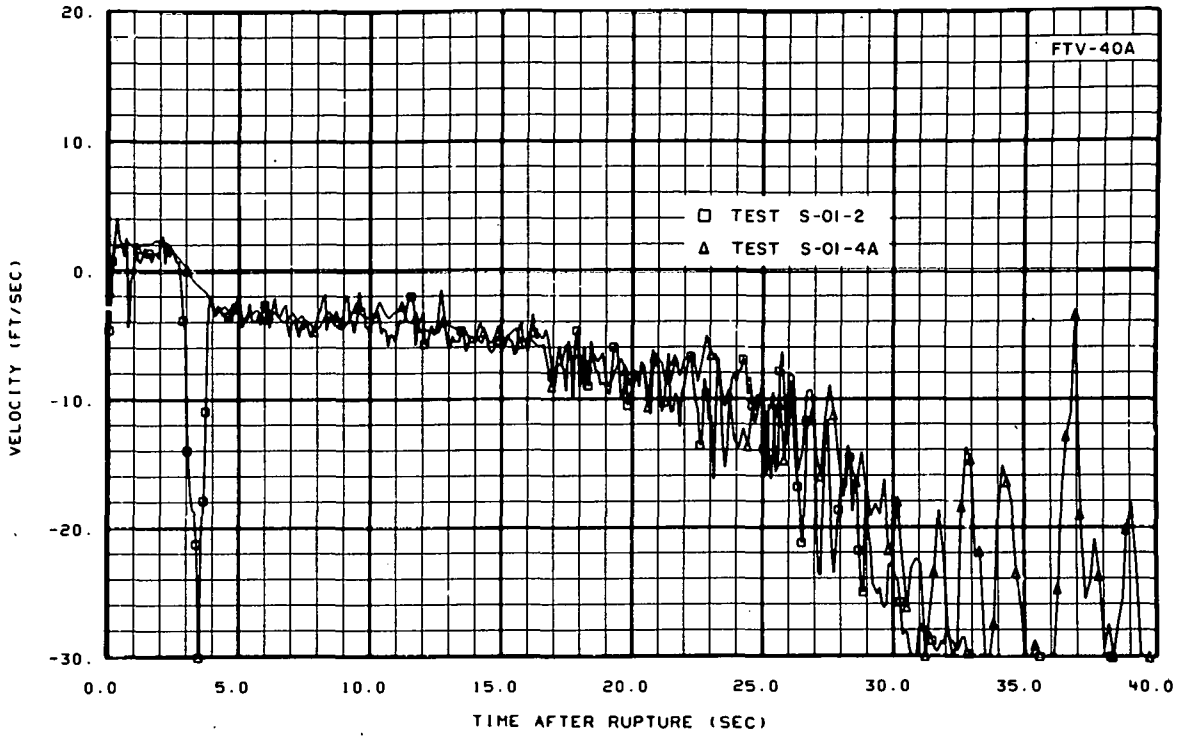

Fig. B-3 Downcomer fluid velocity – Tests S-01-2 and S-01-4A.

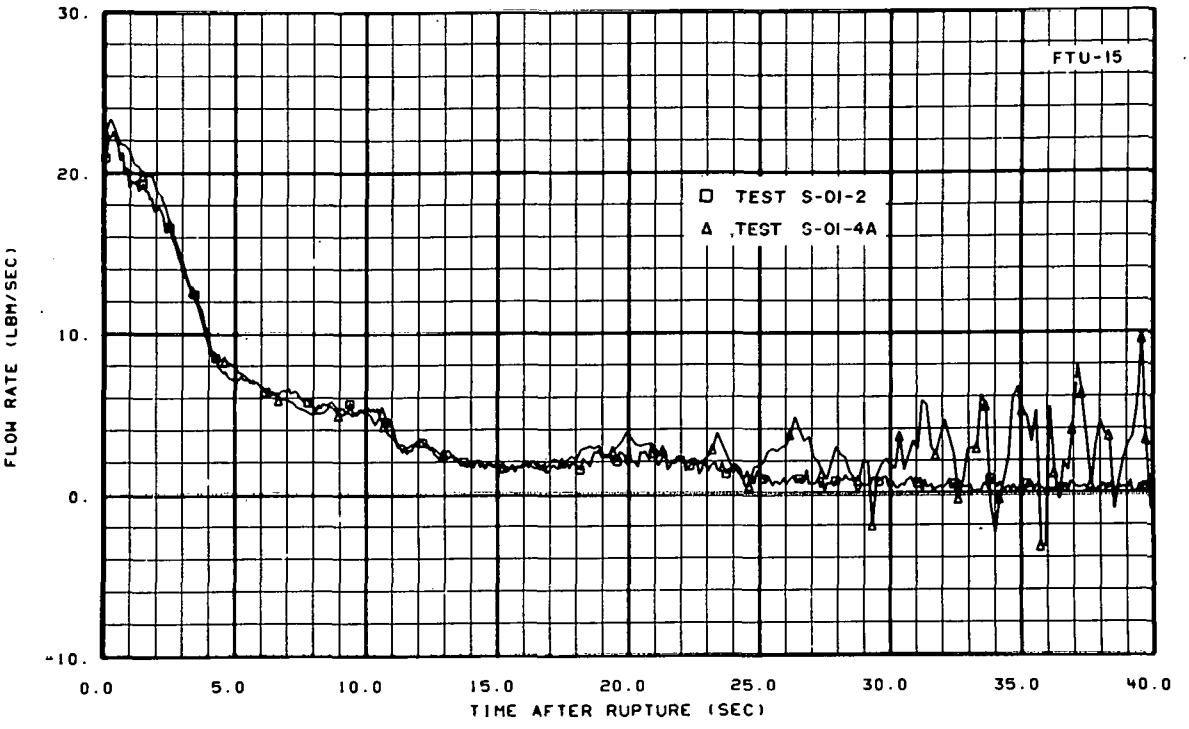

Fig. B-4 Flow rate at intact loop vessel inlet – Tests S-01-2 and S-01-4A.

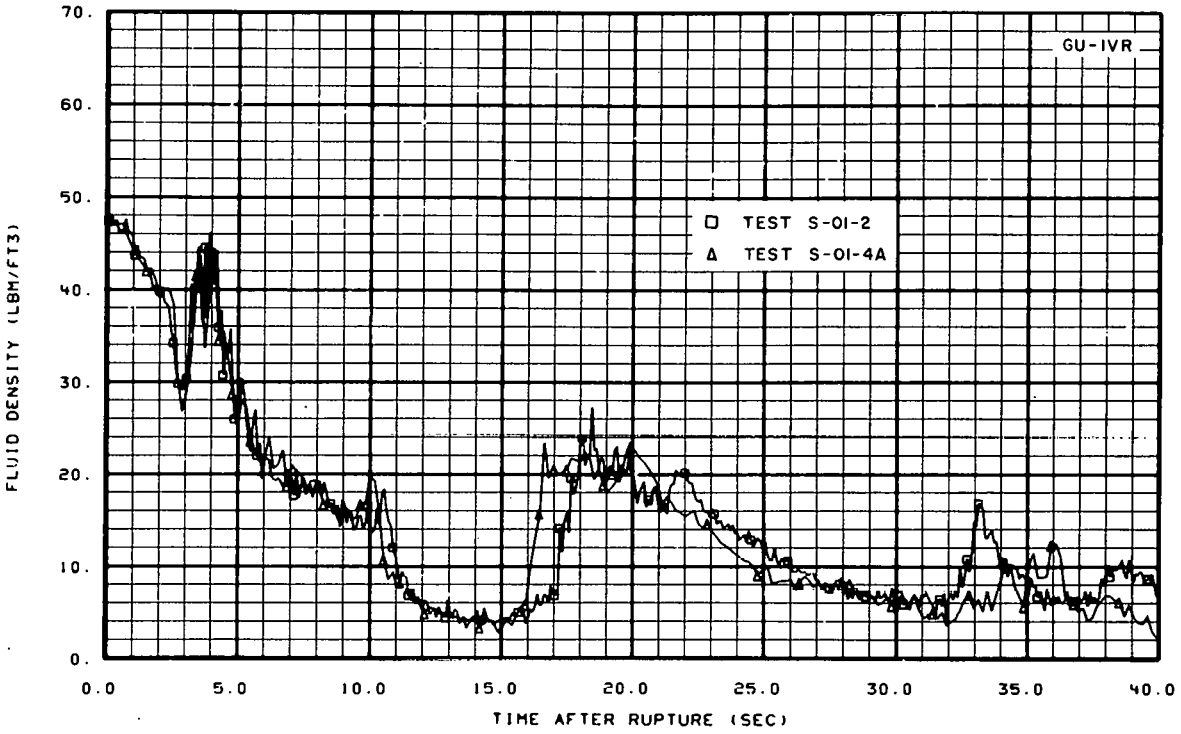

Fig. B-5 Fluid density at intact loop hot leg vessel outlet – Tests S-01-2 and S-01-4A.

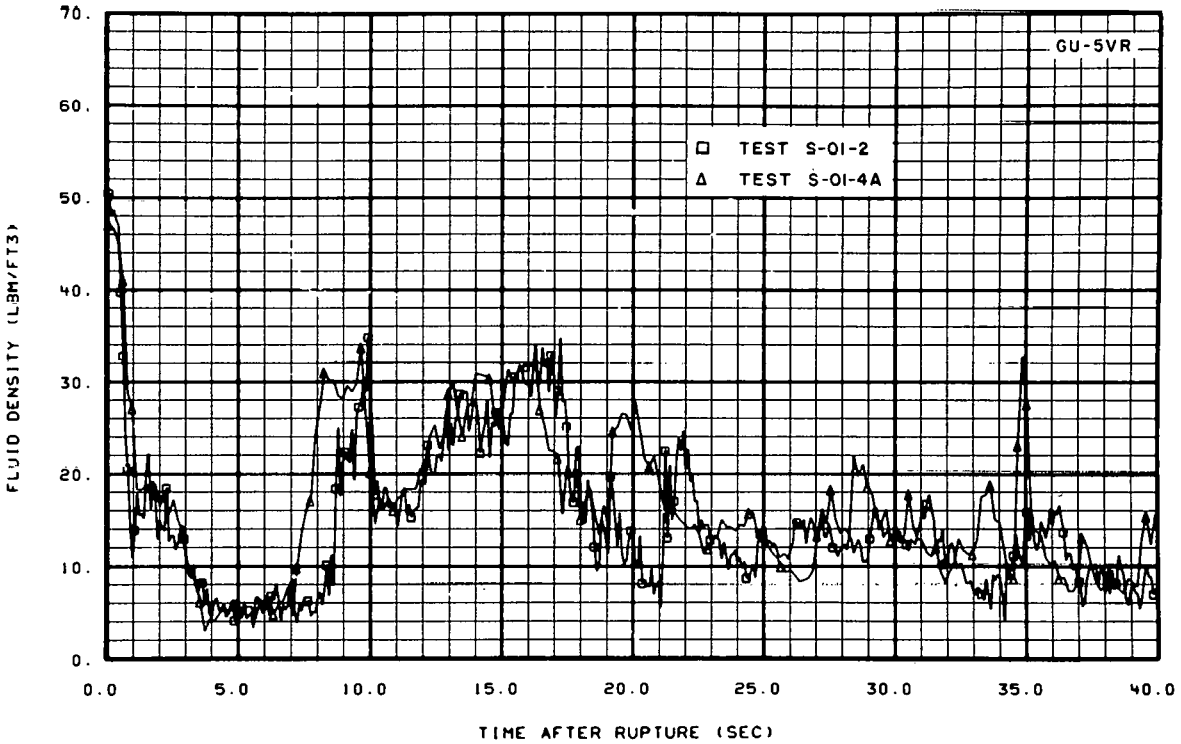

Fig. B-6 Fluid density at intact loop hot leg – Tests S-01-2 and S-01-4A.

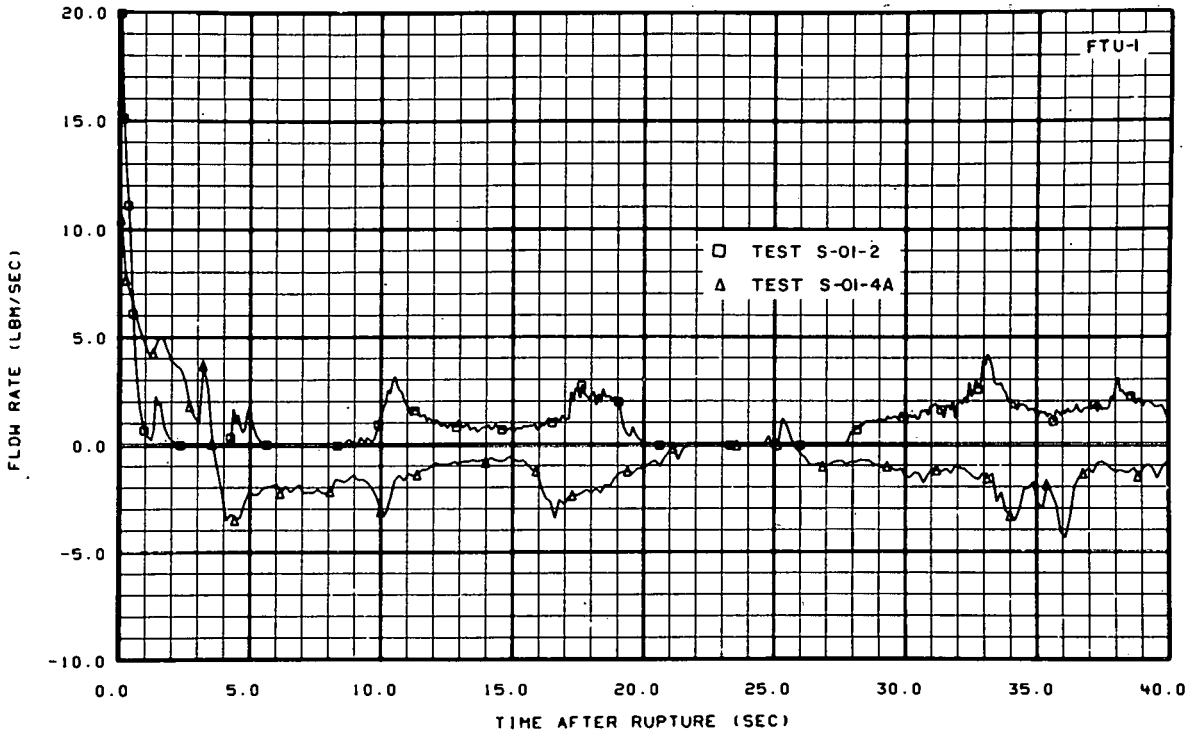

Fig. B-7 Flow rate at intact loop hot leg vessel outlet – Tests S-01-2 and S-01-4A.

unidirectional, and the drag disc within the core failed. The measured pressure drop from the lower plenum to the upper plenum (through the core) would also have resolved the flow direction for the two tests; however, this measurement also failed during Test S-01-2.

Although the core turbine flowmeter data are in question for Test S-01-2, the density measurement did function properly and does show a difference relative to results for Test S-01-4A. Figure B-8 shows a much higher density for Test S-01-2 between 16 and 24 seconds after rupture. Results from other cold leg break tests are consistent with the results of Test S-01-4A, indicating that the core density during this time interval is affected by the intact loop flow resistance. However, the RELAP4 calculations show no difference in core density for the two resistance cases and agree reasonably well with Test S-01-4A results. Also, the density values about two feet lower in the core do not show the strong differences exhibited at the core barrel inlet, as indicated by the results shown in Figure B-9.

An additional factor in considering the flow direction through the core is the fluid inventory in the lower plenum during the time period of concern. If flow were positive through the core for Test S-01-2, the integrated mass through the core during the stated time interval should be large enough to significantly deplete the liquid inventory in the lower plenum. The integrated mass through the core, and the liquid inventory in the lower plenum for Test S-01-2, do not support this concept, as shown in Figures B-10 and B-11, indicating that the flow through the core for Test S-01-2 may not have been positive.

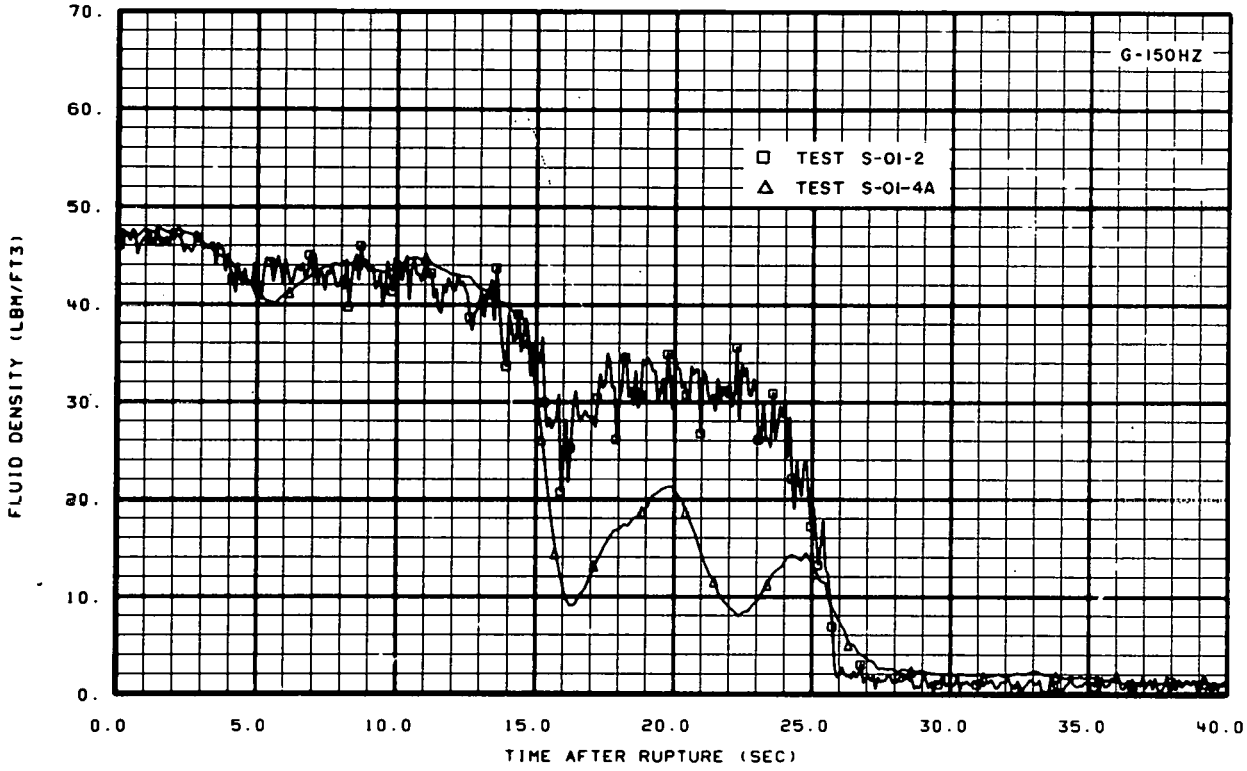

Fig. B-8 Fluid density at entrance to core – Tests S-01-2 and S-01-4A.

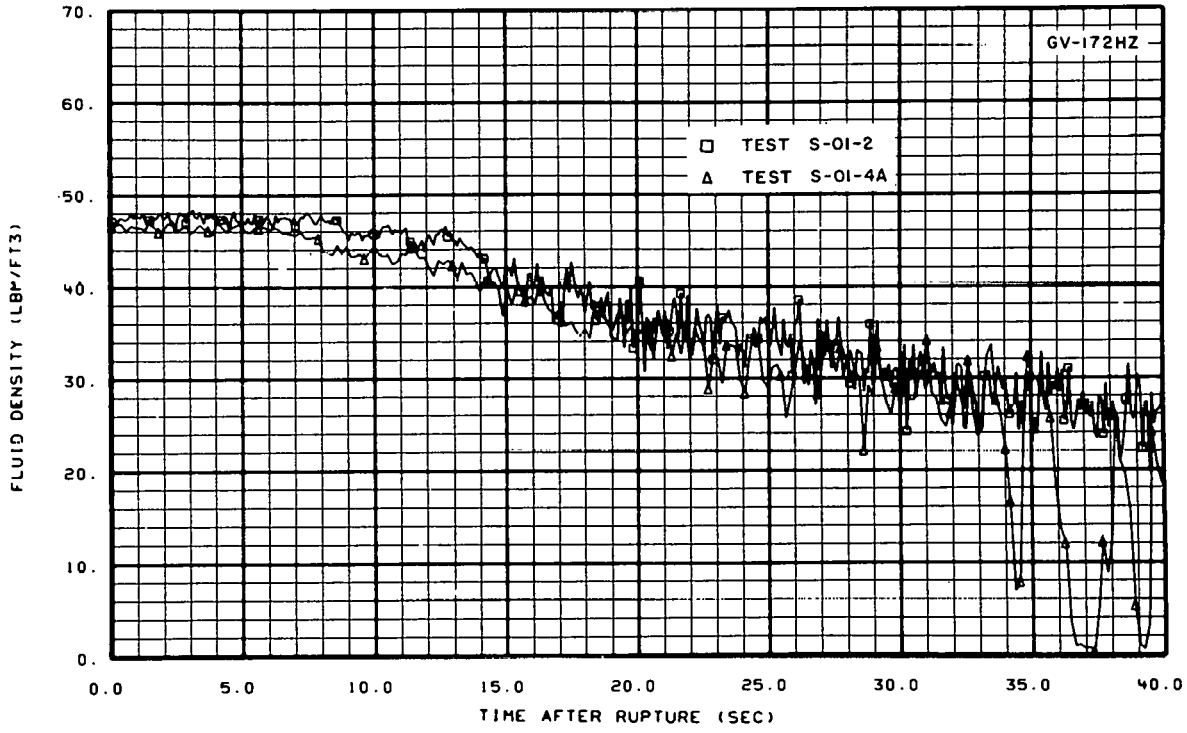

Fig. B-9 Fluid density in lower plenum – Tests S-01-2 and S-01-4A.

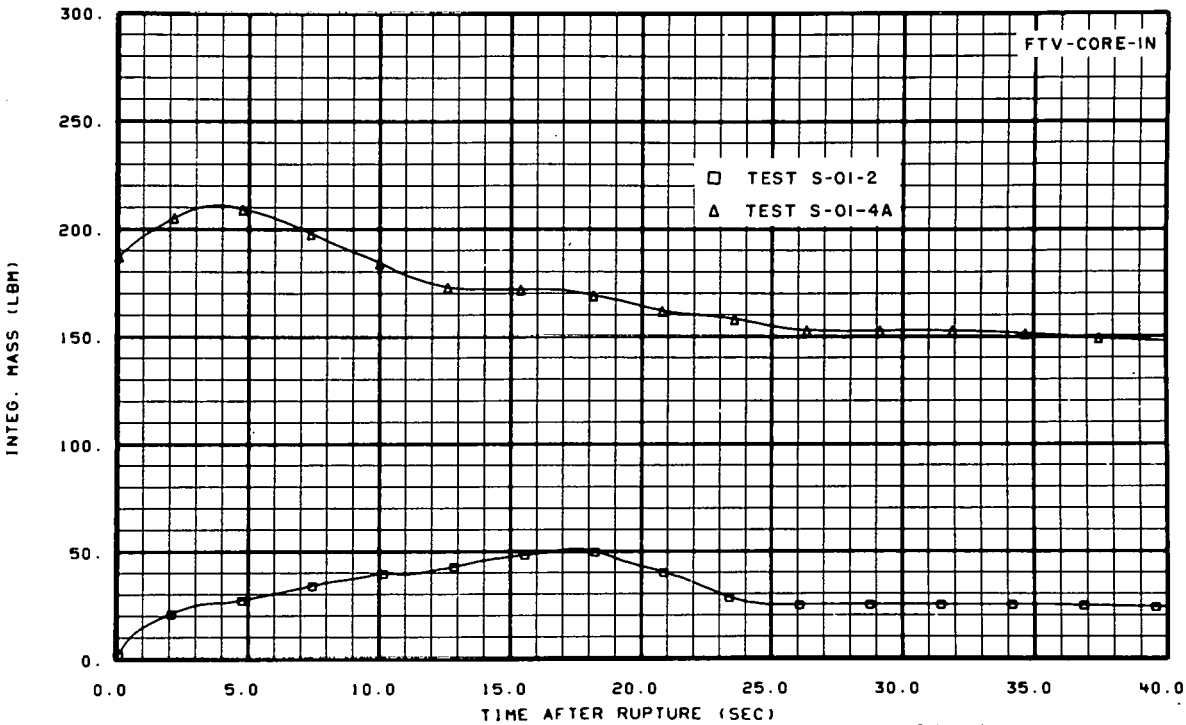

Fig. B-10 Integrated mass through core entrance – Tests S-01-2 and S-01-4A.

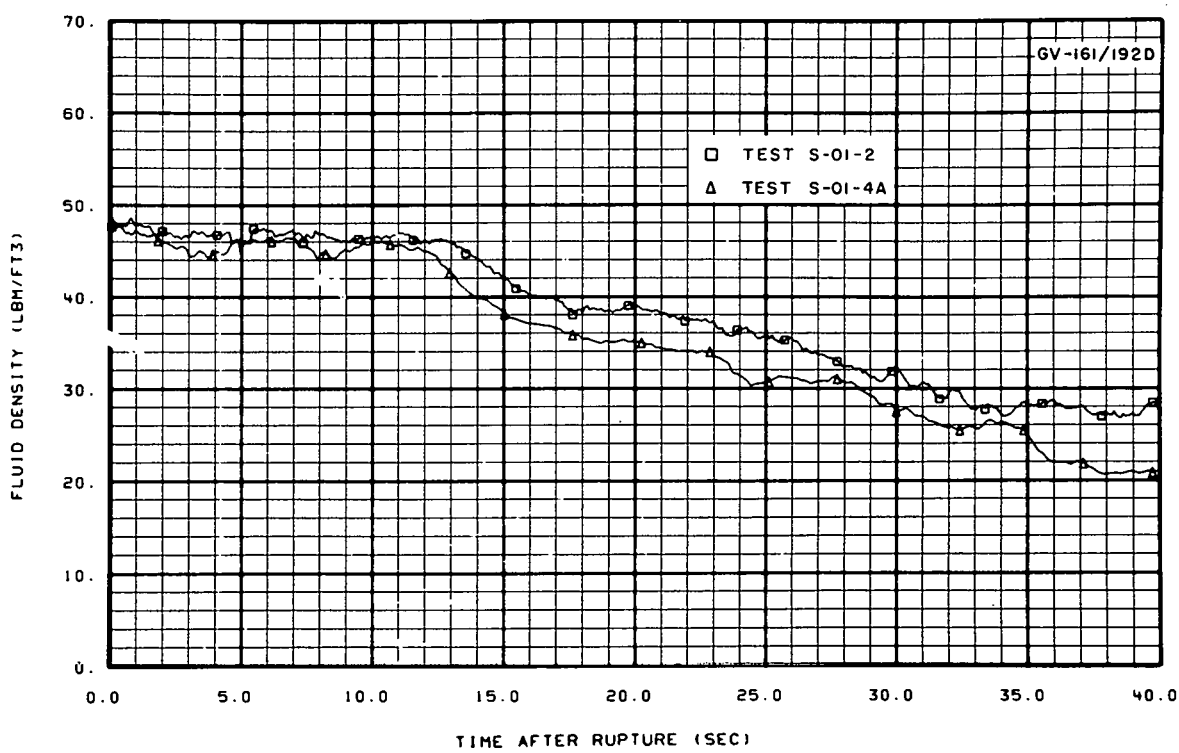

Fig. B-11 Diagonal fluid density measurement in the lower plenum – Tests S-01-2 and S-01-4A.

Since the discussed influences of data do not clearly indicate a positive flow direction through the core for Test S-01-2, and since six of the nine measurements in the vessel region support negative flow through the core, after thorough evaluation, the flow turbine flowmeter measurement appears to be in error.

DISTRIBUTION RECORD FOR ANCR- 1228

External -

287 - NRC-2 - Water Reactor Safety Systems Engineering

2 - H. J. C. Kouts, NRC

Internal

1 - Chicago Patent Group - ERDA
9800 South Cass Avenue
Argonne, Illinois 60439

3 - A. T. Morphew, Classification and Technical Information Officer
ERDA-ID
Idaho Falls, Idaho 83401

1 - R. J. Beers, ID

1 - P. E. Litteneker, ID

1 - R. E. Swanson, ID

1 - V. A. Walker, ID

1 - R. E. Wood, ID

11 - INEL Technical Library

80 - Author

Total Copies Printed - 389